NATIONAL CENTRE FOR NUCLEAR RESEARCH

DOCTORAL THESIS

---

# Aspects of Lorentz and CPT Violation in Cosmology

---


*Author:*

Nils Albin NILSSON

*Supervisor:*

Prof. Dr Hab. Mariusz P. DĄBROWSKI


*A thesis submitted in fulfillment of the requirements*

*for the degree of Doctor of Physical Sciences*

*at the*

National Centre for Nuclear Research


March 10, 2020

# Declaration of Authorship

I, Nils Albin NILSSON, declare that this thesis titled, "Aspects of Lorentz and CPT Violation in Cosmology" and the work presented in it are my own. I confirm that:

- This work was done wholly or mainly while in candidature for a research degree at the National Centre for Nuclear Research.
- Where any part of this thesis has previously been submitted for a degree or any other qualification at the National Centre for Nuclear Research or any other institution, this has been clearly stated.
- Where I have consulted the published work of others, this is always clearly attributed.
- Where I have quoted from the work of others, the source is always given. With the exception of such quotations, this thesis is entirely my own work.
- I have acknowledged all main sources of help.
- Where the thesis is based on work done by myself jointly with others, I have made clear exactly what was done by others and what I have contributed myself.

Signed:

_____

Date:

_____

*"Nature never deceives us; it is always we who deceive ourselves"*

Jean-Jaques Rousseau

NATIONAL CENTRE FOR NUCLEAR RESEARCH

# *Abstract*

National Centre for Nuclear Research

Doctor of Physical Sciences

**Aspects of Lorentz and CPT Violation in Cosmology**

by Nils Albin NILSSON

The breaking of Lorentz symmetry can give rise to a wealth of observational consequences. The main topic of this thesis is to explore models of gravitation and cosmology with Lorentz symmetry violation (closely linked to Charge-Parity-Time (CPT) violation). Five Lorentz-violating models or frameworks are outlined in this thesis, and three of these are subsequently chosen and studied in the following chapters. Doubly General Relativity breaks Lorentz symmetry through a modification of the dispersion relation of particles. This is combined with the kinematic modified dispersion relations common in phenomenological studies of Lorentz violation with high-energy gamma rays. By applying a large cosmological dataset to the resulting model, it is found that the *lower* limit on the energy scale of Lorentz violation is $E_{LV} \sim 10^{16}$ GeV ($1\sigma$). Hořava-Lifshitz gravity is a possibly UV-complete quantum-gravity theory candidate. By again applying a large updated cosmological dataset new constraints on the cosmological parameters are found. In particular, the curvature density parameter $\Omega_k$ found to be non-zero $(-3.30 \pm 0.20) \times 10^{-3}$ ($1\sigma$). Moreover, this model is discussed in context of the Hubble parameter tension, through which the Hořava-Lifshitz coupling parameter $\lambda$is given new contraints. It is found that Lorentz violation can contribute up to 38% of the Hubble tension. The Standard-Model Extension is a general, theory-agnostic framework for testing Lorentz and CPT violation. Here, the Hamiltonian formulation of the Standard-Model Extension gravitational sector is presented.

## Polski:

Łamanie symetrii Lorentza może prowadzić do wielu konsekwencji obserwacyjnych. Głównym tematem rozprawy jest zbadanie modeli grawitacyjnych i kosmologicznych, w których zachodzi scenariusz naruszenia tej symetrii (blisko spokrewnione ze złamaniem symetrii CPT – Ładunku, Parzystości, Czasu). W pracy opisano pięć różnych modeli ze scenariuszem łamania symetrii Lorentza, z czego trzy są wybrane do dalszej analizy w kolejnych rozdziałach. Podwójna Ogólna Teoria Względności (Doubly General Relativity) łamie symetrię Lorentza poprzez modyfikację relacji dyspersyjnych cząstek. Powyższy model jest połączony z kinematycznie zmodyfikowanymi relacjami dyspersyjnymi powszechnymi w badaniach fenomenologicznych łamania symetrii Lorentza za pomocą wysokoenergetycznych promieni gamma. Porównując uzyskany model z szerokim zestawem danych kosmologicznych stwierdzono, że *dolna* granica skali energii łamiącej symetrię Lorentza wynosi $E_{LV} \sim 10^{16}$GeV ($1\sigma$). Teoria grawitacji Hořavy-Lifszyca jest potencjalnym kandydatem na kompletną w ultrafiolecie teorię kwantowej grawitacji. Ponownie, poprzez zastosowanie wielkich zestawów danych kosmologicznych do tego modelu, udało się wyznaczyć nowe ograniczenia na wartości jego parametrów kosmologicznych. W szczególności stwierdzono, że krzywizna przestrzeni jest niezerowa $(-3,30 \pm 0,20) \times 10^{-3}$ ($1\sigma$). Co więcej, model ten jest omawiany w kontekście rozbieżności dotyczących parametru Hubble'a (Hubble parameter tension), w wyniku czego otrzymuje się nowe ograniczenia na wartość parametru $\lambda$ w teorii Hořavy-Lifszyca. Stwierdzono, że scenariusz łamania symetrii Lorentza może przyczynić się w 38% do rozwiązania problemu rozbieżności parametru Hubble'a. Rozszerzony Model Standardowy jest ogólną, efektywną teorią pola mogącą posłużyć do testowania scenariuszy łamania symetrii Lorentza. W rozprawie, zaprezentowane jest Hamiltonowskie sformułowanie sektora grawitacyjnego dla Rozszerzonego Modelu Standardowego.

## Svenska:

Lorentzbrott kan ge upphov till mängder av observerbara konsekvenser. Denna avhandlings huvudtema är att utforska gravitations- och kosmologimodeller som inkluderar Lorentzbrott (kopplat till Laddning-Paritet-Tidbrott (CPT)). Fem Lorentzbrytande modeller och ramverk skissas i början av denna avhandling och tre av dessa väljs sedermera ut och studeras i efterföljande kapitel. Dubbelt Allmän Relativitetsteori (Doubly General Relativity) bryter Lorentzsymmetri genom att modifiera dispersionsrelationen för partiklar. Detta kombineras med de kinematiskt modifierade dispersionsrelationerna som är vanliga i fenomenologiska studier av högenergifotoner. Genom att applicera ett stort kosmologiskt dataset på den resulterande kosmologiska modellen bestämdes det lägre värdet för den karakteristiska energiskalan för Lorentzbrott till $E_{LV} \sim 10^{16}$ GeV ($1\sigma$). Hořava-Lifshitzgravitation är en möjligen UV-komplett kvantgravitationskandidat. Genom att återigen applicera ett stort uppdaterat kosmologiskt dataset bestäms nya värden på de kosmologiska parametrarna. I synnerhet kan den spatiala kurvaturen bestämmas till $(-3.30 \pm 0.20) \times 10^{-3}$ ($1\sigma$). Hubblespänningen (Hubble tension) diskuteras också inom denna modell som en effekt av föredragna referensramar (preferred-frame effects), och värden på Hořava-Lifshitzparametrar bestäms från Hubblespänningsdata. Det fastställs också att Lorentzbrott kan bidra med upp till 38% av Hubblespänningen. Standardmodellutvidgningen (Standard-Model Extension) är ett allmännt ramverk för att parametrisera och testa Lorentz- och CPT-brott. Här härleds och presenteras Hamiltonformuleringen av Standardmodellutvidgningens gravitationssektor.

# *Acknowledgements*

The writing of this thesis would not have been possible without the support and guidance of my supervisor, Mariusz P. Dąbrowski, who gave me a lot of research freedom and encouraged me to be independent. His influence has made me the researcher who I am today and has helped shape this thesis into what is printed within these pages. To Ewa Czuchry, who took me in when all I had was an idea and encouraged me to tackle hard problems. To Vincenzo Salzano who taught me about MCMC and patiently answered my endless questions. To Quentin Bailey and Kellie O'Neal-Ault who helped open the door to an exciting field and for helping me develop a long-term collaboration, and to all the people at Embry-Riddle for treating me like one of their own from day one. To Artur and Viktor, with whom I could always discuss ideas, and to Harrison for proofreading parts of this thesis. To my parents, who supported me even when it brought me far from home, and to Sarah, for her unwaivering support.

Special thanks goes to the National Centre for Nuclear Research and National Science Center. Their financial support made it possible for me to attend conferences and visit scientists in Poland, Germany, Italy, Greece, Portugal, Canada, and the USA. I also thank the National Centre for Nuclear Research for the use of the CIŚ high-performance computing cluster.

To all the people who have helped me along the way, thank you.

# Contents

# List of Figures

# List of Tables

# List of Abbreviations

| | |
|---|---|
| **ADM** | **A**rnowit-**D**eser-**M**isner |
| **BAO** | **B**aryon **A**coustic **O**scillations |
| **BBN** | **B**ig-**B**ang **N**ucleosynthesis |
| **BDB** | **B**eyond **D**etailed **B**alance |
| **CMB** | **C**osmic **M**icrowave **B**ackground |
| **CPT** | **C**harge-**P**arity-**T**ime |
| **CTA** | **C**herenkov **T**elescope **A**rray |
| **DB** | **D**etailed **B**alance |
| **DGR** | **D**oubly **G**eneral **R**elativity |
| **DSR** | **D**oubly **S**pecial **R**elativity |
| **FLRW** | **F**riedmann-**L**emaître-**R**obertson-**W**alker |
| **GR** | **G**eneral **R**elativity |
| **GRB** | **G**amma-**r**ay **B**urst |
| **GUT** | **G**rand **U**nified **T**heory |
| **Gyr** | **G**iga**y**ear |
| **GZK** | **G**reisen-**Z**atsepin-**K**uzmin |
| **HL** | **H**ořava-**L**ifshitz |
| **IR** | **I**nfra**r**ed |
| **ΛCDM** | **Λ** **C**old **D**ark **M**atter |
| **LI** | **L**orentz **I**nvariant |
| **LIGO** | **L**aser **I**nterferometer **G**ravitational-Wave **O**bservatory |
| **LIV** | **L**orentz **I**nvariance **V**iolation |
| **LV** | **L**orentz-**V**iolating |
| **MCMC** | **M**arkov-**C**hain **M**onte **Ca**rlo |
| **PPN** | **P**arametrised **P**ost-**N**ewtonian |
| **QED** | **Q**uantum **E**lectrodynamics |

| | |
|---|---|
| **QFT** | **Q**uantum **F**ield **T**heory |
| **SME** | **S**tandard-**M**odel **E**xtension |
| **SNeIa** | **S**upernova**e** Type **Ia** |
| **UV** | **U**ltra**V**iolet |

*To Agne, who taught me to get on with it.*

# 1

# Introduction

SYMMETRY is reassuring. It gives us the impression of predictability and control. It seems that humans are hardwired to spot symmetries in our surroundings. It is then fortunate that modern physics is built on symmetries and their consequenses. At first glance this is less than intuitive, as the natural world around us appears to contain very little symmetry. A straight line or perfect circle would certainly stand out in a forest or desert. However, when we look closer we can see symmetric structures, such as pentagonal flower petals and hexagonal honeycombs in beehives. In fact, the closer we look, the purer the summetries seem to become, and when we study the fundamental physical processes which govern the physical world, we realise that everything is built on symmetries.

In mankind's present understanding of nature, there are two distinct regimes, one governed by quantum field theory and one by general relativity. Quantum field theory describes all fundamental interactions except gravity with remarkable accuracy and has been successfully used to construct the Standard Model of particle physics. General relativity, on the other hand, describes gravity and is important on very large scales and very large masses, such as stars, galaxies, black holes, and the like. Both of these theories claim to be universally valid, but when scaling out from the very small to the very large, there comes a point where we have to switch theories. Moreover, there are regions and regimes where classical General Relativity simply is not predictive, such as the initial and black hole singularity. Therefore, for the past few decades, physicists have been searching for a theory of Quantum Gravity, to either unify or replace these two highly successful descriptions of nature. However, when trying to formulate a theory of Quantum Gravity one encounters several types of obstacles, such as renormalisability in gravity [1, 2], loss of unitarity [3, 4], and the problem of time [5–7]. One can also see the need for Quantum Gravity from a reductionist point of view which permeates modern physics.

As any theory of Quantum Gravity has to encompass General Relativity (with characteristic constant $G$), quantum mechanics (with characteristic constant $\hbar$), and special relativity (with characteristic constant $c$), this theory should reasonably contain the fundamental constants of these three paradigms; ($G$, $\hbar$, and $c$). As such, by dimensional analysis we can construct a characteristic energy scale for such a theory, the *Planck energy*: $E_{Pl} = \sqrt{\hbar c^5 / G}$. This energy scale is around $10^{19}$ GeV, so any

signals of quantum gravity will most likely be found in phenomena involving high energies, short length scales, and strong gravity. As can be seen from the Bronstein-Zelmanov-Okun cube in Figure 1.1, standard classical mechanics can be obtained from quantum mechanics if we let Planck's constant $\hbar$ go to 0 or from special relativity if we let the speed of light $c$ go to infinity. In this figure, efforts to obtain information about quantum gravity can be thought of as the red arrows. These paradigms can also be characterised by the *dimensionless* fine-structure and gravitational constant, which give a measure of the strength of the interactions. The fine-structure constant, $\alpha = e^2/4\pi\epsilon_0\hbar c \approx 1/137$, is *much larger* than the gravitational constant, $\alpha_G = Gm_e^2/\hbar c \approx 10^{-44}$. Since the Planck scale ($\sim 10^{19}$ GeV) can reasonably be thought of as the characteristic energy scale of Quantum Gravity it may seem unlikely that this ever could fall within the observationally accessible regime for any experiment. However, it has been realised, through the study of gravity models beyond General Relativity and several models of Quantum Gravity that there may exist several low energy trickle-down signatures from high-energy Quantum Gravity effects which may be visible in either the gravitational or particle physics regime. For example, some of these effects may be imprints on primordial perturbations [8], spacetime variation of coupling constants [9, 10], TeV black holes from the existence of extra dimensions [11], violation of spacetime and/or discrete symmetries [12], to name a few. In this thesis I will focus on possible deviations or modifications of Lorentz symmetry, a cornerstone spacetime symmetry which permeates all of relativity and particle physics and thus offers rich phenomenology in several sectors. Lorentz symmetry violation is a large, active field of research, with big efforts being put forth both in theory and experiment. Detecting any sign of Lorentz violation would be a clear signal of new physics with large implications. Possible observable effects include *i)* sidereal variations of coupling constants as the Earth moves with respect to a fixed background field [13], *ii)* canonically forbidden reactions, such as vacuum Cherenkov radiation and photon decay [14, 15], *iii)* propagation effects, such as birefringence of gravitational-wave polarisations [16, 17], *iv)* modified reaction thresholds, for example photon extinction from active galactic nuclei [18], to name a few examples.

Another symmetry which is intimately tied to Lorentz symmetry is that of **CPT**

**symmetry**, which is, as far as we know, a fundamental property of nature. It is defined as the invariance of physical laws under simultaneous reversal of Charge, Parity, and Time. The CPT theorem [19] states that any unitary, Lorentz invariant local quantum field theory described by a hermitian Hamiltonian must be CPT invariant. As such, there is a one-way implication between Lorentz and CPT symmetry; A detection of CPT violation implies that Lorentz symmetry is also broken [20]. At the same time, if Lorentz symmetry is broken, the CPT theorem does not hold, and CPT symmetry must be imposed as an extra constraint if we wish to keep it. As a result, CPT violation has received a lot of attention in particle physics, such as the neutral kaon system [21, 22], as well as in high-energy astroparticle physics. In recent years, this notion has received a lot of attention, which is mainly motivated by the introduction of theoretical models which allow or explicitly contain Lorentz (and CPT) violation. The publications which make up the bulk of this thesis focus on Lorentz rather than CPT violation, since Lorentz violation phenomenology is more accessible to gravity and cosmology; however, because of the tight link between the two, CPT violation has been discussed wherever appropriate.

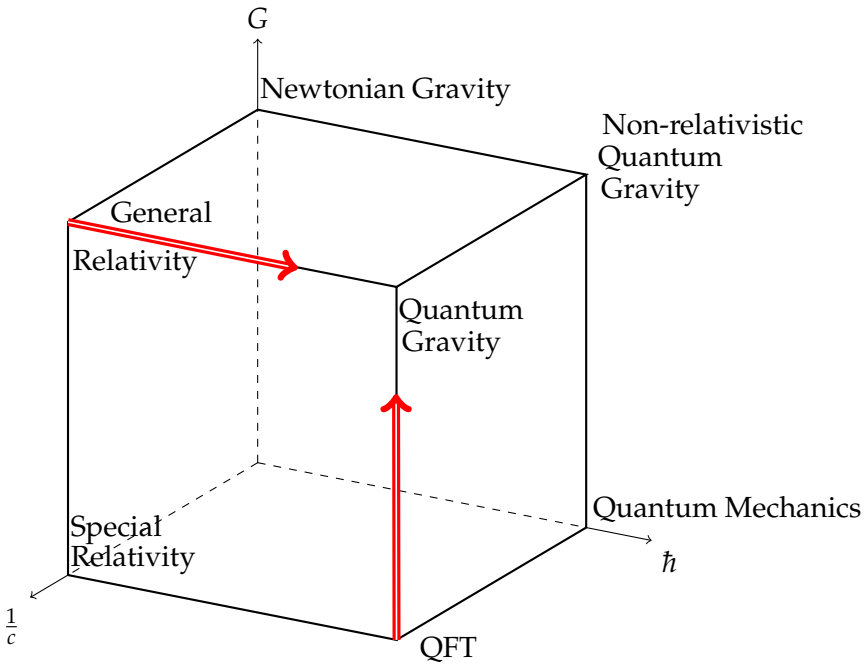


FIGURE 1.1: A Bronstein-Zelmanov-Okun cube depicting relations between physical theories with their respective fundamental constants. The (red) arrows represent Effective Field Theory approaches to probe quantum-gravity effects.

## 1.1 Research Aims and Scope

The overarching aim of this research was to gain a better understanding of Lorentz and CPT symmetry in gravitation and cosmology. In particular, the goal was to find constraints on the possible breaking of Lorentz symmetry in regions of strong gravity. This is motivated by the fact that Lorentz violation is an expected signal of quantum gravity. Moreover, it is clear that any deviation from perfect Lorentz symmetry would be a clear sign of new physics. The work in this thesis makes no attempt to provide a fundamental theory (which would be a Herculean task) but rather focuses on exploring and contraining the possible phenomenological consequences of Lorentz violation and its possible impact on cosmological evolution and gravitational phenomena.

The different pieces of research in this thesis can be roughly divided into three parts; Modified Dispersion Relations, Ultraviolet Completions of Gravity, and Effective Field Theory, as different approaches to studying Lorentz violation.

*Modified Dispersion Relations* is a purely phenomenological approach, where it is assumed that high-energy particles (usually photons) interact with a quantum spacetime (for example, the quantum foam [23, 24]) which perturbs its dispersion relation. This can lead to frequency-dependent photon masses, birefringence, and the like. These types of models offer rich phenomenology and can be readily tested. In this thesis a modified dispersion relation model has been combined with Doubly General Relativity to provide limits on the energy scale at which Lorentz-violating effects become strong. Through the CPT theorem, this energy scale is also where departures from CPT symmetry might manifest [25].

*Ultraviolet Completions of Gravity* are models of gravity where the ultraviolet behaviour has been altered. The model under study in this thesis is Hořava-Lifshitz gravity, where Lorentz invariance is explicitly broken in the ultraviolet regime, which renders the theory perturbatively renormalisable. As such, Hořava-Lifshitz gravity is a quantum-gravity candidate. In this thesis, this model has been explored on a phenomenological level. New limits on cosmological parameters have been provided, and Lorentz violation has been discussed as one source of the Hubble tension.

*Effective Field Theory* is a general way to study Lorentz and CPT violation. In this

thesis the focus has been on the effective field theory known as the Standard-Model Extension, which contains all the sectors of the Standard Model (as well as gravity) along with every observer-covariant and gauge invariant operators, both CPT odd and even. In the gravitational sector, the linearised limit has been thoroughly studied to date. In this thesis, the first steps towards writing the gravitational sector of the Standard-Model Extension in its 3+1 decomposed form are taken. This will eventually allow for the Standard-Model Extension to be included in fully non-linear numerical relativity and compact binary merger simulations.

## 1.2 Linkage of Scientific Papers

The main body of research presented in Chapters 3-6 has been published in peer-reviewed journals, as conference proceedings, or are published on arXiv. These pieces of work have been reproduced more or less verbatim here and put into a larger context by the introductory material. Out of these contributions, Two are peer-reviewed publications [26, 27], one is a manuscript available on arXiv (and submitted to a journal) [28] and one is a set of conference proceedings [29]. The author also has three manuscripts currently under development [231, 238]. The other manuscript in preparation lies outside of the scope of thesis.

These papers and manuscripts all discuss Lorentz violation, albeit focusing on different aspects, from pure phenomenology (Modified dispersion relations), to a specific model exhibiting ultraviolet Lorentz violation (Hořava-Lifshitz gravity), as well as a general effective field theory for parametrising deviations from Lorentz symmetry (the Standard-Model Extension).

# 2

# The Role of Lorentz and CPT Symmetry in Modern Physics

THE combination of General Relativity and the Standard Model of particle physics makes up our most accurate description of Nature currently. General relativity describes gravitation at the classical level, whereas the Standard Model describes the interactions of elementary particles and forces at the quantum level. This quantum description is based on global Lorentz symmetry in flat spacetime, the symmetry under the three rotations and three boosts which make up the set of generators of the Lorentz group. These are spacetime symmetries, as they transform the physical space. In General Relativity it is reduced to *local* Lorentz symmetry, since at every point in spacetime we may define a locally freely falling Lorentz frame where Lorentz symmetry is preserved. As such, Lorentz symmetry is one of the fundamental principles of modern physics and offers ample phenomenological opportunities for testing its validity in several sectors. Another closely related symmetry is CPT; Charge conjugation, Parity inversion, and Time reversal. These are *discrete* symmetries, related to Lorentz symmetry (which is *continuous*) though the CPT theorem, which states that any local, Lorentz invariant quantum field theory with a Hermitian Hamiltonian must be CPT invariant in flat space [30]. The converse (and particularly interesting for the purposes of this thesis) was proved in [20] (see [31–34] for the ensuing discussion) and states that an interacting theory which violates CPT also violates Lorentz symmetry.

## 2.1 Explicit versus Spontaneous Lorentz Symmetry Breaking

There are, in general, two different mechanisms through which to break symmetries in field theory, dubbed *explicit* and *spontaneous* symmetry breaking. Since we are interested in Lorentz violation, the symmetry we will choose to break will be Lorentz symmetry). Explicit Lorentz violation is signalled by the existence of a fixed background tensor $\bar{k}_\chi$ put "by hand" into the Lagrangian of the theory [12, 35]. These fixed tensors do not transform under the Lorentz group; therefore, Lorentz symmetry is broken on the level of the Lagranian $\mathcal{L}$. On the other hand, spontaneous Lorentz violation arises as a Lorentz-violating solution to the otherwise Lorentz invariant theory when a dynamical field acquires a vacuum expectation value $\bar{k}_\chi = \langle k_\chi \rangle$ [12, 35–39]. It is possible to move from spontaneous to explicit breaking through

a coarse-graining procedure in which a Lorentz-violating solution to the Euler-Lagrange equations is found, and then plugged in to the original action, which then acquires explicit Lorentz violation. We may write that

$$\mathcal{L}\left[k_\chi\right] \text{ (Lorentz invariant)}, \quad \mathcal{L}\left[\bar{k}_\chi\right] \text{ (Lorentz-violating)}. \tag{2.1}$$

In the Standard Model, spontaneous breaking of the $SU(2) \times U(1)$ electroweak symmetry, which fills spacetime with a scalar condensate, this being the vacuum expectation value of the Higgs field. In general, spontaneous breaking of a local gauge symmetry yields massive gauge bosons (such as the $W^\pm$ and $Z^0$), whereas breaking a global one generates massless Nambu-Goldstone modes [35]. If we consider Minkowski space, then explicit and spontaneous Lorentz symmetry are equivalent, but when moving to curved spacetimes explicit symmetry breaking generally leads to inconsistencies with energy-momentum conservation and the Bianchi identities, which is the main reason why this approach is usually avoided in the gravity sector. Theories with explicit symmetry breaking are usually regarded as less aesthetically pleasing, as they contain prior geometry (see also Section 2.3); however, theories such as Hořava-Lifshitz gravity (see Section 2.4.2 and Chapters 4, 5) incorporate prior geometry in the form of a preferred foliation of spacetime. Indeed, if we wish to write down a gravity theory with explicit Lorentz violation we will be faced with solutions incompatible with Riemannian geometry, or having to impose extra constraint equations in order to satisfy $\nabla_\mu T^{\mu\nu} = 0$ in a rather contrived way. The reason for this incompatibility lies in the structure of the gravitational bundle of frames, where the geometry satisfies $\nabla_\mu G^{\mu\nu} = 0$, and substitution of the equations of motion (Einstein equations) leads to the Bianchi identities $\nabla_\mu T^{\mu\nu} = 0$. Other sectors have a different base geometry. In QED, which is based on a principal $U(1)$ fiber bundle on a static background spacetime, the bundle geometry is determined through the equations of motion $\partial_\mu F^{\mu\nu} = j^\nu$, where the electromagnetic field strength tensor $F^{\mu\nu}$ is the curvature of the bundle, satisfying $\partial_{[\lambda} F_{\mu\nu]} = 0$. Because $F^{\mu\nu}$ is antisymmetric we may immediately deduce that $\partial_\nu j^\nu = 0$, but we can *not* find this conservation equation by substituting the equations of motion into the Bianchi identities as in gravity, and matter and geometry are not coupled in the same way; therefore we

may have explicit breaking in non-gravitational scenarios without any issues [12, 35–39]. It should also be mentioned that the breaking of Lorentz symmetry violates one of the conditions for the CPT theorem. In simple scenarios one can encounter minimally suppressed Lorentz (and thus CPT) violation, in which case the order of violation can be said to be $\mathcal{O}\left(E^2/M_{\text{Pl}}\right)$, where $E$ is some typical energy probe. In this case, *any constraint on the energy scale of Lorentz violation is also a constraint on CPT violation*.

## 2.2 CPT Symmetry in an Expanding Universe

The brief introduction to CPT symmetry at the beginning of this chapter assumed Minkowski space; however, when gravity is added CPT symmetry may be violated due to possible problems with unitarity around singular backgrounds and horizons. Indeed, Hawking radiation from black holes may lead to loss of unitarity, leading to CPT violation [25]. When the black hole has been sufficently reduced in size it will be perceived as background perturbations to asymptotic observers, who will then trace out this information, it being captured behind the horizons. So an asymptotic out state will be built from density matrices

$$\rho = \text{Tr}|\blacksquare\rangle\langle\blacksquare|, \tag{2.2}$$

which inevitably leads to loss of unitarity as the system evolves from a pure to a mixed state, and also makes it impossible to properly define an S-matrix, and the strong CPT theorem cannot hold [40].

For several decades, the consensus has been that the expansion of the Universe is accelerating, which is substantiated by many probes, such as the local distance ladder, Cepheid-type stars, TRGB data (Tip of the Red Giant Branch), and others [41–45]. If the Universe is truly of Friedmann-Lemaitre-Robertson-Walker plus a positive cosmological constant $\Lambda > 0$, the Universe will eventually enter a de Sitter phase, when all other energy density contributions have decayed sufficently, and the scale factor will read

$$a(t)|_{t\to\infty} = e^{\sqrt{\Lambda/3}t}. \tag{2.3}$$

At this point there will exist an event horizon, beyond which an observer at the origin can never see. The coordinate size of this region is

$$\eta(t) = \int_t^\infty \frac{dt'}{a\left(t'\right)}, \tag{2.4}$$

whereas its physical size is $\ell_{\rm dS} = a(t)\eta(t) = \sqrt{3/\Lambda} = H_{\rm dS}^{-1}$. Information behind the horizon is hidden from the observer, which just like for the evaporating black hole makes it impossible to define asymptotic out states, and CPT invariance is expected to be broken [40]. It is worth mentioning that there is an ongoing discussion about whether the Universe actually is accelerating. In [46], the authors analyse the lightcurves of Type Ia supernovae, and find only "marginal" evidence for cosmic acceleration. This has sparked an extensive debate (see e.g. [47–51]), and the matter seems far from settled. Here we assume that the Universe is dominated by a cosmological-constant type dark energy, which will eventually [25] lead to CPT violation in the Universe.

## 2.3 General Properties of Models with Lorentz Violation

In order to introduce Lorentz violation to General Relativity, it is necessary to add new tensor fields which break Lorentz symmetry; however, it is still desirable to keep as many properties of General Relativity as possible, in particular:

*i)* general covariance,

*ii)* the Equivalence Principle,

*iii)* the absence of prior geometry.

A Lorentz-violating gravity model will in general exhibit modifications of one or more of those three properties. It is generally accepted that observer invariance needs to hold, as physics should not depend on the orientation or location of the observer. The equivalence principle is in general altered, as in a Lorentz-violating theory, particle worldlines are species-dependent and not fully determined by the mass;

however, the equivalence principle is broken even when worldlines are species-independent. Consider a modified dispersion relation of the form [52]:

$$E^2 = m^2 + p^2 + \frac{f_\star}{E_{\rm Pl}}|p|^4, \tag{2.5}$$

where $f_\star$ does not depend on the particle species. The corresponding Hamiltonian for a non-relativistic particle in a weak gravitational field is:

$$H = m + \frac{p^2}{2m} + f_\star \frac{p^4}{2mE_{\rm Pl}} + m\phi(x), \tag{2.6}$$

which through Hamilton's equations leads to a mass-dependent acceleration:

$$\ddot{x}_i = -\frac{\partial \phi}{\partial x^i}\left(1 + 6f_\star \frac{m^2 \dot{x}^i \cdot \dot{x}^i}{E_{\rm Pl}}\right). \tag{2.7}$$

which means that the equivalence principle is broken in such a model, and tests of the equivalence principle are able to put stringent constraints on Lorentz violation [53–55]. The lack of prior geometry in general relativity causes problems when breaking Lorentz invariance explicitly, leading to conflicts with the Bianchi identities, as discussed in Section 2.1. In general, the only option for obtaining a consistent theory is to introduce constraint equations by hand, forcing adherence to the Bianchi identities.

## 2.4 Common Lorentz-Violating Models and Frameworks

### 2.4.1 Doubly General Relativity

In recent years, the Rainbow Gravity framework [56] has been given a lot of attention. [57–71]. This is a phenomenological approach based on Doubly Special Relativity (DSR), where the spacetime metric includes energy-dependent functions, and hence describes [72, 73] universes which evolve depending on the energy of the probe particle. With the correct choice of energy dependence, problems such as singularities may be avoided in Rainbow Gravity [58]. Exploring semiclassical or phenomenological theories of quantum gravity is of vital importance to understanding

the low-energy quantum gravitational regime and to reaching an understanding of the underlying fundamental framework.

The key idea of Rainbow Gravity is the modification of the spacetime metric to include energy dependent functions $f_1(E)$ and $f_2(E)$ [56], leading to a modified dispersion relation for relativistic particles of the form:

$$-E^2 f_1^2(E) + p^2 f_2^2(E) = m_0^2, \tag{2.8}$$

and position-space invariant of the form:

$$\mathrm{ds}^2 = -\frac{(\mathrm{dx}^0)^2}{f_1^2(E)} + \frac{(\mathrm{dx}^i)^2}{f_2^2(E)}. \tag{2.9}$$

where $m_0$ is the rest mass of the particle. $x^0$ and $x^i$ are the time and space coordinates, respectively. These functions are introduced by deforming the Lorentz group to include the Planck energy as a second invariant, using the formalism developed in Doubly Special Relativity (DSR) [56, 72, 73]. By introducing the dilatation $D = p_\mu(\partial/\partial p_\mu)$, which preserves rotations but modifies boosts, the boost generators are deformed as follows:

$$K^i \equiv L_0^i + l_p p^i D \Rightarrow K^i = U^{-1} L_0^i U, \tag{2.10}$$

where $l_p$ is the Planck length and $L_0^i$ are the conventional generators of the Lorentz group, $L_{\mu\nu} = p_\mu(\partial/\partial p^\nu) - p_\nu(\partial/\partial p^\mu)$ [72]. $U$ is a non-linear momentum map. $U$ in momentum space becomes:

$$U_\mu(E, p_i) = (U_0, U_i) = (E f_1, p_i f_2)\,. \tag{2.11}$$

By demanding plane-wave solutions to free field theories, $p_\mu x^\mu = p_0 x^0 + p_i x^i$, the momentum map in position space is given by:

$$U^\alpha(x) = \left(U^0, U^i\right) = \left(\frac{t}{f_1}, \frac{x^i}{f_2}\right), \tag{2.12}$$

which leads to the position space invariant (and hence the metric):

$$s^2 = \eta_{\alpha\beta}U^{\alpha}(x)U^{\beta}(x) = -\frac{t^2}{f_1^2} + \frac{(x^i)^2}{f_2^2} \Rightarrow g_{\alpha\beta}(E) = \text{diag}\left(-f_1^{-2}, f_2^{-2}, f_2^{-2}, f_2^{-2}\right), \tag{2.13}$$

where $\eta_{\alpha\beta}$ are the components of the Minkowski metric. In order to satisfy the correspondence principle, it is necessary to introduce a constraint on $f_1$ and $f_2$, namely

$$\lim_{E\to 0} f_k = 1,\ k = 1,2 \quad \Rightarrow \quad \lim_{E\to 0} g_{\mu\nu}(E) = \eta_{\mu\nu}, \tag{2.14}$$

which restores Minkowski space in the low-energy limit [56]. In DSR, invariants of the modified Lorentz group are accompanied by a singularity in the momentum map $U$ [72]. But in standard special relativity, the only energy invariant is the infinite one. Hence, to introduce a new invariant in the theory, the following relations must be fullfilled:

$$U(\tilde{E}) = \tilde{E} f_1(\tilde{E}) = \infty, \tag{2.15}$$

where $\tilde{E}$ is some new invariant energy scale. This constraint, however, is not used by all authors; phenomenologically motivated rainbow functions $f_{1,2}$ which do not fulfill the criterium (2.15) can be found in [58, 74] among others.

The new metric $g_{\mu\nu}(E)$ defines a family of flat metrics parameterised by the energy $E$. Hence probe particles see "different universes"; they measure different cosmological quantities and travel on different geodesics, but share the same set of inertial frames [56].

In order to apply DSR to cosmology it is necessary to find the Friedmann-Lemaitre-Robertson-Walker (FLRW) metric, as modified by Rainbow Gravity. Here the following system of units is implied: $dx^0 = c_0 dt$, $c_0 = 1$, where $c_0$ is the low-energy limit of the energy-dependent speed of light, $c(E) \in [1, 0]$. Now, we need to modify the FLRW metric. The resulting expression is:

$$\mathrm{ds}^2 = -\frac{\mathrm{dt}^2}{f_1^2(E)} + \frac{a^2(t)}{f_2^2(E)}\gamma_{ij}\mathrm{dx}^i\mathrm{dx}^j, \tag{2.16}$$

where $\gamma_{ij}$ represents the 3-metrics defined in Friedmann cosmology for the three different spacetime geometries ($K = 0, \pm 1$), and $a(t)$ is the scale factor. From the

metric (2.16) we find the Einstein equations:

$$G_{\mu\nu}(E) = 8\pi G(E)T_{\mu\nu}(E) + g_{\mu\nu}(E)\Lambda(E), \tag{2.17}$$

where all quantities now vary with energy. The tensorial quantities gain their energy dependence from the rainbow functions contained in the metric, whereas $G(E)$ and $\Lambda(E)$ get theirs from renormalisation group flow arguments, as outlined in [56]. It is usually assumed that $G$ and $\Lambda$ have the same energy-dependence:

$$\begin{cases} G(E) = h^2(E)G_0 \\ \Lambda(E) = h^2(E)\Lambda_0 \end{cases} \tag{2.18}$$

where the index 0 indicates the standard table value. The function $h(E)$, which we will now call the 'scaling function' is constructed in such a way that the standard constants $G_0$, $\Lambda_0$ are recovered in the limit $E \to 0$. Such form of the $h$-dependence for the gravitational and cosmological constants allows the constancy of the vacuum energy density $\rho_\Lambda = \Lambda_0/8\pi G_0$.

### 2.4.2 Hořava-Lifshitz Gravity

One of the main obstacles on the road to quantum gravity is the fact that general relativity is non-renormalisable. This is easy to see if we notice that the expansion of any quantity $\mathcal{F}$ in terms of the gravitational constant can be written as [75]:

$$\mathcal{F} = \sum_{n=0}^{\infty} a_n \left(G_N E^2\right)^n, \tag{2.19}$$

where $E$ is the energy of the system, $a_n$ is a numerical coefficient and $G_N$ is the gravitational coupling constant. From this we see that then $E^2 \geq G^{-1}$, this expansion diverges, and it is expected that general relativity loses perturbative renormalisability at such high energies.

It is possible to improve the ultraviolet behaviour of general relativity by introducing higher-order derivative terms to the Einstein-Hilbert Lagrangian. For example, we can write it as: $S = \int \mathrm{d}^4x\sqrt{-g}(R + R_{\mu\nu}R^{\mu\nu})$, which changes the graviton propagator from $1/k^2$ into $1/(k^2 - G_N k^4)$. The new term proportional to $k^{-4}$

will indeed cancel the ultraviolet divergence, but the theory is now non-unitary and equipped with a massive spin-2 ghost [75]. In fact, this ghost comes from the fact that this higher-order gravity theory has time derivatives of $\mathcal{O} > 2$. In the example above, the resulting field equations are fourth order. In order to address this problem, Hořava decided to evade the ghost by constructing a higher-order theory of gravity where only the *spatial* derivatives are of $\mathcal{O} > 2$, while keeping second-order time derivatives only [76]. This requires an explicit breaking of Lorentz invariance in the ultraviolet, but to be consistent with all current experiments, which have so far failed to detect any significant signals of Lorentz invariance violation, this symmetry has to be *restored* in the infrared limit. The way Hořava overcame this hurdle was to introduce an anisotropic scaling of space and time in the ultraviolet (also known as Lifshitz scaling). This scaling takes the form (in a 4-dimensional spacetime):

$$t \to b^{-z}t,\ x^i \to b^{-1}x^i,\ (i = 1, 2, 3), \tag{2.20}$$

where $z$ is a critical exponent. To restore Lorentz invariance we need to set $z = 1$, but to have power-counting renormalisability we need to have $z \geq 4$ [75]. The most common choice is to set $z = 3$. Thus, ultraviolet Lorentz violation lies at the core of Hořava-Lifshitz gravity and cosmology. Hořava assumed that it is broken down to $t \to \xi_0(t)$, $x^i \to \xi^i(t, x^k)$, which preserves the spatial diffeomorphisms. This theory acquires a symmetry group denoted Diff[M,$\mathcal{F}$], which is known as foliation-preserving diffeomorphisms [75, 76], where $\mathcal{F}$ is the preferred frame. This allows for arbitrary changes of the spatial coordinates on each constant time slice, and also picks out a preferred time foliation of spacetime, which breaks Lorentz invariance.

Because of the anisotropic scaling between space and time, it is convenient to introduce the ADM decomposition of the spacetime metric in a preferred foliation:

$$\mathrm{d}s^2 = -N^2\mathrm{d}t^2 + g_{ij}(\mathrm{d}x^i + N^i\mathrm{d}t)(\mathrm{d}x^j + N^j\mathrm{d}t), \tag{2.21}$$

where the dynamical variables of the theory now are the lapse function $N$, the shift vector $N^i$, and the spatial metric $g_{ij}$ $(i, j = 1, 2, 3)$. Given this, we can write down the

most general action for the theory as:

$$S = \int \mathrm{d}^3x\mathrm{d}tN\sqrt{g}\left[K^{ij}K_{ij} - \lambda K^2 - \mathcal{V}(g_{ij})\right], \tag{2.22}$$

where $g$ is the determinant of the spatial metric $g_{ij}$, $\lambda$ is a running coupling parameter (dimensionless), and $\mathcal{V}$ is a potential term. Moreover, $K_{ij}$ is the extrinsic curvature:

$$K_{ij} = \frac{1}{2N}\left(\dot{g}_{ij} - \nabla_i N_j - \nabla_j N_i\right), \tag{2.23}$$

where an overdot denotes a full derivative with respect to the time $t$. The trace of $K_{ij}$ is denoted $K$. The potential $\mathcal{V}$ depends only on the spatial metric and its spatial derivatives, and is also invariant under three-dimensional diffeomorphisms [77]. It contains *only* operators of dimension 4 and 6 which can be constructed from the spatial metric $g_{ij}$.

### 2.4.3 Einstein-Aether Theory

Another theory which breaks Lorentz invariance is Einstein-Aether theory, which is related to low-energy Hořava-Lifshitz gravity [78–80]. In this model Lorentz invariance is broken by a timelike unit vector field called the *aether* (or khronon). Since we are interested in studying Lorentz violation the aether field arises as a natural way to ensure that this theory lacks a Lorentz-invariant phase completely, and by introducing the aether field, a preferred frame is always present. The current formulation of Einstein-Aether theory as a low energy effective field theory passes all observational tests when choosing the parameters of the theory appropriately [78, 80–88]. The only discrepancy lies in the two Parametrised post-Newtonian PPN parameters which relate to preferred-frame effects.

The most general action of the theory can be written as:

$$S = \frac{1}{16\pi G_{\mathrm{ae}}}\int d^4x\sqrt{-g}\left(R + K^{\alpha\beta}K_{\mu\nu}\nabla_\alpha u^\mu \nabla_\beta u^\nu + \lambda(u^\alpha u_\alpha - 1)\right), \tag{2.24}$$

where

$$K^{\alpha\beta}_{\mu\nu} = c_1 g^{\alpha\beta}g_{\mu\nu} + c_2\delta^\alpha_\mu\delta^\beta_\nu + c_3\delta^\alpha_\nu\delta^\beta_\mu + c_4 u^\alpha u^\beta g_{\mu\nu}. \tag{2.25}$$

In the above expressions, $R$ is the Ricci scalar, $\lambda$ is a Lagrange multiplier ensuring that $u^\alpha$ is always timelike, and $c_i$ are dimensionless constants. Moreover, as is a general feature of Lorentz-violating field theories, the gravitational coupling constant $G_{\text{ae}}$ differs from the Newtonian one through $G_N/G_{\text{ae}} = 1 - (c_1 + c_4)/2$.

By varying the action (2.24) with respect to the aether field and the metric, respectively, leads to the following field equations:

$$\lambda u_\mu = \nabla_\alpha \left( K^{\alpha\beta}_{\mu\nu} \nabla_\beta u\nu \right) - c_4 \dot{u}_\alpha \nabla_\mu u^\alpha \tag{2.26}$$

$$G_{\alpha\beta} = T^{\text{ae}}_{\alpha\beta} + 8\pi G_{\text{ae}} T^{\text{m}}_{\alpha\beta}, \tag{2.27}$$

where $G_{\alpha\beta}$ is the Einstein tensor, $T^{\text{ae}}_{\alpha\beta}$, and we have added a matter Lagrangian. In a cosmological setting with FLRW geometry, the aether field $u^\alpha$ coincides with the 4-velocity of a comoving observer and is thus completely determined by the geometry and lies on-shell. Therefore we can write the stress-energy tensor for the aether as a combination of covariantly conserved tensors derived from FLRW geometry. The exact form reads [88–91]:

$$T^{\text{ae}}_{\alpha\beta} = -\frac{1}{2}(c_1 + 3c_2 + c_3) \left[ G_{\alpha\beta} - \frac{1}{6} R (g_{\alpha\beta} + 2u_\alpha u_\beta) \right], \tag{2.28}$$

and the effect of adding the aether is to renormalise the gravitational constant and add a perfect fluid which renormalising the contribution of the spatial curvature [88, 89]. Thus we can expect to find traces of the aether in the expansion history of the Universe along with possible imprints on the Hubble parameter tension [28, 88].

### 2.4.4 Bumblebee Gravity

One of the simplest models for studying spontaneous Lorentz violation in gravity is called *bumblebee gravity*. In this model Lorentz symmetry is broken when an axial vector field $B_\mu$ takes on a non-zero vacuum expectation value. Bumblebee gravity is of particular interest since it features rotation, boost, and CPT violation whilst still having relatively simple field equations [12]. The bumblebee field comes with an associated 2-tensor field strength usually defined as $B_{\mu\nu} \equiv \partial_\mu B_\nu - \partial_\nu B_\mu$, which bears close resemblance to the electromagnetic field strength tensor $F_{\mu\nu}$. In fact, it was

found in [92, 93] that by linearising the bumblebee model on a flat background a type of "pseudo-Maxwell" theory with a bumblebee photon can be found. A detailed discussion and observational constraints on these features can be found in [92].

Several interesting features of bumblebee gravity have been pointed out in the literature. For example, it was pointed out in [94] that the model possesses consistent vacuum solutions, and that the nature of the preferred frame influenced the nature of these solutions. Moreover, it was shown in [95] that the theory has an exact Schwarzchild solution, and provided bounds on Lorentz violation from a series of solar-system gravitational tests. It was also shown that for certain parameter values, bumblebee gravity can also be applied to cosmology and has Gödel solutions [96].

The action for a non-minimal pure-gravity bumblebee model can be written as [95]:

$$S_B = \int d^4x\sqrt{-g}\frac{1}{16\pi G}\left[R + \xi B^\mu B^\nu R_{\mu\nu} - \frac{1}{4}B_{\mu\nu}B^{\mu\nu} - V\right], \tag{2.29}$$

where $R_{\mu\nu}$ is the Ricci tensor, $\xi$ is a real coupling constant with mass dimension 1, and $V = V(B^\mu B_\mu \pm b^2)$ is the potential driving the formation of a non-zero vacuum expectation value $\langle B^\mu \rangle = b^\mu$, breaking Lorentz symmetry. We arrive at the equation of motion for the bumblebee field as $\nabla^\mu B_{\mu\nu} = 2V' B_\nu - \xi B^\mu R_{\mu\nu}/8\pi G$, and the Einstein equations resulting from the action (2.29) read:

$$G_{\mu\nu} = R_{\mu\nu} - \frac{1}{2}g_{\mu\nu}R = 8\pi T^B_{\mu\nu}, \tag{2.30}$$

where the stress-energy tensor for the bumblebee field is

$$\begin{aligned} T^B_{\mu\nu} \;=\; & -B_{\mu\alpha}B^\alpha_{\ \nu} - \frac{1}{4}B_{\alpha\beta}B^{\alpha\beta}g_{\mu\nu} - Vg_{\mu\nu} + 2V'B_\mu B_\nu \\ & + \frac{\xi}{\kappa}\left[\frac{1}{2}B^\alpha B^\beta R_{\alpha\beta}g_{\mu\nu} - B_\mu B^\alpha R_{\alpha\nu} - B_\nu B^\alpha R_{\alpha\mu}\right. \\ & + \frac{1}{2}\nabla_\alpha\nabla_\mu\left(B^\alpha B_\nu\right) + \frac{1}{2}\nabla_\alpha\nabla_\nu\left(B^\alpha B_\mu\right) \\ & \left. - \frac{1}{2}\nabla^2\left(B_\mu B_\nu\right) - \frac{1}{2}g_{\mu\nu}\nabla_\alpha\nabla_\beta\left(B^\alpha B^\beta\right)\right], \end{aligned} \tag{2.31}$$

which is covariantly conserved since the vacuum expectation value of the bumblebee field is generated dynamically.

The potential $V$ has so far been kept arbitrary, but may simply be chosen as $V(x) = \lambda x^2/2$ or $V(x) = \lambda x$ (Lagrange-multiplier potential). The second case is actually equivalent to non-linear gauge electrodynamics as explored in [97]. Moreover, different subcases of the bumblebee gravity model have been studied in for example [80, 91, 98–102].

### 2.4.5 The Standard-Model Extension

The framework called the Standard-Model Extension has become the de-facto standard for putting constraints on Lorentz violation. It is an effective field theory which encompasses all the sectors of the Standard Model and General Relativity, as well as all possible Lorentz-violating terms up to arbitrary order in the operators [12, 103, 104]. The terms breaking Lorentz invariance are constructed by combining Lorentz-violating operators with coefficients carrying Lorentz indices, called *coefficients of Lorentz violation*, which are subsequently constrained through experiment. Each term respects observer symmetry while breaking particle invariance with respect to diffeomorphism symmetry and local Lorentz symmetry. A significant advantage of the Standard-Model Extension is that, being a complete effective field theory, it also offers great predictive power and allows us to predict which experiments will provide the best constraints. As such, it also provides a good way to catalogue results and compare models, as well as a solid theory for theoretical studies of Lorentz violation. Using the vierbein formalism, the pure-gravity action can be written as [12]:

$$S_{\text{gravity}} = \frac{1}{16\pi G}\int d^4x \underbrace{(eR - 2e\Lambda + \ldots)}_{\mathcal{L}^{\text{LI}}} + \underbrace{\left(e\,(k_T)^{\lambda\mu\nu}\,T_{\lambda\mu\nu} + \ldots\right)}_{\mathcal{L}^{\text{LV}}}, \tag{2.32}$$

where $e$ is the vierbein, $\Lambda$ is the cosmological constant, and $T_{\lambda\mu\nu}$ is the torsion tensor. $\mathcal{L}^{\text{LI}}$ and $\mathcal{L}^{\text{LV}}$ stand for the Lorentz invariant and Lorentz-violating Lagrangian density, respectively. Since this framework in principle contains an infinite number of operators suppressed by increasing inverse powers of the Planck energy, it is common to restrict attention to the so-called minimal Standard-Model Extension. The operators in this subset are of mass dimension 4 or less and characterise leading-order Lorentz-violating effects. Working in the Riemannian limit only one term in

(2.32) survives, which reads [12]: $(k_R)^{\kappa\lambda\mu\nu} R_{\kappa\lambda\mu\nu}$, proportional to the Riemann tensor. After a Ricci decomposition of this term and noticing that the coefficient tensors can be taken to be traceless, the gravitational action can then be written as:

$$S_{\text{gravity}} = \frac{1}{16\pi G} \int d^4x \sqrt{-g} \left[ (1-u)R - 2\Lambda + s^{\mu\nu} R^{(T)}_{\mu\nu} + t_{\mu\nu\alpha\beta} W^{\mu\nu\alpha\beta} \right], \tag{2.33}$$

where $R^{(T)}_{\mu\nu}$ is the trace-free Ricci tensor and $W^{\mu\nu\alpha\beta}$ is the Weyl tensor. $u$, $s^{\mu\nu}$, and $t^{\mu\nu\alpha\beta}$ are the coefficients of Lorentz violation in the minimal gravitational sector. As discussed in Section 2.1 it is in general necessary for the coefficients for Lorentz violation in the gravity sector to be dynamical. This formulation is especially useful since it distinguishes between effects proportional to the Weyl, Ricci, and scalar curvatures. The SME coefficients may be either CPT odd or even; in general, a CPT even coefficient will have an even number of spacetime indices and vice versa. Thus, the minimal Standard-Model Extension gravitational sector is CPT even. Note that this does not preclude CPT violation from other sources, such as cosmological loss of unitarity discussed in Section 2.2.

Many limits have been set on gravitational sector coefficients, primarily from solar-system tests and weak-field tests, which generally use the linearised limit ($g_{\mu\nu} = \eta_{\mu\nu} + h_{\mu\nu}$) of the Standard-Model Extension, for example gravimeters [105, 106], spin precession [107], gravitational waves [108], solar-system tests [109, 110], Weak Equivalence Principle [109, 111–114], pulsar timing [54, 115], and very-long baseline interferometry [116]. (For a full list of all constraints in all sectors see the "Data Tables" [117]); however, work in the full theory has been limited to date [29, 118, 119].

# 3

# Modified Dispersion Relations in Gravity; Doubly General Relativity

It is expected that any theory which aspires to bridge quantum theory and gravity will need to include the Planck length $\ell_P = \sqrt{\hbar G/c^3}$, where $\hbar$ is the reduced Planck constant, $G$ is Newton's gravitational constant, and $c$ is the speed of light. This characteristic length is derived by dimensional considerations of the constants which should appear in a regime where quantum theory, relativity, and gravity all are significant. It is expected that the Planck length is the minimum length which one can measure in a meaningful way. Associated with the Planck length is the Planck energy $E_{Pl} = \sqrt{\hbar c^5/G}$, which is simply the energy of a photon with de Broglie wavelength $\ell_P$. The concept of a minimum length lies at the heart of approaches to quantum gravity such as string theory and loop quantum gravity, and has inspired a lot of theoretical work [74, 120–124]. The idea of spacetime foam was put forth in [23] and has inspired research since then. According to this idea, quantum effects make spacetime nontrivial at small scales (the Planck scale), where particle-antiparticle pairs are continuously created and annihilated, curving spacetime at extremely small length- and time scales. This "chaotic" picture inspired the term "spacetime foam", or "quantum foam".

For some time the main approach to non-trivial spacetimes and Planck-scale effects has been Lorentz violation scenarios, which have been widely studied both theoretically and observationally. In this approach, Lorentz invariance is assumed to be broken at high energies, which introduces high-energy corrections to, for example, the dispersion relations of high-energy particles of cosmological origin.

It has been recently reported in [125] that the Rainbow framework is suitable for exploring scenarios with broken Lorentz symmetry [14, 103, 126–131]. In the light of this, we present the following analysis which will be concentrated on the determination of the Lorentz violation energy scale for relativistic particles by the observational data from cosmology.

This Chapter is organised as follows. In Section 3.1 we describe the modified homogeneous Friedmann universe in the Rainbow Gravity formalism. The formalism of Rainbow Gravity was outlined in Chapter 2.4.1. In Section 3.2 we interpret our results and present some concluding remarks. Unless explicitly stated, $c = \hbar = 1$,

Greek indices $\mu, \nu = 0, 1, 2, 3$, Roman indices $i, j, k = 1, 2, 3$, and the metric signature is $(-, +, +, +)$.

## 3.1 Lorentz Invariance Violation in Rainbow Gravity

### 3.1.1 Lorentz Invariance Violation

Motivated by the notion of quantum foam coined by Wheeler [23], it has been suggested in theories of quantum gravity that Lorentz symmetry breaks down at high energies and short timescales [74, 103]. A common approach when studying these effects from a phenomenological point of view is to assume an effective modified dispersion relation, manifesting itself at high energies [14, 131, 132]. In relation to that we consider a modified dispersion relation which for massless particles (whom we study from now on) takes the form:

$$p^2 = E^2 \;\rightarrow\; p^2 = E^2 \left[1 + f(E)\right], \tag{3.1}$$

A modified dispersion relation such as the one in Eq. (3.1) would lead to highly energetic particles travelling slower or faster (depending on the quantum gravitational model) than their low-energy counterparts. For studies on Lorentz violation and possible observational tests, see [18, 52, 103, 132–137].

In the framework of Lorentz Violation, it is often assumed that $f(E)$ in Eq. (3.1) can be expressed in a series expansion at low energies ($E \ll E_c$) [74, 131, 138]:

$$f(E) = \chi_1 \left(\frac{E}{E_c}\right)^1 + \chi_2 \left(\frac{E}{E_c}\right)^2 + \mathcal{O}\left(\frac{E^3}{E_c^3}\right), \tag{3.2}$$

where $E_c$ is the energy scale at which Lorentz violating effects become strong, and the couplings $\chi_n = \pm 1$ ($n = 1, 2$) are determined by the dynamical framework being studied. It is also assumed that the effects of Lorentz violation enter in either a linear or a quadratic term, and thus the low-energy approximation of $f(E)$ can be written as [131]:

$$f(E) \approx \chi_n \left(\frac{E}{E_c}\right)^n. \tag{3.3}$$

The modified dispersion relation in the present scenario then reads as:

$$p^2 \approx E^2 \left[1 + \chi_n \left(\frac{E}{E_c}\right)^n\right], \tag{3.4}$$

which leads to a speed of light (or any other massless particle) [131]:

$$c(E) = \frac{\partial E}{\partial p} \approx 1 - \chi_n \left(\frac{E}{E_c}\right)^n, \quad E \ll E_c, \tag{3.5}$$

which changes its value as in VSL theories [139–142]. In quantum foam scenarios, the non-trivial features of spacetime at the Planck-scale are expected to slow particle propagation, and hence we will take $\chi_n = 1$ from now on.

It is now important to make the connection between this framework and Rainbow Gravity. In the latter, the invariant energy scale is the Planck scale. This is the energy scale which all observers agree on, and hence we identify $E_c = E_{Pl}$. Secondly, what we are ultimately interested in is the minimum energy which is needed for a massless particle to be subject to Lorentz violating effects. Hence, we will build a cosmological model in this framework and constrain the energy $E$ against data. Since no compelling evidence for Lorentz violation has yet been presented, the energy scale for Lorentz violation, $E_{LV}$, must be larger than the energy $E$. Hence, the only constraints we will be able to obtain will be lower limits.

### 3.1.2 Simple Lorentz Invariance Violating Cosmological Framework

It was recently reported in [125] that the Rainbow formalism is suitable for describing Lorentz Violating scenarios [14, 103, 126–131]. It was shown that even though the Poisson bracket between the deformed boost and the flat-space limit Hamiltonian vanishes, $\{\mathcal{N}, \mathcal{H}\} = 0$, the Rainbow line element (2.13) is not invariant under the same boost. The authors of [125] remark that this makes vector norms non-invariant and makes it impossible to define local invariant observers, which makes it necessary to break Lorentz invariance [125]. In the light of this, we present below a concatenation of Lorentz violation phenomenology and the Rainbow formalism, and we show that it is possible to combine the two in a consistent and logical way.

It is now possible to write down the Friedmann equation as follows [56]:

$$\left(\frac{\dot{a}}{a}\right)^2 = \frac{8\pi G(E)\rho}{3f_1^2(E)} - \frac{K}{a^2}\left[\frac{f_2(E)}{f_1(E)}\right]^2 + \frac{\Lambda(E)}{3f_1^2(E)}, \tag{3.6}$$

and the acceleration equation becomes:

$$\frac{\ddot{a}}{a} = -\frac{4\pi G(E)(3p+\rho)}{3f_1^2(E)} + \frac{\Lambda(E)}{3f_1^2(E)}. \tag{3.7}$$

Combining Eq. (3.6) and Eq. (3.7) yields the conservation equation, which is *independent* of the rainbow functions:

$$\dot{\rho} = 3\frac{\dot{a}}{a}(\rho + p). \tag{3.8}$$

The fact that the conservation equation does not include extra energy dependence from the rainbow functions is a clear advantage of this framework, since it implies that there is no dissipation of energy. Comparing the Lorentz Violation and Rainbow dispersion relations (3.1) and (2.8) and matching coefficients, it is possible to identify the following:

$$f_1(E) = \sqrt{1 + \left(\frac{E}{E_{Pl}}\right)^n}, \quad f_2(E) = 1 \tag{3.9}$$

From the dispersion relation (3.1) and the correspondence principle it is possible to extract that $\lim_E \to 0, f(E) = 0$, which means that the map $U$ satisfies Eq. (2.15).

In order to calculate any useful cosmological quantities, it is neccessary to define $h(E)$. There are several suggestions in the literature, and the following two will be investigated. One suggestion comes from the field of *varying constants cosmology*, where the running of physical constants is used to solve cosmological issues such as singularities. In analogy with [143], we suggest here that the evolution takes the following novel form:

$$G(E) = \left(1 - \frac{E}{E_{Pl}}\right)^{-1} G_0. \tag{3.10}$$

Comparing (2.18) and (3.10), $h(E)$ is found to be (we will denote the first case $h_-$):

$$h_-(E) = \left(1 - \frac{E}{E_{Pl}}\right)^{-1/2}. \tag{3.11}$$

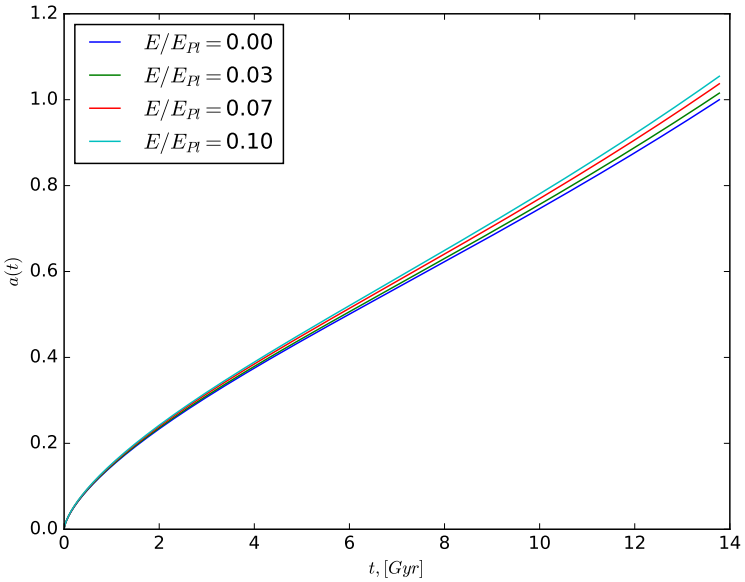


FIGURE 3.1: The modified Friedmann scale factor for rainbow function 3.11 with $n = 2$ for probe particles of different energies.

Another suggestion for the form of $h(E)$ can be found in [64], and in analogy with this we suggest the following:

$$h_+(E) = \sqrt{1 + \left(\frac{E}{E_{Pl}}\right)^4}. \tag{3.12}$$

Choosing to look at a matter dominated universe with cosmological constant, $\rho = \rho_m$ and $\Lambda \neq 0$, the following solution to Eq. (3.6) is found:

$$a(t) = a_0 \left(\frac{\Omega_m}{\Omega_\Lambda}\right)^{1/3} \left[\sinh \frac{3}{2}\sqrt{\Omega_\Lambda}\frac{h_\pm(E)}{f_1(E)}H_0 t\right]^{2/3}, \tag{3.13}$$

where $a_0$ is the present day value of the scale factor. It is easy to see that (3.13) takes the standard form when $E \to 0$, so $h_\pm(E) \to 0$, which satisfies the correspondence principle.

As an example, we show here the case of $h_-(E) = (1 - E/E_{Pl})^{-1/2}$. Using the rainbow function (3.11) in (3.13), with $n = 2$, which in Lorentz violating scenarios is referred to as *quadratic* Lorentz violation, the following result is obtained: In Figure 3.1, the scale factors for the different probe energies clearly separate after $2 - 3$

Gyr, and the *rainbow* in Rainbow Gravity can be clearly seen. Linear Lorentz violation, $n = 1$ produces results which are difficult to distinguish when plotted. This is rather counterintuitive, as one would expect the less suppressed case ($n = 1$) to be more important phenomenologically. The explanation to this lies in the function $h_-(E)$ which contains a minus sign in the denominator. Because of this the ratio $h_-/f_1$ contains terms such as

$$1 - \epsilon + \epsilon - \epsilon^2 = 1 - \epsilon^2$$

in the case for $n = 1$. (Here, $\epsilon = E/E_{Pl}$). The minus sign in $h_-$ causes this cancellation. For $n = 2$, the corresponding term is $1 - \epsilon$, when $\epsilon \ll 1$. Hence $h_-/f_1$, and more importantly, its derivative, will always be smaller for $n = 1$ than $n = 2$. This accounts for the somewhat surprising behavior of Figure 1.

In the more general case, when all the contributions to the energy density are taken into account, the Friedmann equation takes the following form:

$$\left(\frac{\dot{a}}{a}\right)^2 = \frac{8\pi G_0}{3}\frac{h_\pm^2(E)}{f_1^2(E)}\rho_c\left[\Omega_m\left(\frac{a_0}{a}\right)^3 + \Omega_{\rm rad}\left(\frac{a_0}{a}\right)^4 + \Omega_\Lambda + \Omega_k\left(\frac{a_0}{a}\right)^2\frac{1}{h_\pm^2(E)}\right], \tag{3.14}$$

where

$$\Omega_{\{m,{\rm rad},\Lambda,k\}} = \frac{\rho}{\rho_c} = \frac{8\pi G}{3H_0^2}\rho_{\{m,{\rm rad},\Lambda,k\}}, \tag{3.15}$$

are the energy density parameters (for matter, radiation, dark energy, and curvature) as measured today and $\rho_c$ is the conventional critical energy density, $\rho_c = 3H_0^2/8\pi G$. The extra factor on $\Omega_k$ comes from the definition of the curvature energy contribution:

$$\frac{h_\pm^2(E)}{f_1^2(E)}\frac{8\pi G}{3}\rho_k = -\frac{K}{a^2 f_1^2(E)} \tag{3.16}$$

### 3.1.3 Two specific choices of the scaling function $h_\pm(E)$

The analysis described above was carried out for the two choices of the function $h_\pm(E)$ in Eq. (3.11) and Eq. (3.12) and limits on $E$ were derived for both linear and quadratic Lorentz violation ($n = 1, 2$). The results are stated in Table 3.1. In order to obtain these results, we employed an MCMC method, in which we ran three chains of $10^5$ steps each, to obtain bounds on the energy $E$. These results are interpreted as

| | |
|---|---|
| $h_-(E) = \sqrt{1 - \frac{E}{E_{Pl}}}$ | $n = 1 : 0.0033\ (1\sigma), 0.0076\ (2\sigma), 0.0121\ (3\sigma)$<br>$n = 2 : 0.0067\ (1\sigma), 0.0152\ (2\sigma), 0.0243\ (3\sigma)$ |
| $h_+(E) = \sqrt{1 + \left(\frac{E}{E_{Pl}}\right)^4}$ | $n = 1 : 0.0068\ (1\sigma), 0.0154\ (2\sigma), 0.0262\ (3\sigma)$ |

TABLE 3.1: $1, 2$, and $3\sigma$ constraints on the ratio $(E/E_{Pl})$ for linear and quadratic Lorentz violation ($n = 1, 2$) for the scaling function $h_-(E)$. For $h_+(E)$, only the case $n = 1$ is included.

follows; when constraining the energy $E$, we have looked for the values of $E$ which fit to our current understanding of the Universe, through the data available. Since Lorentz violating effects have not yet been observed, the energy scale $E_{LV}$ must lie *outside* of the likely range for $E$. As such, we obtain lower limits on $E_{LV}$. The limits placed correspond to the Grand Unified Theory (GUT) energy scale $E_{LV} \sim 10^{16}$ GeV at the $1\sigma$ limit and are even higher reaching $E_{LV} \sim 10^{17}$ GeV at $3\sigma$ limit.

In Table 3.1 the case of $h_+(E)$ and $n = 2$ is not included. Due to some artefact in the parametrisation this case contains *both* upper and lower limits on the energy scale $E$. We have discarded this case as it suggests we now live in a Lorentz violating era. Hence we deem it unphysical and do not consider it further.

At this stage it is very important to note that this is not the "energy of spacetime", but rather the energy scale of a probe particle travelling through spacetime and feeling a metric determined by its energy. This statement takes a central role in [56], where it is used to derive several modified cosmological quantities. In this chapter, we interpret the limits obtained as decoupling limits, at which Lorentz violating effects become statistically significant. This is even clearer for the three models were we only obtained upper limits. This may be interpreted as a kind of arrival probability, and drops monotonically with energy. In analogy with the GZK cutoff, for example, we find this behavior reasonable.

### 3.1.4 Comparison with the ΛCDM model

In our model, the decoupling energy scale from Lorentz violating effects leaves an imprint on the equations of cosmological evolution. As expected, this results in a different cosmological evolution compared to that of the ΛCDM. In order to quantify

this difference, we notice that it is possible to write Eq. (3.6) in the following form:

$$\left(\frac{\dot{a}}{a}\right)^2 = \frac{8\pi G_0}{3}\rho_c \left[\Omega'_m \left(\frac{a_0}{a}\right)^3 + \Omega'_{rad}\left(\frac{a_0}{a}\right)^4 + \Omega'_\Lambda + \Omega'_k \left(\frac{a_0}{a}\right)^2\right], \tag{3.17}$$

i.e. the standard form of the Friedmann equation. Here, the primed quantities are defined as:

$$\Omega'_m = \frac{h_\pm^2(E)}{f_1^2(E)}\Omega_m, \quad \Omega'_\Lambda = \frac{h_\pm^2(E)}{f_1^2(E)}\Omega_\Lambda, \quad \Omega'_k = \frac{1}{f_1^2(E)}\Omega_k, \quad \Omega'_{rad} = \frac{h_\pm^2(E)}{f_1^2(E)}\Omega_{rad}. \tag{3.18}$$

Besides, it is easy to notice from (3.18) that

$$\frac{\Omega'_m}{\Omega_m} = \frac{\Omega'_\Lambda}{\Omega_\Lambda} = \frac{\Omega'_{rad}}{\Omega_{rad}}, \tag{3.19}$$

and also that

$$\Omega_m + \Omega_{rad} + \Omega_k + \Omega_\Lambda = \frac{h_\pm^2}{f_1^2}; \quad \Omega'_m + \Omega'_{rad} + \Omega'_k + \Omega'_\Lambda = 1. \tag{3.20}$$

As our analysis has provided bounds and estimates on the energy scale $E_{LV}$ as well as the energy densities $\Omega_X$, it is now a simple task to compare the primed and unprimed quantities. We present here the results for the model $h_-(E) = \sqrt{1 - E/E_{Pl}}$ with $n = 1$. In Figure 3.2 one sees the histograms for the matter and dark energy densities, both primed and unprimed. From Figure 3.2 we can see that when rearranged to the standard Friedmann form, the primed quantities diminish in comparison to the unprimed ones. This was to be expected, as the ratio $h_\pm^2(E)/f_1^2(E)$ is consistently less than unity (in this model). As such, the imprint of the rainbow and scaling function on cosmological evolution can be thought of as mimicking dark energy in the sense that there is a weaker repulsion ($\Omega'_\Lambda < \Omega_\Lambda$) accompanying weaker attraction ($\Omega'_m < \Omega_m$) giving a net effect of a stronger global repulsion (acceleration). It is important to note that because of how the numerical analysis was carried out, the normalisation of primed and unprimed quantities are different.

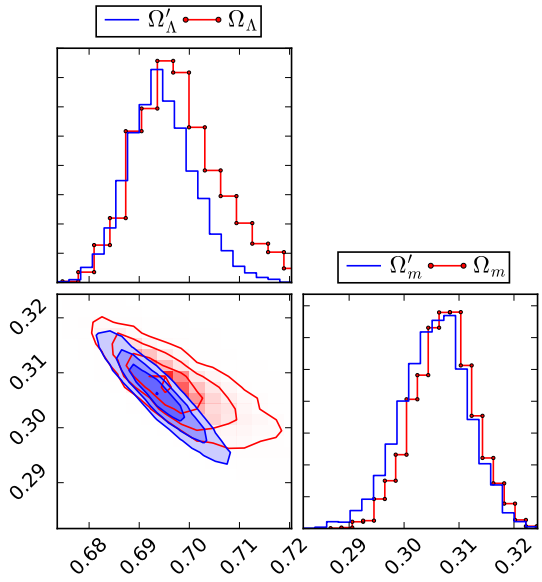


FIGURE 3.2: One and two dimensional projections of the posterior probability distributions for linear Lorentz violation ($n = 1$) and $h_-(E) = \sqrt{1 - E/E_{Pl}}$. $\Omega_m$ and $\Omega_\Lambda$ (without primes) correspond to the energy densities in Eq. (3.6), whereas $\Omega'_m$ and $\Omega'_\Lambda$ (with primes) are the rescaled quantities in Eq. (3.17). The histograms show the one dimensional marginalised distributions for the parameters independently, and the scatter plot shows the two dimensional parameter space.

## 3.2 Discussion and Conclusions

In this chapter we have studied Lorentz symmetry violating scenarios which are predicted in the high-energy regime of some theories of quantum gravity. We have shown that it is possible to realise such scenarios within the framework of Rainbow Gravity due to modification of the dispersion relation by introducing new functions of particle energy $f_1(E)$ and $f_2(E)$. We have studied such a theory in the cosmological context assuming additionally the energy-dependence of the gravitational constant $G(E)$ and the cosmological constant $\Lambda(E)$ which change according to the scaling function $h_\pm(E)$.

We have shown that it is possible to consistently express the low-energy limit of Lorentz violating theories within the framework of Gravity's Rainbow, when only one of the rainbow functions is non-trivial. We have proven that the Rainbow function $f_1(E)$ and the scaling functions $h_\pm(E)$ influence the evolution of the cosmological scale factor in the Friedmann equation. Our main point was to carry

out an Markov-Chain Monte Carlo analysis in order to compare our theory with observational data such as: Hubble + Supernovae Type Ia + Baryon Acoustic Oscillations (Baryon Oscillation Spectroscopic Survey+Lyman $\alpha$) + Cosmic Microwave Background. Due to this we were able to constrain model parameters and in particular the energy scale $E_{LV}$ to be of the order of $10^{16}$ GeV at $1\sigma$ which is a Grand Unified Theory (GUT) energy scale up to $10^{17}$ GeV at $3\sigma$.

We suggest the interpretation of this energy as a Lorentz invariance decoupling scale since it is much higher than any observed particle energy. Just as the decoupling of the Cosmic Microwave Background in the early universe occurs at the recombination energy, the energy $E_{LV}$ may be interpreted as a decoupling energy from spacetime Lorentz violating effects. In the quantum foam picture, this occurs when the energy of a massless particle is too low to interact with the nontrivial spacetime, statistically. It may still happen through other mechanisms [136] and there are some possible observational signals of this (see for example [18]).

We argue that the energy $E_{LV}$ should be viewed as the energy at which massless particles are decoupled from nontrivial background effects. This cutoff energy is generally assumed to be around the Planck energy, which this study indeed verifies. Moreover, the nontrivial structure of the quantum foam is expected to implicitly break Lorentz invariance, which can be modelled phenomenologically with a modified dispersion relation. This also fits well with our notion of $E_{LV}$, and as our assumptions on the structure of the function $f(E)$ stems from low-energy quantum gravity, our framework may be used for general quantum gravity phenomenology. The value of $E_{LV}$ also serves as the energy scale at whcih CPT symmetry might be broken, and due to the sign of the cosmological constant in this model one might expect cosmological CPT violation, albeit at a different time because of the altered cosmological behaviour. It may be noted that our results are in agreement with some of the limits obtained in [144]. It is also worth noting the behavior of Lorentz invariance hinted at in this chapter is not a new idea; the notion of Lorentz symmetry being an *emergent* symmetry is a key ingredient of Hořava Gravity [145], for example.

Several previous papers have investigated various aspects of the phenomenology of Rainbow Gravity (see for example [146–149]). As a much expected consequence of quantum gravity the effects of Lorentz Violation should also be investigated. Probing the behavior of symmetries at high energies is important in order to understand the limits of the current theories and to gain insight into what may lie beyond. Lorentz symmetry is one of those symmetries. However, as a fundamental ingredient of modern physics, it deserves thorough scrutiny.

# 4

# Ultraviolet Lorentz violation; Hořava-Lifshitz Cosmology

## 4.1 Introduction

One of many challenging problems in modern theoretical physics is how to merge quantum field theory with general relativity. Attempts at formulating a quantum theory for gravitation have been made for many decades, but there is still no theory which clearly stands out from its competitors. One of the main obstacles one encounters when trying to quantise general relativity using standard techniques is that it is not a perturbatively renormalisable theory. This is indeed a serious problem as general relativity breaks down at small scales, and alternative formulations for a quantum theory of gravity have been developed in order to deal with this issue. For example, string theory and loop quantum gravity have been developed for this reason, and although these theories resolve some problems (such as singularities) there are few phenomenological channels through which to test these theories [150, 151]. Although no theory of quantum gravity is known it is possible to predict some of its features. For example, it is likely to contain the three constants $c$ (speed of light, relativity), $G$ (gravitational constant, gravitation), and $\hbar$ (Planck's constant, quantum mechanics). Using these constants, we can construct a characteristic energy scale for quantum gravity as $E_{Pl} = \sqrt{\hbar c^5/G}$. This is to be interpreted at the "frontier" beyond which we can expect quantum gravity effects to manifest themselves. If this is indeed the case, we can only expect to find quantum gravity effects in regions with very high energy, strong gravity, and high velocities. The phenomenological avenues to probe these regions are sparse, and do not in general allow themselves to be recreated in the laboratory, so we are forced to rely on astrophysical observations. One possibility is that of TeV particle astrophysics, as observed with the next generation of telescopes. There are several scenarios in which quantum gravity effects could affect the opacity of the Universe to such high-energy particles [127, 136]. These effects would multiply with the distance, and could in principle be detectable with (for example) the CTA [18].

An area of observation which has recently opened up a new window to the Universe is that of *gravitational wave astronomy*. Recently, LIGO found evidence of a binary black hole merger [152], which was consistent with the prediction from general relativity for such events. Moreover, LIGO and VIRGO have also observed a binary

neutron star merger [153] which was accompanied by a short $\gamma$-ray burst picked up by the FERMI and INTEGRAL $\gamma$-ray telescopes [154]. This put strong constraints on the speed of tensorial gravitational waves, as the difference $\Delta t$ from the speed of light $c$ was found to be $-3 \cdot 10^{-15} < \Delta t/c < 7 \cdot 10^{-16}$ [108]. As opposed to general relativity, which permits only tensor metric perturbations, many alternative models of gravity have more degrees of freedom. For example, scalar-tensor theories such as Brans-Dicke theory permits a transverse-scalar mode, and Hořava-Lifshitz gravity allows both vector and tensor modes [155, 156]. This has also been discussed in the context of Lorentz-violating theories, for example in [157] (Hořava gravity) and in [158] (Einstein-Æther theory). In general, gravitational wave data places strong constraints on the coupling constants of the theories, as well as the speed of the tensor mode. Moreover, these observations also place constraints on the Lorentz breaking scale (often denoted $M_*$) in Hořava gravity [157].

Recently, the LIGO and VIRGO team reported the first ever direct limits of the strain of scalar and vector modes at $< 1.5 \cdot 10^{-26}$ at 95% [159, 160]. Prior to this, the magnitude of scalar modes were completely unconstrained, and this new discovery can place tight bounds on alternative theories of gravity, such as Hořava-Lifshitz. This new field of multimessenger astronomy has the potential to teach us more about strong gravity events and will be some of the most important ways of probing new physics in the future.

The fact that general relativity has been tested and found consistent with virtually all observations tells us that it is a very good model for the IR behaviour of quantum gravity. Thus, any candidate quantum gravity model proposed must have general relativity as its low energy limit. It therefore makes sense to look at proposals for UV-completions of general relativity, for example [161, 162]. In general these include a cutoff energy scale beyond which general relativity breaks down. If this energy scale is low enough (in the TeV range) there may be a lot of accessible phenomenology in these models. Another interesting proposal in this category is Hořava gravity, which is a concrete proposal of a UV complete theory of gravity, and possibly of quantum gravity [76, 163]. It is also referred to as Hořava-Lifshitz (HL) gravity since if contains a fixed point in the UV with an anisotropic Lifshitz scaling between space and time, explicity breaking Lorentz invariance in the UV.

A lot of work has gone into this model, including studies on cosmological solutions [164–166, 173, 181, 210, 211], dark radiation and braneworlds [166, 167], strong coupling [179], and the resolution of the initial singularity [168–170]. Several papers have placed bounds on different regions of the Hořava-Lifshitz framework, for example using cosmological data [171], binary pulsars [81, 82], and in the context of dark energy [172]. This has also been done [173] in the effective field theory formalism of the the extended version of Hořava theory [77]. Other authors have placed bounds on more general Lorentz violation in the context of dark matter and dark energy, for example [174, 175].

The breaking of Lorentz invariance mentioned above may seem counterintuitive, as it is one of the fundamental principles of modern physics and is strongly supported by experiment. In fact, every single experiment so fas been consistent with Lorentz invariance [14, 117]. This means that breaking Lorentz symmetry has to be done with great care. However, there is *no a priori reason* to expect that a theory of quantum gravity should uphold Lorentz invariance, as according to our understanding, spacetime takes on a quantum nature in the Planck regime, and as we have mentioned before, continuous classical spacetime emerges as a low energy limit of this quantum theory. Then, as Lorentz symmetry is a *continuous symmetry* of nature, it bears to reason that it might not exist at all in the quantum regime, but rather emerge as an IR symmetry of nature. Once Lorentz symmetry is no longer a concern, one may include higher-order derivatives in the Lagrangian in order to cure divergencies in the UV [75].

There is an open discussion about instabilities and pathologies in different formulations of HL-type theories (see e.g. [77, 176, 177] or a recent review [75]). The original HL theory suffers from many inconsistencies and shortcomings, the most significant of which being the existence of a parity violating term [176], problems with ghost instabilities and strong coupling at very low energies [178, 179], wrong sign and very large value of cosmological constant [180, 181], problems with power counting renormalisation of the scalar mode propagation [182, 183]. Some of those issues (ghost instabilities and the sign of the cosmological constant) are discussed in more detail later on in this chapter and we discuss alternative solutions to them, like carrying out an analytic continuation of the constant parameters ([184]). Other

problems arise from the conditions imposed in the original Hořava formulation of the theory; the detailed balance condition, where it is assumed that potential part of the action is given from the superpotential, thus limiting the number of its terms and independent couplings. There is also the projectability condition which assumes that the lapse function $\mathcal{N}$ depends only on time $\mathcal{N} = \mathcal{N}(t)$. Some authors ([179], end note) claim that the non-projectable version leads to serious strong coupling problem and does not have a viable GR limit at any energy scale. On the other hand more recent considerations, e.g. [180, 185], claim the opposite. These authors state that most of the shortcomings (like parity violation, problems with renormalisation of the scalar mode and its IR behaviour) can be cured by adding additional terms to the superpotential and relaxing projectability condition, while still keeping detailed balance (or eventually softly breaking it). However later works provide evidence for problems with power-counting renormalizability of the scalar mode (spin-0 graviton) in the detailed balance version of the theory [182]. Recent formulation of the so called "mixed-derivative" Hořava gravity [183, 186] claim that this formulation is actually power counting renormalizable.

There is still an open issue within HL-type theories, namely the large value of the cosmological constant, as there is a descrepancy of at least 60 orders of magnitude between the value demanded by detailed balance [180] and the observed one. It is discussed in [181] that adding the effects of very large vacuum energy of quantum matter fields may cancel out the negative sign and magnitude of the bare cosmological constant leaving the tiny observed residual. There is also problem of a huge predicted value for the quantum vacuum (review in [187]), as there is a large difference between the magnitude of the vacuum energy expected from zero-point fluctuations and scalar potentials and the observed value, and maybe those issues have common solution.

Taking into account various problems and contradicting statements in the works studying different HL-type theories from the analytical side, it is worth to investigate how different formulations fit the observational data. Currently Hořava gravity and its extensions are not ruled out observationally (although the recent binary neutron star merger GW170817 [108] provides tight bounds on some parameters [157]); thus further observational constraints should either rule out its specific scenarios or the

whole model, or in case of agreement with observations provide a better justification for deeper theoretical research. It is still believed that HL theory might provide a promising cosmological scenario solving some shortcomings of classical GR, like non-renormalisability. We are actually interested in fitting cosmological scenarios predicted by different version of HL theories to existing observational data. We believe that it is a separate issue from theoretical analysis, as observational constraints may provide valuable input for theoretical analysis.

Studies providing bounds on HL theory constants and parameters based on observational data already exist in the literature. Some are based on the two simplest HL scenarios and quite old cosmological data, like [171] (non-projectable version with and without detailed balance). Others like [173] fit data to the more general extension of Horava theory [77], and also consider linear perturbations around that background. However, this research is based on a flat model (in our case the curvature density parameter is left as a free parameter). As a part of a bigger project we would like to place new bounds on parameters appearing in Hořava-Lifshitz cosmology based on the more recent data. As a first step we would like to fit the data to the two simplest cosmological models. We will look at scenarios based on the original Hořava formulation [76, 163] with detailed balance condition imposed, as well as one with this condition relaxed and with the generalised form of the gravitational action (Sotiriou-Visser-Weinfurtner (SVW) generalisation) [176]. This way we can see the effect of applying newer observational data and different parameterisation on the values of HL cosmological parameters. In the next step we are going to include bigger sets of data, like PANTHEON SN1a catalogue [188] and gamma-ray bursts [189] and/or apply it to a more general HL formulation, like [77] - the so called "healthy" or "consistent" extension of the original formulation. There are works [173] putting constraints on this extension written in the effective field theory framework, but the latter is based on a flat background, limiting the number of parameters. In this work we have focused on a simpler cosmological model and a smaller data set in order to better capture the influence of new data on the model as compared to earlier works. We also used the least number of free parameters and more natural parameterisation of the other ones. By increasing the size of the data sets incrementally we gain a better understanding as to the sensitivity of the model

to data with higher resolution and range.

In this chapter, we provide improved observational constraints on two basic HL scenarios, which are based on the most recent cosmological data set from Cosmic Microwave Background (Planck CMB) [190], expansion rates of elliptical and lenticular galaxies [191], JLA compilation (Joint Light-Curve Analysis) data for Type Ia supernovae (SneIa) [192], Baryon Acoustic Oscillations (BAO) [193–195] and priors on the Hubble parameter [196]. These updated observational results, together with an alternative parameterisation of the Friedmann equations, provided much tighter constraints on parameters of the HL-type theories, more prone to further observational verification.

The chapter is organised as follows: in Section 4.2 we go through brief review of Hořava-Lifshitz cosmology and describe our setup for observational constraints in two cases, the original one and the SVW generalisation [176]. In Section 3 we present the new bounds on the theory parameters, based on a large updated cosmological dataset, and we conclude in Section 4. The details of our numerical analysis are presented in the Appendix.

## 4.2 Hořava-Lifshitz Cosmology

### 4.2.1 Detailed Balance

A way to simplify the action (2.22) is to impose the so-called detailed balance condition, in which we assume that it should be possible to derive $\mathcal{V}$ from a superpotential $W$ [76, 177, 180]:

$$\mathcal{V} = E^{ij}\mathcal{G}_{ijkl}E^{kl}, \quad E^{ij} = \frac{1}{\sqrt{g}}\frac{\delta W}{\delta g_{ij}}, \tag{4.1}$$

and

$$\mathcal{G}^{ijkl} = \frac{1}{2}\left(g^{ik}g^{jl} + g^{il}g^{jk}\right) - \lambda g^{ij}g^{kl}. \tag{4.2}$$

From this requirement, the most general action for Hořava-Lifshitz gravity is given by [177]:

$$S_{db} = \int \mathrm{d}t\, \mathrm{d}^3x \sqrt{g} N \left[ \frac{2}{\kappa^2} \left( K_{ij}K^{ij} - \lambda K^2 \right) + \frac{\kappa^2}{2\omega^4} C_{ij}C^{ij} - \frac{\kappa^2 \mu}{2\omega^2} \frac{\epsilon^{ijk}}{\sqrt{g}} R_{il} \nabla_j R^l_k \right. \\ \left. + \frac{\kappa^2 \mu^2}{8} R_{ij}R^{ij} + \frac{\kappa^2 \mu^2}{8(1-3\lambda)} \left( \frac{1-4\lambda}{4} R^2 + \Lambda R - 3\Lambda^2 \right) \right], \tag{4.3}$$

where

$$C^{ij} = \epsilon^{ikl} \nabla_k \left( R^j_{\ l} - \frac{1}{4} R \delta^j_l \right) \tag{4.4}$$

is the Cotton tensor, $\epsilon^{ikl}$ is the totally antisymmetric tensor, and the parameters $\kappa, \omega$, and $\mu$ have mass dimension $-1, 0$, and $1$, respectively. The action (4.3) for HL gravity has been obtained from the original one [76] by carrying out an analytic continuation (e.g. [184]) of constant parameters: $\mu \mapsto i\mu$ and $\omega^2 \mapsto -i\omega^2$. This enabled to obtain positive values of the cosmological constant $\Lambda$ (that correspond to current observational results) in the low energy limit of the theory, unlike in the original formulation.

The coupling parameter $\lambda$ is dimensionless. In general, it runs (logarithmically in the high energy limit – in UV) and may eventually reach one the three infrared (IR) fixed points ([76]): $\lambda = 1/3$, $\lambda = 1$ or $\lambda = \infty$. The range $1 > \lambda > 1/3$ leads to ghost instabilities in the IR limit of the theory [197]. However, this range of $\lambda$ is exactly the flow-interval between the UV and IR regimes. The only physically interesting case that remains, allowing for a possible flow towards GR – at $\lambda = 1$ – is the regime $\lambda \geq 1$. Region $\lambda \leq 1/3$ is disconnected from $\lambda = 1$ and cannot be included in realistic considerations.

We expect that the action (4.3) corresponds to the Einstein-Hilbert near the IR limit of the theory. This happens for the speed of light $c$ and gravitational constant $G$ expressed in terms of HL parameters as follows:

$$G = \frac{\kappa^2}{32\pi c}, \quad c = \frac{\kappa^4 \mu^2 \Lambda}{8(3\lambda - 1)^2}. \tag{4.5}$$

In order to study cosmology in this model it is necessary to populate the Universe with matter and radiation. Since we are interested in the phenomenological bounds on such a theory we will introduce a cosmological energy-momentum tensor into the modified Einstein field equations with the simple demand that the standard general relativistic expression is recovered in the infrared limit. Therefore, as it is described in one of our previous papers [170], we equip our Universe with a hydrodynamic approximation where $p_m$ and $\rho_m$ (pressure and energy density of the dark plus baryonic matter) are parameters subject to the continuity equation $\dot{\rho}_m + 3H(\rho_m + p_m) = 0$. We also include a standard model radiation component through $p_r$ and $\rho_r$ (note that we already have a cosmological constant $\Lambda$ in $S_{db}$), which are also subject to the evolution equation $\dot{\rho}_m + 3H(\rho_m + p_m) = 0$.

Moreover, we use the *projectability condition* $N = N(t)$ [76] and the standard FLRW line element: $g_{ij} = a^2(t)\gamma_{ij}$, $N_i = 0$, where $\gamma_{ij}$ is a maximally symmetric constant curvature metric:

$$\gamma_{ij}\mathrm{d}x^i\mathrm{d}x^j = \frac{\mathrm{d}r^2}{1-Kr^2} + r^2\mathrm{d}\Omega^2, \tag{4.6}$$

values $K = \{-1, 0, 1\}$ corresponds to closed, flat, and open Universe, respectively. On this background

$$K_{ij} = \frac{H}{N}g_{ij}\,, \qquad R_{ij} = \frac{2K}{a^2}g_{ij}\,, \qquad C_{ij} = 0\,, \tag{4.7}$$

where $H \equiv \dot{a}/a$ is the Hubble parameter.

The equations of motion are obtained by varying the action (4.3) written in the FLRW metrics with respect to $N$ and $a$. After that lapse is set to one: $N = 1$ (if it was set so at the beginning, standard Friedmann equations would have been obtained) and terms with density $\rho$ and pressure $p$ are added). This leads to the Friedmann equations for the projectable Hořava-Lifshitz universe under detailed-balance condition:

$$\left(\frac{\dot{a}}{a}\right)^2 = \frac{\kappa^2}{6(3\lambda-1)}\left[\rho_m + \rho_r\right] + \frac{\kappa^2}{6(3\lambda-1)}\left[\frac{3\kappa^2\mu^2K^2}{8(3\lambda-1)a^4} + \frac{3\kappa^2\mu^2\Lambda^2}{8(3\lambda-1)}\right] - \frac{\kappa^4\mu^2\Lambda K}{8(3\lambda-1)^2a^2}, \tag{4.8}$$

$$\frac{\mathrm{d}}{\mathrm{d}t}\frac{\dot{a}}{a}+\frac{3}{2}\left(\frac{\dot{a}}{a}\right)^2=-\frac{\kappa^2}{4(3\lambda-1)}[p_m+p_r]-\frac{\kappa^2}{4(3\lambda-1)}\Big[\frac{\kappa^2\mu^2K^2}{8(3\lambda-1)a^4}- \\ -\frac{3\kappa^2\mu^2\Lambda^2}{8(3\lambda-1)}\Big]-\frac{\kappa^4\mu^2\Lambda K}{16(3\lambda-1)^2a^2}. \tag{4.9}$$

We can introduce in the above equations the dark energy parameters, namely energy density $\rho_{DE}$ and pressure density $p_{DE}$, defined as follows:

$$\rho_{DE}|_{db}:=\frac{3\kappa^2\mu^2K^2}{8(3\lambda-1)a^4}+\frac{3\kappa^2\mu^2\Lambda^2}{8(3\lambda-1)}, \tag{4.10}$$

$$p_{DE}|_{db}:=\frac{\kappa^2\mu^2K^2}{8(3\lambda-1)a^4}-\frac{3\kappa^2\mu^2\Lambda^2}{8(3\lambda-1)}. \tag{4.11}$$

**Setup for Observational Constraints**

Here we describe the theoretical setup which made it possible to constrain the parameters of the theory. Introducing natural units $8\pi G = 1 = c$ and taking the IR limit $\lambda = 1$ reduces relations (4.5) to the following ones:

$$\kappa^2=4,\quad \mu^2\Lambda=2. \tag{4.12}$$

Substituting these values to the the Friedmann equation (4.8) leads to:

$$\left(\frac{\dot{a}}{a}\right)^2=\frac{1}{3}(\rho_m+\rho_r)+\frac{1}{3}\left(\frac{3K^2}{2\Lambda a^4}+\frac{3\Lambda}{2}\right)-\frac{K}{a^2}, \tag{4.13}$$

We also define in the IR limit the canonical density parameters for the current universe $a_0 = 1$ (subscript 0 indicates the value as measured today) as follows

$$\Omega_m^0=\frac{\rho_m}{3H_0^2},\quad \Omega_r^0=\frac{\rho_r}{3H_0^2},\quad \Omega_k^0=-\frac{K}{H_0^2a_0^2}, \tag{4.14}$$

where $H_0$ is the Hubble parameter. Using these parameter we rewrite equation (4.13) as follows:

$$\left(\frac{\dot{a}}{a}\right)^2=H_0^2\left[\Omega_m^0a^{-3}+\Omega_r^0a^{-4}+\Omega_k^0a^{-2}+\frac{(\Omega_k^0)^2H_0^2}{2\Lambda}a^{-4}+\frac{\Lambda}{2H_0^2}\right], \tag{4.15}$$

where the last two term correspond to dark energy density parameter obtained from equations (4.10) and (4.14):

$$\Omega_{DE} = \frac{\rho_{DE}|_{db}}{3H_0^2} = \frac{(\Omega_k^0)^2 H_0}{2\Lambda} a^{-4} + \frac{\Lambda}{2H_0^2}. \tag{4.16}$$

In the above Friedmann equation (4.15) we encounter the term $\Omega_k^2 H_0^2/2\Lambda a^4$, which is the coefficient of dark radiation in Hořava-Lifshitz. We can conveniently express this in terms of the effective number of neutrino species present in the BBN époque. This is because the dark radiation must have been present during that time and is thus subject to BBN constraints from other experiments. As such, we can obtain a constraint equation for the dark radiation component [198, 199]:

$$\frac{(\Omega_k^0)^2 H_0^2}{2\Lambda} = 0.135 \Delta N_\nu \Omega_r^0, \tag{4.17}$$

where $\Delta N_\nu$ is the deviation of the effective number of massless neutrino species from the standard $\Lambda$CDM value ($N_\nu = 3 + \Delta N_\nu$). There are already several bounds on $\Delta N_\nu$ from different experiments. The limits from [199, 200]: $-1.7 \leq \Delta N_\nu \leq 2.0$ originate from a BBN analysis, and in [201], the authors use data from BBN and CMB (Planck) to arrive at an upper limit of $\Delta N_\nu < 0.2$. Moreover, using Planck CMB data, the authors of [202] arrive at the limits $-0.32 \leq \Delta N_\nu \leq 0.44$ (TTTEEE+lensing). Other approaches and bounds can be found in [203, 204], for example. Through the relation (4.17) we see that $\Delta N_\nu = 0$ leads to the possibility of a flat Universe. This is concerning, since it has been established that a flat Hořava-Lifshitz coincide with the standard $\Lambda$CDM model [165, 166]. Therefore the constraints on the curvature parameter $\Omega_k$ and the BBN neutrino parameter $\Delta N_\nu$ are of utmost importance, and they have been left as free parameters in our analysis. That is, we have not imposed the BBN limit on $\Delta N_\nu$, but the limits we found on this parameter automatically satisfied the BBN constraint. Now, since all the density parameters have to add up to unity we have:

$$\Omega_m^0 + \Omega_r^0 + \Omega_k^0 + \frac{(\Omega_k^0)^2}{4 \cdot 0.135 \Delta N_\nu \Omega_r^0} + 0.135 \Delta N_\nu \Omega_r^0 = 1, \tag{4.18}$$

and we can rewrite the Friedmann equation (4.15) as:

$$\left(\frac{\dot{a}}{a}\right)^2 = H_0^2\left[\Omega_m^0 a^{-3} + \Omega_r^0 a^{-4} + \Omega_k^0 a^{-2} + \frac{(\Omega_k^0)^2}{4\cdot 0.135\Delta N_\nu \Omega_r^0} + 0.135\Delta N_\nu \Omega_r^0 a^{-4}\right], \tag{4.19}$$

and this is the equation that we have used in our MCMC analysis of detailed balance.

### 4.2.2 Beyond Detailed Balance

Since there has been a discussion in the literature about whether detailed balance is too restrictive ([75, 165, 166]) it is important to investigate the case when we do not impose this condition. When we relax the detailed balance condition we open up for including more terms into the potential $\mathcal{V}$. In this case, the Friedmann equations can be expressed as [177, 179]:

$$\left(\frac{\dot{a}}{a}\right)^2 = \frac{2\sigma_0}{3\lambda-1}(\rho_m+\rho_r) + \frac{2}{3\lambda-1}\left[\frac{\Lambda}{2} + \frac{\sigma_3 K^2}{6a^4} + \frac{\sigma_4 K}{6a^6}\right] + \frac{\sigma_2}{3(3\lambda-1)}\frac{K}{a^2}, \tag{4.20}$$

$$\frac{\mathrm{d}}{\mathrm{d}t}\frac{\dot{a}}{a} + \frac{3}{2}\left(\frac{\dot{a}}{a}\right)^2 = -\frac{3\sigma_0}{3\lambda-1}\frac{\rho_r}{3} - \frac{3}{3\lambda-1}\left[-\frac{\Lambda}{2} + \frac{\sigma_3 K^2}{18a^4} + \frac{\sigma_4 K}{6a^6}\right] + \frac{\sigma_2}{6(3\lambda-1)}\frac{K}{a^2}, \tag{4.21}$$

where $\sigma_i$ are arbitrary constants ($\sigma_2 < 0$) and in analogy with the detailed balance scenario:

$$G = \frac{6\sigma_0}{16\pi}, \quad \frac{\sigma_2}{3(3\lambda-1)} = -1. \tag{4.22}$$

Dark energy and pressure densities may be defined as follows:

$$\rho_{DE}|_{bdb} := 3\left(\frac{\Lambda}{2} + \frac{\sigma_3 K^2}{6a^4} + \frac{\sigma_4 K}{6a^6}\right), \tag{4.23}$$

$$p_{DE}|_{bdb} := 3\left(-\frac{\Lambda}{2} + \frac{\sigma_3 K^2}{6a^4} + \frac{\sigma_4 K}{6a^6}\right). \tag{4.24}$$

#### Setup for Observational Constraints

Here, we follow the setup for the detailed balance scenario, with $8\pi G = 1 = c$, and the same definition of the density parameters ($\Omega_X^0$). Following the notation in [171] we introduce similar parameters in the IR limit $\lambda = 1$:

$$\omega_1 = \frac{\Lambda}{2H_0^2}, \quad \omega_3 = \frac{\sigma_3 H_0^2 \Omega_k^0}{6}, \quad \omega_4 = -\frac{\sigma_4 \Omega_k^0}{6}, \tag{4.25}$$

and introducing the following Bing Bang nucleosynthesis (BBN) constraint [198]:

$$\omega_3 + \omega_4(1 + z_{BBN})^2 = 0.135\Delta N_\nu \Omega_r^0, \tag{4.26}$$

where $z_{BBN}$ is the redshift at BBN ($\sim 4 \times 10^8$). Moreover, we have the following constraint on the density parameters:

$$\Omega_m^0 + \Omega_r^0 + \Omega_k^0 + \omega_1 + \omega_3 + \omega_4 = 1. \tag{4.27}$$

Using the above two equations to eliminate $\omega_4$ along with the $\sigma$-parameters, we can rewrite the Friedmann equation (4.20) for the beyond detailed balance scenario as:

$$\left(\frac{\dot{a}}{a}\right)^2 = H_0^2 \left[\Omega_m^0 a^{-3} + \left(\Omega_r^0 + \omega_3\right) a^{-4} + \Omega_k^0 a^{-2} + \omega_1 + \frac{0.135 \cdot \Delta N_\nu \Omega_r^0 - \omega_3}{(1 + z_{BBN})^2} a^{-6}\right]. \tag{4.28}$$

This is the equation we have used in our MCMC analysis of the beyond detailed balance scenario. Additionally, the dark energy density parameter can be written as:

$$\Omega_{DE}^0 = \omega_1 + \omega_3 + \omega_4 = \omega_1 + \omega_3 + \frac{0.135 \cdot \Delta N_\nu \Omega_r^0 - \omega_3}{(1 + z_{BBN})^2}. \tag{4.29}$$

## 4.3 Results and Discussion

Using the equations (4.8) and (4.20) as a starting point, we now want to find the parameter set which best fits the data. To do this we use a large updated data set with CMB (Planck), SN1a, BAO and more (see Appendix for details). In order to do this, we used a Markov-Chain Monte Carlo (MCMC) method, which was evaluated on the CIŚ computer cluster. The parameters are completely unconstrained but are given initial guesses, which speed up computation. We introduced a Gaussian prior on one parameter: $H_0$, derived from the Hubble constant value in [196], $H_0 = (69.6 \pm 0.7)$ km s$^{-1}$ Mpc$^{-1}$. That was the only prior imposed on any of the parameters. During every step in the computation, the MCMC method calculates the $\chi^2$, and in the end returns the parameter set which minimised the $\chi^2$ function. This way, we are able to obtain information about the posterior probability distribution without knowing it explicitly. For full details about the data and method, see

Appendix.

### 4.3.1 Detailed Balance

To derive the constraints on the detailed balance scenario, we used Eq. (4.19) and (4.19) in our MCMC method. As the detailed balance equations are relatively simple there was no need to introduce many constraints, and the parameters $\Delta N_\nu$ has been left completely free in this section. One interesting result is that we find significant evidence for *positive spatial curvature* at $3\sigma$ confidence (see Figure 4.1). This is an encouraging prospective observational signal, since any measurement of positive spatial curvature would be a step towards validating this model. Parameters with $1\sigma$ limits are presented in Table 4.1.

In our analysis, the parameters $H_0$, $\Omega_m^0$, $\Omega_r^0$ all have familiar and reasonable bounds. The parameters which stand out are $\Omega_k^0$, $\Delta N_\nu$ and $\Lambda$. Our initial simulations revealed that the spatial curvature is actually significantly different from zero, and, instead of expressing the parameters $\omega$ in terms of the above parameters as in [171], we have chosen to leave it as $\omega = \Lambda/2H_0^2$. Therefore there was no need to split the analysis in $\Omega_k^0 > 0$ and $\Omega_k^0 < 0$. Through Eq.(4.17), a non-zero spatial curvature automatically leads to a non-zero $\Delta N_\nu$. Previous works, like [171], have also used $\Delta N_\nu$ as a free parameter, but with this updated data set and different parametrisation we arrive at different results and parameter bounds (compared, for example, to [171]). In this scenario the value of $\Lambda \sim 0.676 \cdot 10^{-35}$ s$^{-2}$ $\sim 0.836 \cdot 10^{-52}$ m$^{-2}$ and the cosmological constant in the $\Lambda$CDM model is of the same order $\Lambda_{\Lambda\text{CDM}} \sim 1.11 \cdot 10^{-52}$ m$^{-2}$ [190]. There is a marginal difference but the overall magnitude is still much smaller than the lower bound on $\Lambda_{\text{HL}}$ estimated by the energy scales at which Lorentz invariance breaking remains undetected in sub-mm precision tests. Authors of [178, 180, 185] provide a rough estimation for the lower bound of $\Lambda_{\text{HL}}$ to be somewhere in the range from 1–100 meV$^2$ (at least) in natural units, which converts to $10^7$–$10^9$ m$^{-2}$ in metric units. The issue of the huge bare value of the cosmological constant demanded by the need for suppression at IR limit of fourth-order operators appearing in the HL action is discussed in the literature, eg. [180, 181] and references therein, that is why the obtained numerical value should be viewed from that perspective.

Additionally, through $\mu^2\Lambda = 2$, $\mu$ acquires finite values, unlike the results in [171], where $\Lambda$ is bound by zero from below, and $\mu$ is unbounded from above.

Moreover, using Eq. (4.16) we arrive to the bounds $\Omega^0_{DE} = 0.686 \pm 0.015$ at $3\sigma$. This is very close to that from Planck 2015 [190] where the tabled value is $\Omega^0_{DE} = 0.6911 \pm 0.0062$ at $1\sigma$ and to the result from [173]. This is interesting as the authors of the latter use effective field theory and a "healthy extension" of HL theory [77] to constrain Hořava-Lifshitz cosmology against data. They arrive at the value $\Omega^0_{DE} = 0.69 \pm 0.02$ at $3\sigma$, which is in close agreement to our findings, although they used not only background Friedmann equation as we do, but also considered linear perturbations on this background. We also use a different HL model, so our background equation (4.15) is slightly different from their Friedmann equation (46). Except different parameters of the theory, (4.15) here contains also curvature term, which arrived to be non-zero, but it does not include massive neutrinos explicitly, as it is contained in eq. (46) of (4.15). In contrast, our results differ from those in [171] which uses older data, and this strengthens the case that our results are more accurate, as we use similar background equation.

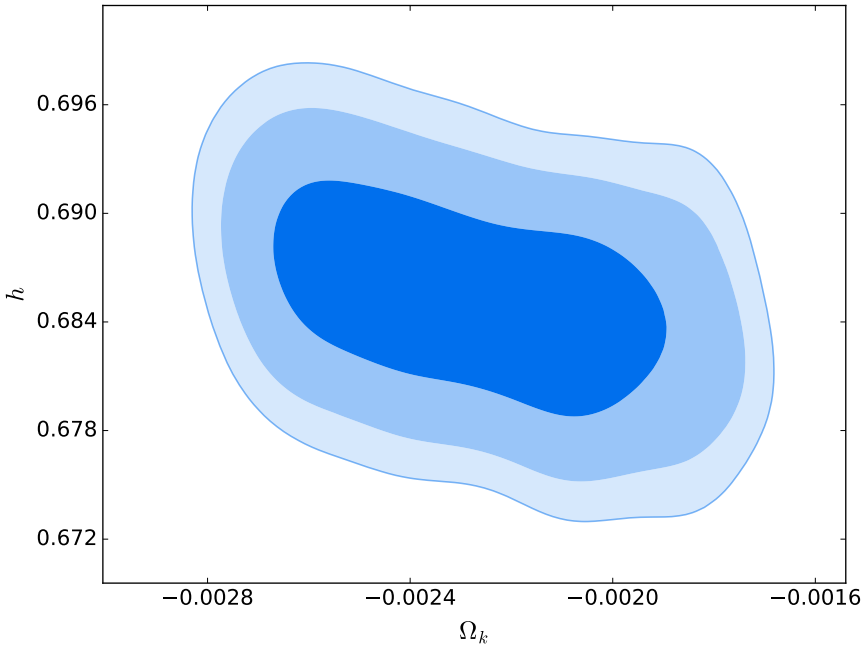


FIGURE 4.1: 1, 2, and $3\sigma$ contours of the curvature parameter $\Omega^0_k$ and the dimensionless Hubble parameter $h$ under detailed balance. Solid (blue) colour corresponds to the $1\sigma$ limit. Spatial flatness ($\Omega^0_k = 0$) is excluded at more than $3\sigma$.

| Parameter | DB: $1\sigma$ limits | BDB: $1\sigma$ limits |
|---|---|---|
| $\Omega_m^0$ | $0.316 \pm 0.0054$ | $0.324 \pm 0.0068$ |
| $\Omega_k^0$ | $(-2.27 \pm 0.25) \cdot 10^{-3}$ | $(-3.30 \pm 0.20) \cdot 10^{-3}$ |
| $\Omega_r^0$ | $(9.08 \pm 0.10) \cdot 10^{-4}$ | $\left(9.24^{+0.17}_{-0.21}\right) \cdot 10^{-4}$ |
| $\Omega_{DE}^0$ | $0.686 \pm 0.0053$ | $0.679 \pm 0.0061$ |
| $H_0$ | $68.530 \pm 0.413$ | $69.630 \pm 0.635$ |
| $\Delta N_\nu$ | $0.155 \pm 0.033$ | $0.54^{+0.15}_{-0.21}$ |
| $\Lambda$ | $\left(0.676^{+0.125}_{-0.128}\right) \cdot 10^{-35}$ | $\left(0.691^{+0.147}_{-0.146}\right) \cdot 10^{-35}$ |
| $\sigma_1 / H_0^2$ | - | $4.073 \pm 0.038$ |
| $\log \sigma_3 H_0^2$ | - | $0.4^{+1.0}_{-1.7}$ |

TABLE 4.1: Constraints on the parameters from both scenarios: detailed balance (DB) and beyond detailed balance (BDB) (The units of $H_0$ are km·s$^{-1}$·Mpc$^{-1}$ and of $\Lambda$ are $s^{-2}$). A dash (-) indicates that a parameter is not used in that particular model.

### 4.3.2 Beyond Detailed Balance

To obtain constraints on parameters in the beyond detailed balance scenario we used equations (4.26), (4.27), and (4.28) in the same MCMC method as for detailed balance. Here, we introduced another constraint equation in order to make sure that the Hubble parameter is always completely real. From equations (4.23) and (4.26) it is possible to identify a generalised dark energy density. As such, this energy density has to be larger than zero. In this way we obtain real values of the Hubble parameters while only making physical assumptions. The constraint can be written

as:

$$\rho_{DE}|_{bdb} = 3H_0^2\left[\omega_1 + \omega_3 a^{-4} + \omega_4 a^{-6}\right] = 3H_0^2\left[\omega_1 + \omega_3 a^{-4} + \frac{0.135 \cdot \Delta N_\nu \Omega_r - \omega_3}{(1+z_{BBN})^2} a^{-6}\right] > 0. \tag{4.30}$$

Using the equations and constraints mentioned above we carried out an MCMC analysis of the beyond detailed balance model. All the results are shown in Table 4.1. Here, it is interesting to note that in this scenario we find evidence for positive spatial curvature at $1\sigma$: $\Omega_k^0 = -0.0033 \pm 0.0020$. The contours showing this is plotted against $h$ in Figure 4.3. Here, the marginalised probability for $\Omega_k^0$ in detailed balance is completely contained inside the beyond detailed balance scenario, away from the best-fit value. This can be seen in Figure 4.2.

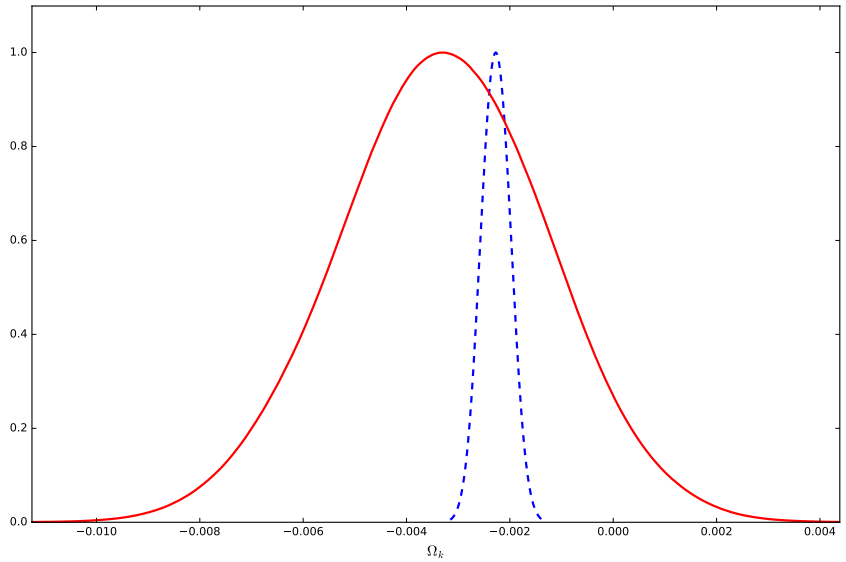


FIGURE 4.2: Marginalised constraints of the curvature parameter $\Omega_k^0$. The dashed (blue) curve represents the detailed balance scenario while the solid (red) curve shows beyond detailed balance. The detailed balance scenario is completely contained within beyond detailed balance.

Moreover, the parameter $\sigma_3 H_0^2$ seems to acquire a log-normal distribution, and the two-sided confidence intervals for this parameter must be considered unreliable. Because of the log-normal distribution, however, it was possible to find limits on $\log \sigma_3 H_0^2$, which is shown in Figure 4.4. The errors on this parameter are very large,

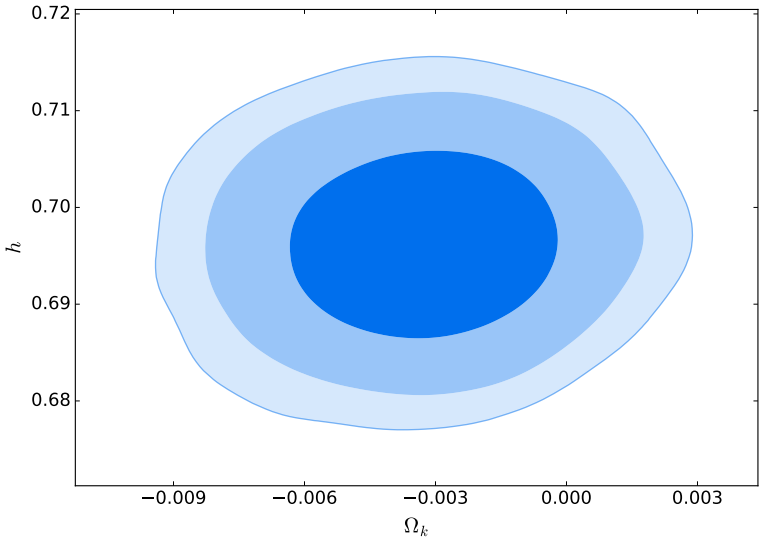


FIGURE 4.3: 1, 2, and $3\sigma$ contours of the curvature parameter $\Omega_k^0$ and the dimensionless Hubble parameter $h$ in the beyond detailed balance scenario. Solid (blue) colour corresponds to the $1\sigma$ limit. Spatial flatness is excluded at $1\sigma$.

which is an artefact of the log-normal distribution which has long tails on both ends. We express the two $\sigma$ parameters as $\sigma_1/H_0^2$ and $\sigma_3 H_0^2$ (see Eq. (4.25)) as there is no need to specify units or value for $H_0$.

It is also worth noting that it is possible to differentiate between the two scenarios by looking at the neutrino species parameter $\Delta N_\nu$. As can be seen in Figure 4.5, only some of the marginalised probability of the detailed balance model is contained within the range of beyond detailed balance, and a large part of the curve lies outside. Thus, $\Delta N_\nu$ is a promising parameter to help differentiate between the two scenarios. Remarkably, the lower bound of $\Delta N_\nu$ from Table 4.1 is in conflict with the bound ($\Delta N_\nu < 0.2$) derived from BBN and Planck CMB (mentioned in Section 2.2.1). In fact, looking at the $2\sigma$ and $3\sigma$ bounds on $\Delta N_\nu$ $(0.21, 0.17)$ we see that our analysis yields a significantly different result at more than $2\sigma$ confidence.

Using Eq. (4.29) we find the bounds $\Omega_{DE}^0 = 0.678^{+0.017}_{-0.019}$ at $3\sigma$ confidence level, which is close to the value from Planck 2015 ($\Omega_{DE}^0 = 0.6911 \pm 0.0062$ at $1\sigma$), but not as close as for the detailed balance scenario. This is mainly due to different estimated

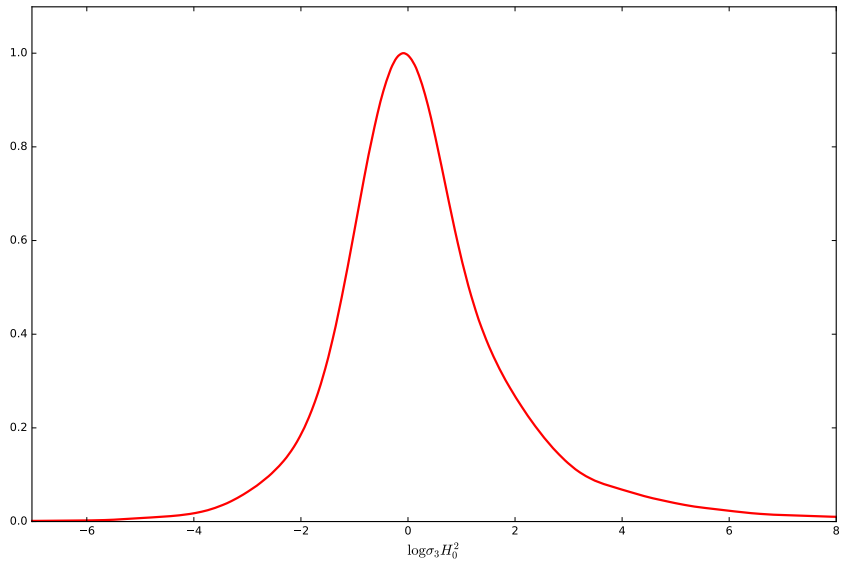


FIGURE 4.4: Marginalised constraints of the parameter $\log(\sigma_3 H_0^2)$. The slightly elongated tail on the right hand side shifts the mean away from 0.

values of $\Lambda/2H_0^2$, makes up the main part of $\Omega_{DE}^0$ in both scenarios. Beyond detailed balance parameters at $3\sigma$ are $\omega_1 = 0.679^{+0.017}_{-0.019}$ (the leading term in $\Omega_{DE}^0$), $\omega_3 = (2.05^{+4.38}_{-2.04}) \cdot 10^{-6}$ and $\omega_4(1+z_{BBN})^2 = (4.18 \cdot 10^{-6})^{+0.0056}_{-0.0064}$ (the errors on $\omega_3$ and $\omega_4$ are very large, so only order is relevant here).

## 4.4 Conclusions

Using an updated cosmological data set we calculated new observational constraints on cosmological parameters of different formulations of Hořava-Lifshitz gravity. Unlike in the previous approaches [171] we use a different parametrisation of our parameters, the most important one is treating $\Omega_k^0$ (together with $\Delta N_\nu$) as completely free parameter. This allowed us to avoid the splitting of considerations and calculations into two separate cases of negative and positive curvature parameters that was used before.

We investigated two basic Hořava-Lifshitz scenarios, the one with detailed balance condition imposed in the action and the other one, the so called Sotiriou-Visser-Weinfurtner (SVW) generalization [176], which relaxes this condition and assumes higher order, i.e. cubic terms in the action. We found very remarkable results, namely detailed balance scenario exhibits positive spatial curvature to more than

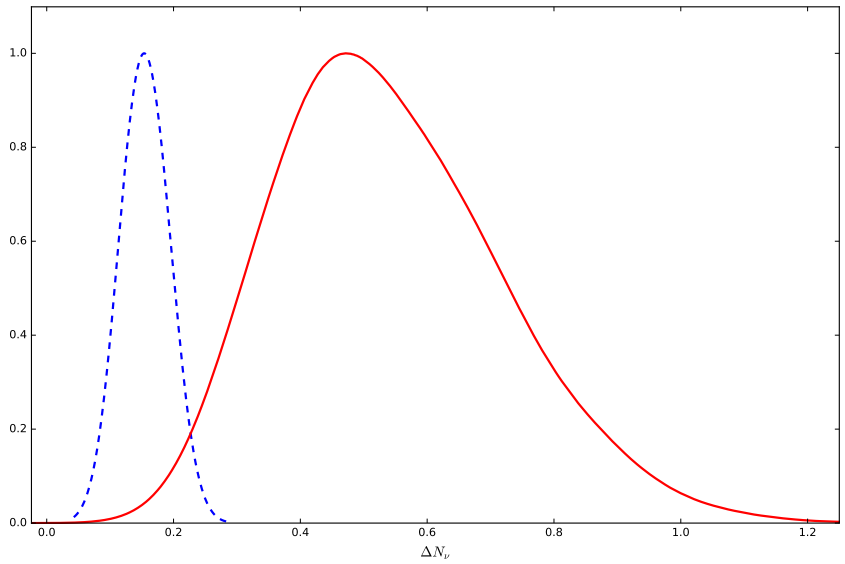


FIGURE 4.5: Marginalised constraint of the parameter $\Delta N_\nu$. The dashed (blue) curve represents the detailed balance scenario, and the solid (red) shows beyond detailed balance. The two scenarios only shows a small amount of overlap.

$3\sigma$ whereas for the SVW generalization there is evidence for positive spatial curvature at $1\sigma$, which could be a smoking gun for observations. Some of our parameters differ quite a lot from previous works, but as we have some different assumptions (for example, in [171] the parameter $\omega_3$ is assumed to be positive for convenience), different values are to be expected.

The best fit value of the parameter $\Delta N_\nu$ (kept as a completely free parameter of the theory) at $1\sigma$ is definitely positive and within BBN limits, as well as within some of the bounds from CMB. Since there is a variety of papers with different bounds on $\Delta N_\nu$ available, it is unclear which one should compare to. In general, more data is needed to make a final verdict on this issue, and we aim to address this in future work as it becomes available. Our analysis, however, excludes from both scenarios the zero-curvature flat universe and corresponds to the non-zero positive cosmological constant $\Lambda$. This means that we might expect late-time cosmological CPT violation as in $\Lambda$CDM and Doubly General Relativity (see Section 2.2).

Most values of the parameters of the theory are similar as in $\Lambda$CDM model. For example, our values for $\Omega_m = 0.316 \pm 0.0054 (0.324 \pm 0.0068)$ for detailed balance (beyond detailed balance) are both within $1\sigma$ of $\Lambda$CDM [190]. We are also close to the dark energy density parameter, as discussed in Section 4.3.1. However, what sets

the HL model apart is the non-zero curvature parameter $\Omega_k$. We found it to be different from zero to $1\sigma$ ($3\sigma$). We also found bounds on the Hořava-Lifshitz parameters $\sigma_1$ and $\sigma_3$, which enter the Lagrange density when Lorentz invariance is no longer imposed. We found that $\sigma_1 H_0^2 = 4.073 \pm 0.038$ and $\log \sigma_3 H_0^2 = 0.4^{+1.0}_{-1.7}$. According to Planck 2015 (when including BAO's) $\Omega_k$ is a Gaussian centered around zero [190]. As our analysis also includes BAO's, further investigation of this parameter may be the way to finally exclude one of these models. Naively, one must still prefer the $\Lambda$CDM model, as it has fewer parameters than HL and fits the data well. However, bearing in mind the theoretical basis of HL cosmology (candidate for a UV-complete theory of gravity) there are, in our opinion, plenty of reasons to keep investigating this model.

It is also worth mentioning that different experiments measuring the Hubble constant $H_0$ provide different values (the so-called $H_0$ tension). Our results: $68.5 \pm 0.4$ and $69.6 \pm 0.6$ km s$^{-1}$ Mpc$^{-1}$ for detailed balance and beyond detailed balance, respectively, lie close to the Planck 2018 result $67.27 \pm 0.6$ km s$^{-1}$ Mpc$^{-1}$ in mean, but our $1\sigma$ confidence levels overlap with those from e.g. strong gravitational lensing, $71.9^{+2.4}_{-3}$ [205] and lies close to those of cosmic ladder experiments like the Sh0es project, where the Hubble constant was found to be $73.8 \pm 2.4$ km s$^{-1}$ Mpc$^{-1}$ [206]. However, this experiment used a Gaussian prior on $H_0$ which we have also done, so this agreement might be an artifact of this choice. In short, $H_0$ is not a good parameter for differentiating between HL models or to cast any light on the $H_0$ tension.

In this chapter we were mostly interested in the IR regime of the HL theory and wanted to know if the values of cosmological observables predicted within the considered models fit observational data, and also whether they may be used to distinguish HL cosmology from GR, even in the low-energy limit. Therefore we set the value of the running coupling parameter $\lambda$ to its IR value: $\lambda = 1$. There are works [207] where authors estimate the value of $\lambda$ using similar low-energy data sources (however, our data is more recent), providing that this value is restricted to $|\lambda - 1| \leq 0.02$ at $1\sigma$. At the moment we are performing calculations within more general formulation of the theory [77] and wider observational data, with more high-energy sources, where we also investigate the impact of running of $\lambda$ on other results [231].

# 5

# Preferred-Frame Effects and the $H_0$ Tension

RECENTLY, various measurements of the Hubble constant, $H_0$, have revealed a discrepancy between the value at high and low redshift, respectively. In fact, this discrepancy has been confirmed by many independent observations (using $\Lambda$CDM as a background model) at low (quasars [212], gravitational waves [213–215], Cepheid stars [216–218]) and high redshift (Cosmic Microwave Background [219], Baryon Acoustic Oscillations [220, 221], the inverse distance ladder [222, 223]). The difference in the value of the $H_0$ from these different observations lie around 4% - 9%. Many scenarios have been put forth as explanations or alleviations of the $H_0$ tension, for example dynamical dark energy [224], screened fifth forces [225], the late decay of dark matter [226] and more, but the $H_0$ tension has proved diffcult to resolve. In this chapter we investigate the presence of a preferred frame in the Universe and its effect of the $H_0$ tension. Working in the beyond detailed balance scenario in Hořava-Lifshitz gravity from Chapter 4 the we constrain the discrepancy between our local frame and the preferred frame; moreover, we suggest that part of the Hubble constant discrepancy is due to Lorentz violation in the ultraviolet regime.

## 5.1 Bounds on Hořava-Lifshitz Gravity from the $H_0$ Tension

### 5.1.1 $H_0$ tension as a preferred-frame effect

In [227] the authors suggest that the discrepancy [216, 228] between the value of the Hubble parameter $H_0$ from CMB measurements and from local data is in fact a reference-frame artefact. Since Hořava-Lifshitz gravity is based on a preferred frame (see Section 2.4.2) is it natural to also pose this question in this model. Following [227] we use a flat FLRW metric and define a geodesic observer in the CMB frame as $v^\mu = (\sqrt{1+(\zeta/a)^2}, 0, 0, \zeta/a^2)$, where $\zeta$ is a parameter and $a$ is the FLRW scale factor. For this observer, the metric takes the form:

$$ds^2 = -dT^2 + a^2(T;Z)\left(dX^2 + dY^2 + (1+(\zeta/a)^2)/(1+\zeta^2)dZ^2\right). \tag{5.1}$$

Following [227] we use the transformation which relates the Hubble constant in the local geodesic frame to that in the CMB frame:

$$\frac{H_0^{\rm CMB}}{H_0^{\rm local}} = \frac{1}{\sqrt{1+\zeta^2}}. \tag{5.2}$$

Hence, the local measurement has to be larger than or equal to its CMB counterpart. The two values will coincide when $\zeta \to 0$. We find the low and high redshift values of the Hubble parameter using a Markov-Chain Monte Carlo analysis. Here, we adopt a methodology similar to [229] by using several different data sets from a wide, yet local, redshift range. For the local value of the Hubble constant we use the PANTHEON dataset of supernovae type Ia [188], along with expansion rates of elliptical and lenticular galaxies [191], gamma-ray bursts [189] and quasars [230]. These sources are all within redshift range $0.01 < z < 8.2$, a large redshift range with multiple sources which we define as our "local" frame, as compared to the $z \sim 1040$ for the CMB frame. For details of the method, see [27] and for a detailed discussion of how to obtain cosmological parameters in Hořava-Lifshitz gravity, see [231]. We find that $H_0^{\rm local} = 70.18 \pm 0.02$ km s$^{-1}$ Mpc$^{-1}$ at 99.7%. Moverover, for the high-redshift (early Universe) value of the Hubble parameter we use Planck CMB data [219]. We find that, at 99.7%, the Hubble constant is $67.21^{+5.1}_{-4.4}$ km s$^{-1}$ Mpc$^{-1}$, and using these two values of the Hubble constant in (5.2) we find that the parameter $\zeta$, quantifying the discrepancy between the local frame and CMB frame, is (disregarding any negative values in order to keep $\zeta$ real):

$$0 \leq \zeta^2 \leq 0.25. \tag{5.3}$$

As suggested in [227] we have found bounds on the parameter $\zeta$ from observations of the Hubble parameter. Thus, $\zeta$ defines a geodesic reference frame where the observed $H_0$ tension would emerge naturally.

### 5.1.2 The $H_0$ tension and the Hořava-Lifshitz coupling parameter $\lambda$

It is known that in Lorentz-violating field theories, the gravitational constant measured locally, $G^{\rm local}$ does not coincide with the cosmological one [88]. In fact, we will

show that also the gravitational constant can be thought of as frame dependent, and we will give it a superscript, $G^{\rm CMB}$, to show that this is the value in the CMB frame. In the beyond detailed balance scenario, we may derive from Eq. (4.28) that the value of the gravitational constant at different energy scales are related by a single Hořava parameter [207]:

$$G^{\rm CMB} = \frac{2}{3\lambda^{\rm CMB} - 1} G^{\rm local}, \tag{5.4}$$

where the superscript on $\lambda$ is to highlight that it is the value of $\lambda$ at the time of recombination. The infrared fixed point $\lambda \to 1$ represents General Relativity, which is also when $G^{\rm CMB} = G^{\rm local}$. Clearly, in this scenario, dynamics will be different on cosmologcal scales. This also has implications for the Hubble tension. We can write down a general form of the first Friedmann equation in the two frames as:

$$(H_0^{\rm CMB})^2 = \frac{8\pi}{3} G^{\rm CMB} \rho_0 \tag{5.5}$$

$$(H_0^{\rm local})^2 = \frac{8\pi}{3} G^{\rm local} \rho_0 \tag{5.6}$$

where $\rho_0$ is the total energy density, which is the same in the two frames. On this basis we arrive to the same as Eq. (5.5) by dividing (5.5) by (5.6):

$$\left( \frac{H_0^{\rm CMB}}{H_0^{\rm local}} \right)^2 = \frac{G^{\rm CMB}}{G^{\rm local}} = \frac{2}{3\lambda^{\rm CMB} - 1}. \tag{5.7}$$

In the above relation we have to assume that Lorentz violation only *contributes* to the Hubble tension rather than being the only cause of it. In light of this it would be more accurate to write the right-hand side as $2/(3\lambda^{\rm CMB} - 1) + f(\theta)$, where $f(\theta)$ is an unknown function of one or more parameters. We can now use available Hubble constant data to put constraints on the parameter $\lambda$, and also estimate the contribution of Lorentz violation to the Hubble tension.

#### Constraints on $\lambda^{\rm CMB}$

Currently, the most accurate measurements of the Hubble constant come from the local distance ladder ($74.03 \pm 1.42$ km s$^{-1}$ Mpc$^{-1}$ [216, 228, 232]) and Planck CMB ($67.4 \pm 0.5$ km s$^{-1}$ Mpc$^{-1}$ [219]). Ignoring any model dependence of these bounds

we use Eq. (5.7) to find that $\lambda^{\rm CMB} = (0.86, 0.92)$ at 99.7%. Note that loverlooking the model dependence of these constraints is a strong assumption (especially for the CMB value). Also note that all bounds on $\lambda$ (with one exception) are *derived* constraints; in [231] we consider $\lambda$ a free parameter and place constraints on it from cosmological data. This can be compared to the limits on $H_0$ which we obtained in Hořava-Lifshitz using the beyond detailed balance formulation ($H_0^{\rm local} = 70.18 \pm 0.02$ km s$^{-1}$ Mpc$^{-1}$, $H_0^{\rm CMB} = 67.21^{+5.1}_{-4.4}$ km s$^{-1}$ Mpc$^{-1}$). Indeed, using those values of the Hubble parameters we arrive at $0.95 \leq \lambda^{\rm CMB} \leq 1.16$ at 99.7% confidence level. The bounds on $\lambda^{\rm CMB}$ from local distance ladder and Planck data are problematic, since $1/3 < \lambda < 1$ generally leads to ghost instabilities in the IR limit [197], whereas the limit from the Hubble parameters found from MCMC analysis of Hořava-Lifshitz still overlap with a non-pathological region.

From the same MCMC analysis which provided the bounds on the Hubble parameters we also obtained direct constraints on $\lambda^{\rm CMB} = 1.06 \pm 0.024$. This is encouraging, since the whole range lies in the non-pathological region for $\lambda$; however, these constraints are less stringent than those in [231] and should be seen as indicative only. A summary of all derived limits can be seen in Table 1.

**Constraints on the Hubble parameter**

Using available constraints on $\lambda$ we can get a value of the Hubble tension through Eq. (5.7). To our knowledge there is only one bound in the published literature, namely $\lambda = (0.97, 1.01)$ [207]. Using this we find that $H^{\rm CMB}/H^{\rm local} = (0.98, 1.01)$. This can be compared to the value from local distance ladder and Planck CMB measurements, where the same ratio works out to $H^{\rm CMB}/H^{\rm local} = (0.89, 0.94)$. The central value of this interval is 0.915, leading to a Hubble tension of 8.5%. Taking a conservative approach we use the upper bound of the calculated Hubble ratio from [207] and comparing to the observed 8.5% Hubble tension means that in this scenario, Lorentz violation can be the source of up to 12% of the Hubble tension. It is important to keep in mind that the constraints on $\lambda$ in [207] were derived using a large set of cosmological data from both high and low redshift, and the resulting value must be considered an *average* $\lambda$. However, since it is the only (to our knowledge) published constraint on $\lambda$ so far, we have used it, keeping in mind the above

discussion. Since $\lambda$ runs with energy we can assume that it was larger in the early Universe and therefore likely contributes more to the observed Hubble tension than our bound of $\leq 12\%$ indicates.

We may also use our derived constraints on $\lambda^{\rm CMB} = (0.95, 1.16)$ and assuming Lorentz violation is the only source of the Hubble tension, the corresponding tension is 3.8%. By again comparing to the observed 8.5% this we can infer that, at 99.7% confidence level, Lorentz violation can be the source of up to 44.7% of the Hubble tension.

Finally, we may also use our direct constraint $\lambda^{\rm CMB} = 1.04 \pm 0.024$. In order to find the most conservative estimate we use the upper bound of $\lambda^{\rm CMB}$, which combined with the measured Hubble tension of 8.5% leads to a possible contribution of Lorentz violation of up to 38%. This is our main result.

| **Preferred frame** | **Constraint** |
|---|---|
| Hořava model + Planck CMB [219] | $0 \leq \zeta^2 \leq 0.25$ |
| **Constraints on $\lambda^{\rm CMB}$ from $H_0^{\rm CMB}$** | **Constraint** |
| Hořava model + Planck CMB [219] | $\lambda^{\rm CMB} = 1.06 \pm 0.024$ |
| Derived from Hořava bounds on $H_0^{\rm CMB}$ | $0.95 \leq \lambda^{\rm CMB} \leq 1.16$ |
| **Hubble tension data** | **Lorentz violation contribution** |
| $\lambda$ from [207] + MCMC analysis | $\leq 12\%$ |
| Derived from $H_0^{\rm CMB}$ + MCMC analysis | $\leq 44.7\%$ |
| Hořava model + Planck CMB [219] | $\leq 38\%$. |

TABLE 5.1: Summary table of constraints on preferred-frame effects on the Hubble tension, as well as constraints on $\lambda$ and the Lorentz violation contribution to the Hubble tension.

## 5.2 Cosmographic Analysis

Cosmography is a model-independent method for approximating the luminosity distance and scale factor as a series expansion. In doing this one can obtain constraints on the expansion coefficients directly from data, without any of the underlying assumptions except for homogeneity, isotropy, and fixed spatial curvature [233] (for a discussion on cosmography in Hořava-Lifshitz gravity, see [234]). From the expansion of the scale factor it is convenient to define the following quantities:

$$q = -\frac{1}{aH^2}\frac{d^2a}{dt^2}, \quad j = \frac{a}{H^3}\frac{d^3a}{dt^3}, \quad s = \frac{a}{H^4}\frac{d^4a}{dt^4}, \quad l = \frac{a}{H^5}\frac{d^5a}{dt^5}, \tag{5.8}$$

called deceleration, jerk, snap, and lerk, respectively. These quantities can be directly bounded by observation, serving as a model-independent way of characterising the cosmological behaviour of the Universe. For example, the deceleration parameter measured today (denoted by index 0) is $q_0 < 0$, indicating that the Universe is currently dominated by some kind of repulsive dark energy-type field, whereas $s_0$ and $l_0$ characterise the dynamics of the early Universe.

We can rewrite Eq. (4.28) (in the flat case) to

$$\left(\frac{\dot{a}}{a}\right)^2 = \frac{2}{3\lambda - 1}\left[\Omega_m a^{-3} + \Omega_r a^{-4} + \Omega_\Lambda\right], \tag{5.9}$$

where we have also neglected the dark-radiation term since it will be of order $10^{-3}$ even in the very early Universe. As such, this simplified model represents flat $\Lambda$CDM scaled by the parameter $\lambda$. Given Eqs (5.8) and (5.9), and using that $\Omega_m = 0.324$, $\Omega_r = 9.24 \cdot 10^{-3}$ [231], we find the values of the cosmographic parameters for this model, which are presented in Table 2, for both $\lambda^{\text{CMB}} = 1.06$ and $\lambda^{\text{CMB}} = 1.04$ (we set $\lambda^{\text{local}}$ to unity). Here, we have used the central values for $\lambda$. The values for $q_0$ and $j_0$ are the same since those expressions are independent of $\lambda$. All of these values lie within the $1\sigma$ likelihoods presented in [233]; therefore, they deviate very little from the $\Lambda$CDM model. The cosmological behaviour of the cosmographic parameters can be seen in Figure 1.

| | **Using** $\lambda^{\text{CMB}} = 1.06$ | **Using** $\lambda^{\text{CMB}} = 1.04$ |
|---|---|---|
| $q_0$ | -0.50 | -0.50 |
| $j_0$ | 1.02 | 1.02 |
| $s_0$ | -0.44 | -0.45 |
| $l_0$ | 3.28 | 3.31 |

TABLE 5.2: Values of the cosmographic parameters using the central values for $\lambda^{\text{CMB}}$.

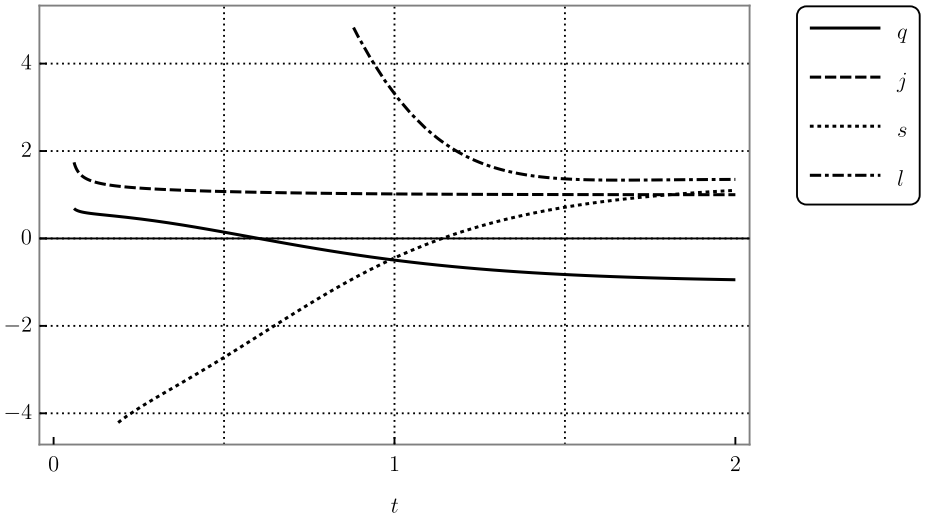


FIGURE 5.1: Cosmological behaviour of the cosmographic functions over time. Here, $t = 1$ represents the value today.

We now wish to examine the behaviour of luminosity distance, which can be written as:

$$d_L(z) = \frac{1+z}{H_0} \int_0^z \left[ \frac{2}{3\lambda - 1} \left( \Omega_m (1+z')^3 + \Omega_r (1+z')^{-4} + \Omega_\Lambda \right) \right]^{-1/2} dz'. \quad (5.10)$$

Here, we do not use a cosmographic expansion; instead, we wish to investigate how the behaviour of $d_L(z)$ differs when using different values for $H_0$ and $\lambda$. This can be seen in Figure 2 along with flat $\Lambda$CDM for comparison. At redshift $z = 8.2$, which is the upper limit for our non-CMB data, the two Hořava models differ from $\Lambda$CDM by 3.6% and 9%, for the different values of $\lambda^{\text{CMB}}$, where the CMB frame discrepancy is to be expected. The Hořava model approaches $\Lambda$CDM as $\lambda \to 1$.

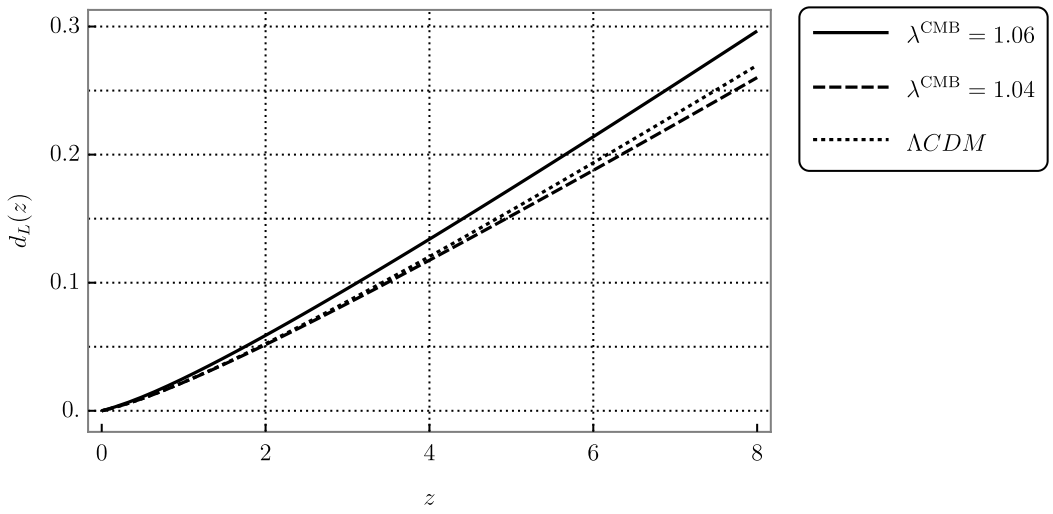


FIGURE 5.2: General behaviour of the luminosity distance $d_L$ as a function of redshift.

In light of the above discussion we note the following: our Hořava-Lifshitz model for flat FLRW is merely a scaling of the ΛCDM model, but with a running scaling parameter; indeed, using the CMB value for $\lambda$ to characterise all of cosmic evolution is something of a worst-case scenario which gives rise to the discrepancy in the luminosity distance in Figure 2. This difference in luminosity distance functions should actually make the Hubble tension even worse in Hořava-Lifshitz gravity, since the discrepancy between the two Hořava curves is larger than compared to the ΛCDM case.

Standard cosmography, where one uses a Taylor expansion of $d_L$ is only accurate for very low redshift; however, it is possible to use Padé or Chebyshev polynomials to get expansions valid out to redshift $z \sim 2 - 3$ [233, 235, 236]. Since we have used analytic expressions for $d_L$ in this analysis (integrated numerically), it is unlikely that using a series expansion will improve upon the situation, as our local data reaches well beyond the convergence radius of the cosmographic method. Since our expressions allow for the possibility of a tension in the Hubble parameter, and since the cosmographic parameters in Table 2 are in agreement with data, we expect similar behaviour as for ΛCDM, albeit with a larger Hubble tension. This may shrink to that of ΛCDM if one consider the case of a dynamical $\lambda$.

## 5.3 Discussion & Conclusions

In this article we have provided new bounds on preferred-frame effects and Hořava-Lifshitz gravity through the $H_0$ tension. Using a value for $H_0$ in the CMB frame for Hořava-Lifshitz gravity along with a local value, we were able to place bounds on $\zeta$, which determines the transformation from the CMB frame to the local geodesic frame. In [15] the authors point out an interesting consequence of a preferred frame. If the frame $\mathcal{F}$ moves relativistically with respect to the CMB frame, there would be an observable effect in the form of a dipole anisotropy of high-energy cosmic rays in the sky. In fact, according to [237], there are indications of this at intermediate scales at $3.4\sigma$ significance, with no known specific sources in the direction of the hotspot. These results are based on the observation of the northern hemisphere between May 2008 to May 2013, yielding 72 cosmic-ray events with energies higher than 57 EeV.

We have also founds tentative bounds on the Hořava-Lifshitz coupling parameter $\lambda$ using Hubble constant data; we find that some of these bounds overlap significantly with regions known to lead to ghost instabilities in the infrared limit of the theory, but that some bounds also cover a non-pathological parameter space of this model and discussed their implications. Furthermore, we have used available bounds on $\lambda$ to estimate how much Lorentz-violating effects could contribute to the Hubble tension. Most significantly, we find that Lorentz violation can contribute to up to 38% of the Hubble tension when using our own bounds on $\lambda$ from the beyond detailed balance scenario along with Planck CMB data. We also derived the cosmographic parameters for our model in a simple case. In light of this discussion it would make sense to also consider Lorentz-violating field theories in the search to find an explanation for the Hubble tension.

# 6

# A 3+1 Decomposition of the Minimal Standard-Model Extension Gravitational Sector

## 6.1 Introduction

LOCAL Lorentz invariance is one of the cornerstones of General Relativity (GR) and modern physics. As such it is an excellent probe of new physics, and Lorentz violation is a large and active area of research.[117] The Standard-Model Extension (SME) is an often-used effective field theory framework which includes all Lorentz and CPT violating terms.[12, 103, 104]

The 3+1 (ADM) version of GR is used in for example canonical quantum gravity and numerical relativity.[4, 239] Here we present a 3+1 decomposition of the minimal SME gravity Lagrangian in the case of explicit Lorentz- symmetry breaking. By decomposing spacetime into three-dimensional constant-time hypersurfaces (denoted $\Sigma_t$), we write the framework in a form which will allow for comparison and matching to other gravity models.

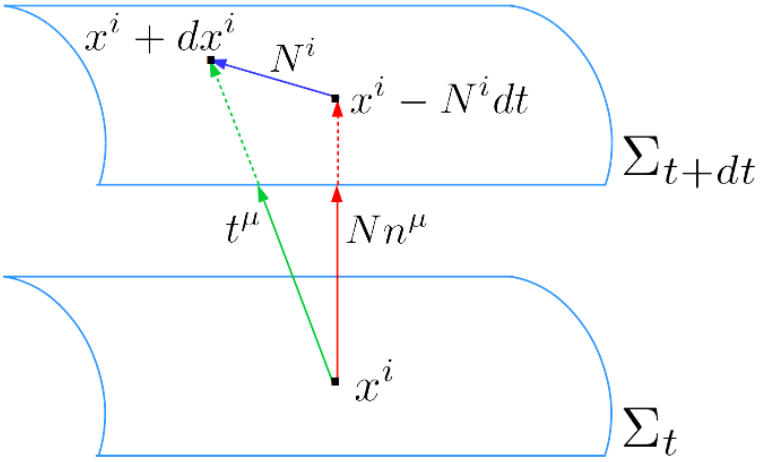


FIGURE 6.1: Constant-time hypersurfaces Σ along with the ADM variables.

## 6.2 General Decomposition

Using the ADM variables, the metric reads:

$$ds^2 = -N^2 dt^2 + \gamma_{ij}\left(dx^i + N^i dt\right)\left(dx^j + N^j dt\right), \tag{6.1}$$

where $N$ is the lapse function and $N^i$ is the shift vector. These ADM variables relate points on different constant-time hypersurfaces (see Figure 6.1), Decomposition of the manifold $\mathcal{M} \to \Sigma \times \mathbb{R}$ induces the metric $\gamma^{\mu\nu} = g^{\mu\nu} + n^\mu n^\nu$, where $n^\mu = (1/N, -N^i/N)$ is a vector normal to the foliation. The minimal gravitational sector of the SME reads as [12, 240]

$$\mathcal{L}_{\text{mSME}} = \frac{\sqrt{-g}}{2\kappa}\left[-uR + s^{\mu\nu}R^T_{\mu\nu} + t^{\mu\nu\alpha\beta}W_{\mu\nu\alpha\beta}\right], \tag{6.2}$$

where $\kappa = 8\pi G$, $R^T_{\mu\nu}$ is the trace-free Ricci tensor, and $W_{\mu\nu\alpha\beta}$ is the Weyl tensor. $u$, $s^{\mu\nu}$, and $t^{\mu\nu\alpha\beta}$ are the SME coefficient fields (mass dimension $M^0$) controlling the size of the Lorentz-violating terms (mass dimension 4). In the isotropic limit we can write the above Lagrangian as:

$$\mathcal{L}_{\text{mSME,iso}} = \frac{\sqrt{-g}}{2\kappa}\left[{}^{(4)}s_{\mu\nu}\,{}^{(4)}R^{\mu\nu}\right], \tag{6.3}$$

where a superscript (4) denotes quantities defined on $\mathcal{M}$. Note that ${}^{(4)}s_{\mu\nu}$ is CPT even, and we can not expect manifest CPT violation except in spacetimes with horizons [25]. Here, we focus on explicit symmetry breaking so that dynamical terms in the action vanish.[37] The above Lagrangian can be rewritten as:

$$\mathcal{L}_{\text{mSME}} = \frac{\sqrt{-g}}{2\kappa}\,{}^{(4)}s^{\mu\nu}\left[\gamma^\alpha{}_\mu\gamma^\beta{}_\nu\,{}^{(4)}R_{\alpha\beta} + n_\mu n_\nu n^\alpha n^\beta\,{}^{(4)}R_{\alpha\beta} - 2\gamma^\alpha{}_\mu n_\nu n^\beta\,{}^{(4)}R_{\alpha\beta}\right], \tag{6.4}$$

and by using the Gauss, Gauss-Codazzi, and Ricci equations, the Ricci tensor can be decomposed to:

$$\begin{aligned}{}^{(4)}R^{\mu\nu} = {} & R^{\mu\nu} + n^\mu K^{\nu\alpha}a_\alpha - n^\nu a^\mu K - \nabla_\alpha\left(n^\alpha K^{\mu\nu} + a^\nu\gamma^{\mu\alpha}\right) - \\ & - 2n^{(\mu}\left(D^{\nu)}K - D_\alpha K^{\nu)\alpha}\right) + n^\mu n^\nu\left(K^2 - K_{\alpha\beta}K^{\alpha\beta} + \nabla_\alpha\left(n^\alpha K + a^\alpha\right)\right).\end{aligned} \tag{6.5}$$

By contracting the decomposed Ricci tensor with ${}^{(4)}s_{\mu\nu}$ we can write down the fully decomposed formulation of the gravitational sector (GR + minimal SME):

$$\begin{aligned}\mathcal{L}_{\text{EH+mSME}} = \frac{\sqrt{-g}}{2\kappa}\Big\{ & R + {}^{(4)}s_{\mu\nu}R^{\mu\nu} + \left(K_{\mu\nu}K^{\mu\nu} - K^2\right)\left(1 + {}^{(4)}s_{\mu\nu}n^\mu n^\nu\right) + \\ & + {}^{(4)}s_{\mu\nu}\left[n^\mu a^\alpha K_\alpha{}^\nu - n^\mu a^\nu K - 2KK^{\mu\nu} - 2K^{\nu\alpha}K_\alpha{}^\nu\right] + \\ & + \nabla^{(4)}_\alpha s_{\mu\nu}\left[\gamma^{\mu\alpha}a^\nu + n^\alpha K^{\mu\nu} + 2n^\mu\left(\gamma^{\nu\alpha}K - K^{\nu\alpha}\right) - n^\mu n^\nu\left(n^\alpha K + a^\alpha\right)\right]\Big\}, \end{aligned} \tag{6.6}$$

where $R^{\mu\nu}$ and $R$ are the Ricci tensor and scalar associated with the induced spatial metric $\gamma^{\mu\nu}$, $K_{\mu\nu}$ denotes the extrinsic curvature of the foliation. Moreover, we define the acceleration vector $a_\mu = D_\mu \ln N$, where $D_\mu$ is the covariant derivative associated with the induced spatial metric. General Relativity is recovered when ${}^{(4)}s_{\mu\nu} \to 0$.

## 6.3 ADM coordinates

For simplicity we make the assumption that $s_{\alpha\beta}$ only has a 00-component, and that $\partial_\alpha s_{00} = 0$ in ADM coordinates. We also define $\lambda' = s_{00}/N^2$. In this case, the total Lagrange density (6.6) can be expressed as:

$$\mathcal{L}_{\text{EH+mSME}} = \alpha\sqrt{\gamma}\left[R + \left(1-\lambda'\right)\left(K_{ij}K^{ij} - K^2\right) + \frac{2\lambda'}{N^2}K\dot{N} - \frac{2\lambda'}{N}\left(\frac{N^j}{N}K - a^j\right)\partial_j N\right]. \tag{6.7}$$

The conjugate momenta associated to this Lagrangian are:

$$\begin{aligned}\Pi^{ij}_\gamma =& \sqrt{\gamma}\left[\lambda'\left(N^k\partial_k \ln N - \frac{\dot{N}}{N}\right)\frac{\gamma^{ij}}{N} - \left(1-\lambda'\right)\left(K^{ij} - K\gamma^{ij}\right)\right], \\ \Pi^i_{N^i} =& 0, \\ \Pi_N =& \frac{2\sqrt{\gamma}\lambda'}{N}K, \end{aligned} \tag{6.8}$$

and we see that the inclusion of the SME term added a scalar momentum absent in GR. The corresponding Hamiltonian density reads as:

$$\begin{aligned}\mathcal{H} =& \frac{N}{\sqrt{\gamma}(1-\lambda')}\left((\Pi_\gamma)_{ij}(\Pi_\gamma)^{ij} - \frac{1}{3}\Pi_\gamma^2\right) - \\ &- \frac{N^2}{3\lambda'\sqrt{\gamma}}\left(\Pi_N\Pi_\gamma - \frac{N(1-\lambda')}{2\lambda'}\Pi_N^2\right) + \\ &+ \Pi_N N^i\partial_i\alpha + 2(\Pi_\gamma)^{ij}D_iN_j - N\sqrt{\gamma}R - 2\lambda'\sqrt{\gamma}a^j\partial_jN \end{aligned} \tag{6.9}$$

## 6.4 Discussion & Conclusions

Using standard tools in numerical relativity theory we have derived a 3+1 decomposition of the minimal SME gravity Lagrangian in the isotropic limit, using a simple form of the SME coefficient. We have also derived the associated conjugate momenta and the corresponding Hamiltonian density in ADM coordinates. We make no linearised gravity approximations, and thus this is an *exact* result. This complements other exact studies of the SME [119]. Our results can be used in ongoing work on identifying the dynamical degrees of freedom in the explicit symmetry breaking case and matching to proposed models of quantum gravity.

# 7

# Conclusions

In In this thesis I have explored aspects of Lorentz violation in a cosmological context; since Lorentz and CPT symmetry are intimately connected, some of the limits derived here also apply to the breaking of CPT symmetry. By using a combination of analytical and numerical work in the form of Markov-Chain Monte Carlo methods I have been able to derive constraints on Lorentz symmetry and the standard cosmological parameters in several models; first through a modified geometry scenario and later on using quantum gravity model candidates and effective field theory.

The most important results contained in this thesis are:

- In the context of Doubly General Relativity, when the modified dispersion relation is taken to be that of a massless particle, the *energy scale of Lorentz violation* can be constrained to be higher than $E_{\mathrm{LV}} \sim 10^{16}$ GeV at $1\sigma$.

- In the quantum gravity model candidate known as Hořava-Lifshitz gravity, when applied to a large cosmological data set and a Markov-Chain Monte Carlo method, the *curvature density* $\Omega_k$ *was found to be non-zero* at more than $1\sigma$ $(-3.30 \pm 0.20) \cdot 10^{-3}$. We also found bounds on the Hořava-Lifshitz parameters $\sigma_1$ and $\sigma_3$, which enter the Lagrange density when Lorentz invariance is no longer imposed. We found that $\sigma_1 H_0^2 = 4.073 \pm 0.038$ and $\log \sigma_3 H_0^2 = 0.4^{+1.0}_{-1.7}$.

- Using available Hubble constant data in the context of Hořava-Lifshitz gravity, the Hubble tension was considered as a preferred-frame effect. Then, using available constraints on model parameters, it was found that *Lorentz violation may contribute up to* 36% *of the Hubble tension*.

- Working in the gravitational sector of the Standard-Model Extension effective field theory in the case of explicit symmetry breaking, the 3+1 formulation of the Lagrangian was found; moreover, the full Hamiltonian and canonical degrees of freedom were derived. It was found that the Standard-Model Extension has *one additional scalar degree of freedom proportional to the coefficient for Lorentz violation*.

## 7.1 Author's Final Remarks

The open question on the nature of Quantum Gravity is clearly a weighty one, as it has kept physicists busy for over five decades with no clear end in sight. A veritable zoo of models and theories has been put forth and analysed over the years, giving us no shortage of models to modify or test with data. In this thesis I have deliberately remained agnostic about which, if any, of the candidate theories might prove to be the correct one. Instead I have picked my favourite quantum-gravity signal candidate and explored it from several points of view, as explained in Chapter 1. Some of these considerations are more general than others, starting with my formal work on the gravitational sector of the Standard-Model Extension to the consideration of specific phenomenological models like Doubly General Relativity. I have simply attempted to shine a light on Lorentz violation from as many angles as possible during these past four years, and I will continue doing so as I move to the next step in my research career.

The natural direction in which to move is, in my opinion, towards the study of gravitational waves. With the discovery of the binary black-hole merger GW150914, the stakes for any modified theory of gravity were raised significantly, giving us access to a truly strong-gravity environment for the first time and as such, many new avenues for testing gravity. It is therefore natural that the next step in testing Lorentz-violating gravity is in the nonlinear regime, for example gravitational-wave generation and binary mergers. A new constraint on models of gravity would therefore have to be the very existence of black holes which are stable to perturbations, and which can merge with an associated quadropolar gravitational-wave emission. It is this direction that I will take my research after finishing this thesis, building upon the gravitational sector of the Standard-Model Extension combined with everything else I have learnt during this journey.

I hope to find something interesting.

# A

# Cosmological Data

In order to estimate the values of the parameters present in Doubly General Relativity and Hořava-Lifshitz we used a large updated cosmological data set. The data used includes expansion rates of elliptical and lenticular galaxies [191], Type Ia Supernovae [192], Baryon Acoustic Oscillations [193–195], Cosmic Microwave Background [190] and priors on the Hubble parameter [196]. We used the parallelised Markov-Chain Monte Carlo (MCMC) code developed in Mathematica and used in many papers, for example [26, 241]. There are many cosmological MCMC codes readily available, for example CosmoMC [242] and Monte Python [243], but the advantages of our code of choice is that it is easy to add new data, and it is also simple to modify. Things such as the cosmological model, statistical method, and parameters used can easily be changed. Moreover, thanks to the flexible way in which the code is written, introducing more exotic models with varying $c$ or $G$ is also straightforward. Even though Mathematica code is generally slower than C or FORTRAN, for example, the simplicity and transparency of the code makes up for this small drawback.

All expressions below are written in the flat case ($\Omega_k^0 = 0$) for simplicity. However, $\Omega_k^0$ is left as a free parameter in the MCMC analysis, and thus all equations extend to the more general case of [244].

With this in mind, the expression for the comoving distance is:

$$D_M(z) = \begin{cases} \frac{D_H}{\sqrt{\Omega_k}} \sinh\left(\sqrt{\Omega_k}\frac{D_C(z)}{D_H}\right) & \text{for } \Omega_k^0 > 0 \\ D_C(z) & \text{for } \Omega_k^0 = 0 \\ \frac{D_H}{\sqrt{|\Omega_k^0|}} \sin\left(\sqrt{|\Omega_k^0|}\frac{D_C(z)}{D_H}\right) & \text{for } \Omega_k^0 < 0\,, \end{cases} \tag{A.1}$$

where $D_H = c_0/H_0$ is the Hubble distance, $D_C(z) = D_H \int_0^z dz'/\mathcal{E}(z')$ is the line-of-sight comoving distance, and $\mathcal{E}(z) = H(z)/H_0$. Also, luminosity distance ($D_L(z)$) and angular diameter distance ($D_A(z)$) are given by:

$$D_L(z) = (1+z)D_M(z)\,, \tag{A.2}$$

$$D_A(z) = \frac{D_M(z)}{1+z}\,. \tag{A.3}$$

### Hubble data

For Hubble parameter data, we use the compilation from [191], which is derived from the evolution of elliptical and lenticular galaxies at redshifts $0 < z < 1.97$. The expression for $\chi^2_H$ is:

$$\chi^2_H = \sum_{i=1}^{24} \frac{\left(H(z_i, \boldsymbol{\theta}) - H_{obs}(z_i)\right)^2}{\sigma^2_H(z_i)} \,, \tag{A.4}$$

where $\boldsymbol{\theta}$ is a vector containing the parameters of the model, $H_{obs}(z_i)$ are the measured values of the Hubble constant and $\sigma_H(z_i)$ are the corresponding observational errors. We will also add a prior on the Hubble constant from [196], $H_0 = 69.6 \pm 0.7$ km s$^{-1}$ Mpc$^{-1}$.

### Type Ia Supernovae

We made use of the updated JLA compilation (Joint Light-Curve Analysis) data for Type Ia supernovae (SneIa) [192] at redshifts $0 < z < 1.39$. In this case, the $\chi^2_{SN}$ is:

$$\chi^2_{SN} = \Delta\boldsymbol{\mu} \cdot \mathbf{C}^{-1}_{SN} \cdot \Delta\boldsymbol{\mu} \,, \tag{A.5}$$

where $\Delta\boldsymbol{\mu} = \mu_{theo} - \mu_{obs}$ is the difference between theoretical and observational values of the distance modulus $\mu$. $\mathbf{C}_{SN}$ is the total covariance matrix. The distance modulus is written as:

$$\mu(z, \boldsymbol{\theta}) = 5\log_{10}[D_L(z, \boldsymbol{\theta})] - \alpha X_1 + \beta\mathcal{C} + \mathcal{M}_B \,. \tag{A.6}$$

Here, $X_1$ parametrises the shape of the supernova light-curve, $\mathcal{C}$ is the colour, and $\mathcal{M}_B$ is a nuisance parameter [192], which together with the weighting parameters $\alpha$ and $\beta$ are included in $\boldsymbol{\theta}$. $D_L$ is the luminosity distance which we write as:

$$D_L(z, \boldsymbol{\theta}) = \frac{1+z}{H_0} \int_0^z \frac{\mathrm{d}z'}{\mathcal{E}(z', \boldsymbol{\theta})} \,. \tag{A.7}$$

Here, and only in this Supernova analysis, we do specify $H_0 = 70$ km/s Mpc$^{-1}$ [192].

### Baryon Acoustic Oscillations

The total $\chi^2$ for Baryon Acoustic Oscillations is given by:

$$\chi^2_{BAO} = \Delta\boldsymbol{\mathcal{F}}^{BAO} \cdot \mathbf{C}^{-1}_{BAO} \cdot \Delta\boldsymbol{\mathcal{F}}^{BAO}\,, \tag{A.8}$$

where $\boldsymbol{\mathcal{F}}^{BAO}$ is different from survey to survey. In this work, we used the WiggleZ Dark Energy Survey with redshifts $z = \{0.44, 0.6, 0.73\}$ [193]. For this analysis the acoustic parameter and the Alcock-Paczynski distortion parameter are of interest. The acoustic parameter is defined as follows:

$$A(z,\boldsymbol{\theta}) = 100\sqrt{\Omega^0_m h^2}\frac{D_V(z,\boldsymbol{\theta})}{z}\,, \tag{A.9}$$

and the Alcock-Paczynski parameter is:

$$F(z,\boldsymbol{\theta}) = (1+z)D_A(z,\boldsymbol{\theta})\,H(z,\boldsymbol{\theta})\,, \tag{A.10}$$

where $D_A$ is the angular diameter distance, which is Eq. (A.3) in the case of $\Omega^0_k = 0$:

$$D_A(z,\boldsymbol{\theta}) = \frac{1}{H_0}\frac{1}{1+z}\int_0^z \frac{\mathrm{d}z'}{\mathcal{E}(z',\boldsymbol{\theta})}\,, \tag{A.11}$$

and $D_V$ is the geometric mean of the physical angular diameter distance $D_A$ and the Hubble function $H(z)$. It reads as:

$$D_V(z,\boldsymbol{\theta}) = \left[(1+z)^2 D_A^2(z,\boldsymbol{\theta})\frac{z}{H(z,\boldsymbol{\theta})}\right]^{1/3}. \tag{A.12}$$

Included in the Baryon Acoustic Oscillation analysis is also data from Sloan Digital Sky Survey (SDSS-III) Baryon Oscillation Spectroscopic Survey (BOSS) DR12 [194]. It can be written as:

$$D_M(z)\frac{r_s^{mod}(z_d)}{r_s(z_d)} \qquad \text{and} \qquad H(z)\frac{r_s(z_d)}{r_s^{mod}(z_d)} \tag{A.13}$$

Here, $r_s(z_d)$ represents the sound horizon at the *dragging redshift* $z_d$. $r_s^{mod}(z_d)$ is the same horizon, but evaluated for the given cosmological model. Here, it is used that $r_s^{mod}(z_d) = 147.78$ Mpc as in [194]. A good approximation of the sound horizon can

be found in [245]:

$$z_d = \frac{1291(\Omega_m^0 h^2)^{0.251}}{1+0.659(\Omega_m^0 h^2)^{0.828}}\left[1+b_1(\Omega_b^0 h^2)^{b2}\right] , \tag{A.14}$$

where

$$\begin{aligned} b_1 &= 0.313(\Omega_m^0 h^2)^{-0.419}\left[1+0.607(\Omega_m^0 h^2)^{0.6748}\right], \\ b_2 &= 0.238(\Omega_m^0 h^2)^{0.223}. \end{aligned} \tag{A.15}$$

The sound horizon $r_s$ can then be defined as:

$$r_s(z,\boldsymbol{\theta}) = \int_z^\infty \frac{c_s(z')}{H(z',\boldsymbol{\theta})}\mathrm{d}z' , \tag{A.16}$$

and the sound speed is given by:

$$c_s(z) = \frac{1}{\sqrt{3(1+\overline{R}_b\,(1+z)^{-1})}} , \tag{A.17}$$

and

$$\overline{R}_b = 31500\Omega_b^0 h^2\,(T_{CMB}/2.7)^{-4} , \tag{A.18}$$

with $T_{CMB} = 2.726$ K.

Ending the Baryon Acoustic Oscillation analysis, considered data from the Quasar-Lyman $\alpha$ Forest from Sloan Digital Sky Survey - Baryon Oscillation Spectroscopic Survey DR11 [195]:

$$\frac{D_A(z=2.36)}{r_s(z_d)} = 10.8\pm0.4 , \tag{A.19}$$

$$\frac{1}{H(z=2.36)r_s(z_d)} = 9.0\pm0.3 . \tag{A.20}$$

With the contributions mentioned throughout this section, the total $\chi^2$ for Baryon Acoustic Oscillations will be $\chi^2_{BAO} = \chi^2_{WiggleZ} + \chi^2_{BOSS} + \chi^2_{Lyman}$.

### Cosmic Microwave Background

In this analysis, we write the $\chi^2$ for the Cosmic Microwave Background (CMB) in the following way:

$$\chi^2_{CMB} = \Delta\boldsymbol{\mathcal{F}}^{CMB} \cdot \mathbf{C}^{-1}_{CMB} \cdot \Delta\boldsymbol{\mathcal{F}}^{CMB} \,. \tag{A.21}$$

Here, $\boldsymbol{\mathcal{F}}^{CMB}$ is a vector quantity given in [246], which summarises the information available in the full power spectrum of the Cosmic Microwave Background from the 2015 Planck data release [190]. $\boldsymbol{\mathcal{F}}^{CMB}$ contains the Cosmic Microwave Background shift parameters and the baryonic density parameter. The shift parameters are:

$$\begin{aligned} R(\boldsymbol{\theta}) &\equiv \sqrt{\Omega^0_m H^2_0} r(z_*, \boldsymbol{\theta}) \\ l_a(\boldsymbol{\theta}) &\equiv \pi \frac{r(z_*, \boldsymbol{\theta})}{r_s(z_*, \boldsymbol{\theta})} \,, \end{aligned} \tag{A.22}$$

whereas the baryonic density parameter is simply $\Omega^0_b h^2$. As mentioned before, $r_s$ is the comoving sound horizon at the photon-decoupling redshift $z_*$, which is given by [247]:

$$z_* = 1048 \left[1 + 0.00124(\Omega^0_b h^2)^{-0.738}\right] \left(1 + g_1(\Omega^0_m h^2)^{g_2}\right) \,, \tag{A.23}$$

with:

$$g_1 = \frac{0.0783(\Omega^0_b h^2)^{-0.238}}{1 + 39.5(\Omega^0_b h^2)^{-0.763}} \,, \tag{A.24}$$

$$g_2 = \frac{0.560}{1 + 21.1(\Omega^0_b h^2)^{1.81}} \,; \tag{A.25}$$

and $r$ is the comoving distance:

$$r(z, \boldsymbol{\theta_b}) = \frac{1}{H_0} \int_0^z \frac{\mathrm{d}z'}{\mathcal{E}(z', \boldsymbol{\theta})} \mathrm{d}z' \,. \tag{A.26}$$

All the methods mentioned above all contribute to the total $\chi^2$, and the function to minimise is: $\chi^2_{tot} = \chi^2_{H_0} + \chi^2_H + \chi^2_{SN} + \chi^2_{WiggleZ} + \chi^2_{BOSS} + \chi^2_{Lyman} + \chi^2_{CMB}$.

# Bibliography


[1] Assaf Shomer. A Pedagogical explanation for the non-renormalizability of gravity (2007). arXiv: 0709.3555 [hep-th].

[2] Gerard 't Hooft. Dimensional reduction in quantum gravity. *Conf. Proc.* C930308 (1993), pp. 284–296. arXiv: gr-qc/9310026 [gr-qc].

[3] Claus Kiefer, Rainer Muller, and Tejinder P. Singh. Quantum gravity and nonunitarity in black hole evaporation. *Mod. Phys. Lett.* A9 (1994), pp. 2661–2670. DOI: 10.1142/S0217732394002501.

[4] Claus Kiefer. Quantum gravity. *Int. Ser. Monogr. Phys.* 124 (2004). [Int. Ser. Monogr. Phys.155,1(2012)], pp. 1–308.

[5] Przemyslaw Malkiewicz and Artur Miroszewski. Internal clock formulation of quantum mechanics. *Phys. Rev.* D96.4 (2017), p. 046003. DOI: 10.1103/PhysRevD.96.046003.

[6] Chris J Isham. Canonical quantum gravity and the problem of time. *Integrable systems, quantum groups, and quantum field theories*. Springer, 1993, pp. 157–287.

[7] KV Kuchař. Time and interpretations of quantum gravity. Proceedings of the 4th Canadian Conference on General Relativity and Relativistic Astrophysics. 1992.

[8] Steven Weinberg. Quantum contributions to cosmological correlations. *Phys. Rev.* D72 (2005), p. 043514. DOI: 10.1103/PhysRevD.72.043514.

[9] T. Damour and Alexander M. Polyakov. The String dilaton and a least coupling principle. *Nucl. Phys.* B423 (1994), pp. 532–558. DOI: 10.1016/0550-3213(94)90143-0.

[10] John D. Barrow. Varying G and other constants. *NATO Sci. Ser. C* 511 (1998), pp. 269–305. DOI: 10.1007/978-94-011-5046-0_8.

[11] Marcus Bleicher et al. Black hole production in large extra dimensions at the Tevatron: New limit on the fundamental scale of gravity. *Phys. Lett.* B548 (2002), pp. 73–76. DOI: 10.1016/S0370-2693(02)02732-6.

[12] V. Alan Kostelecky. Gravity, Lorentz violation, and the standard model. *Phys. Rev.* D69 (2004), p. 105009. DOI: 10.1103/PhysRevD.69.105009.

[13] Charles Lane. Using Comparisons of Clock Frequencies and Sidereal Variation to Probe Lorentz Violation. *Symmetry* 9.10 (Oct. 2017), p. 245. ISSN: 2073-8994. DOI: 10.3390/sym9100245. URL: http://dx.doi.org/10.3390/sym9100245.

[14] Sidney Coleman and Sheldon L. Glashow. High-energy tests of Lorentz invariance. *Phys. Rev. D* 59 (11 Apr. 1999), p. 116008. DOI: 10.1103/PhysRevD.59.116008. URL: https://link.aps.org/doi/10.1103/PhysRevD.59.116008.

[15] Sidney Coleman and Sheldon L. Glashow. Cosmic ray and neutrino tests of special relativity. *Physics Letters B* 405.3 (1997), pp. 249–252. ISSN: 0370-2693. DOI: https://doi.org/10.1016/S0370-2693(97)00638-2. URL: http://www.sciencedirect.com/science/article/pii/S0370269397006382.

[16] Matthew Mewes. Signals for Lorentz violation in gravitational waves. *Phys. Rev.* D99.10 (2019), p. 104062. DOI: 10.1103/PhysRevD.99.104062.

[17] Lijing Shao. Combined search for anisotropic birefringence in the gravitational-wave transient catalog GWTC-1 (2020). arXiv: 2002.01185 [hep-ph].

[18] Malcolm Fairbairn et al. The CTA Sensitivity to Lorentz-Violating Effects on the Gamma-Ray Horizon. *JCAP* 1406 (2014), p. 005. DOI: 10.1088/1475-7516/2014/06/005.

[19] Julian S. Schwinger. The Theory of quantized fields. 1. *Phys. Rev.* 82 (1951). [,132(1951)], pp. 914–927. DOI: 10.1103/PhysRev.82.914.

[20] O. W. Greenberg. *CPT* Violation Implies Violation of Lorentz Invariance. *Phys. Rev. Lett.* 89 (23 Nov. 2002), p. 231602. DOI: 10.1103/PhysRevLett.89.231602. URL: https://link.aps.org/doi/10.1103/PhysRevLett.89.231602.

[21] Aleksander Gajos. Tests of discrete symmetries and quantum coherence with neutral kaons at the KLOE-2 experiment. *Acta Phys. Polon.* B48 (2017), p. 1975. DOI: 10.5506/APhysPolB.48.1975.

[22] Jose Bernabeu et al. CPT and Quantum Mechanics Tests with Kaons. *Frascati Phys. Ser.* 43 (2007), pp. 39–83. arXiv: hep-ph/0607322 [hep-ph].

[23] John A. Wheeler. On the Nature of quantum geometrodynamics. *Annals Phys.* 2 (1957), pp. 604–614. DOI: 10.1016/0003-4916(57)90050-7.

[24] John Archibald Wheeler. Geons. *Phys. Rev.* 97 (2 Jan. 1955), pp. 511–536. DOI: 10.1103/PhysRev.97.511. URL: https://link.aps.org/doi/10.1103/PhysRev.97.511.

[25] Nick E Mavromatos. On CPT symmetry: Cosmological, quantum gravitational and other possible violations and their phenomenology. *Springer Proc. Phys.* 92 (2004). [,43(2003)], pp. 43–72. arXiv: hep-ph/0309221 [hep-ph].

[26] Nils Albin Nilsson and Mariusz P. Dabrowski. Energy Scale of Lorentz Violation in Rainbow Gravity. *Phys. Dark Univ.* 18 (2017), pp. 115–122. DOI: 10.1016/j.dark.2017.10.003.

[27] Nils A. Nilsson and Ewa Czuchry. Hořava-Lifshitz cosmology in light of new data. *Phys. Dark Univ.* 23 (2019), p. 100253. DOI: 10.1016/j.dark.2018.100253.

[28] Nils A. Nilsson. Preferred-frame Effects, the $H_0$ Tension, and Probes of Hořava-Lifshitz Gravity (2019). arXiv: 1910.14414 [gr-qc].

[29] Nils A. Nilsson, Kellie O'Neal-Ault, and Quentin G. Bailey. A 3+1 Decomposition of the Minimal Standard-Model Extension Gravitational Sector. *8th Meeting on CPT and Lorentz Symmetry (CPT'19) Bloomington, Indiana, USA, May 12-16, 2019*. 2019. arXiv: 1905.10414 [gr-qc].

[30] V. Alan Kostelecky. The Status of CPT. *Physics beyond the standard model. Proceedings, 5th International WEIN Symposium, Santa Fe, USA, June 14-19, 1998*. 1998, pp. 588–600. arXiv: hep-ph/9810365 [hep-ph].

[31] Masud Chaichian et al. CPT Violation Does Not Lead to Violation of Lorentz Invariance and Vice Versa. *Phys. Lett.* B699 (2011), pp. 177–180. DOI: 10.1016/j.physletb.2011.03.026.

[32] O. W. Greenberg. Why is CPT fundamental? *Found. Phys.* 36 (2006), pp. 1535–1553. DOI: 10.1007/s10701-006-9070-z.

[33] O. W. A Greenberg. Remarks on a Challenge to the Relation between *CPT* and Lorentz Violation (2011). arXiv: 1105.0927 [hep-ph].

[34] Michael Duetsch and Jose M. Gracia-Bondia. On the assertion that PCT violation implies Lorentz non-invariance. *Phys. Lett.* B711 (2012), pp. 428–433. DOI: 10.1016/j.physletb.2012.04.038.

[35] Jay D. Tasson. What Do We Know About Lorentz Invariance? *Rept. Prog. Phys.* 77 (2014), p. 062901. DOI: 10.1088/0034-4885/77/6/062901.

[36] Robert Bluhm, Shu-Hong Fung, and V. Alan Kostelecky. Spontaneous Lorentz and Diffeomorphism Violation, Massive Modes, and Gravity. *Phys. Rev.* D77 (2008), p. 065020. DOI: 10.1103/PhysRevD.77.065020.

[37] Robert Bluhm. Gravity Theories with Background Fields and Spacetime Symmetry Breaking. *Symmetry* 9.10 (2017), p. 230. DOI: 10.3390/sym9100230.

[38] Robert Bluhm. Explicit versus Spontaneous Diffeomorphism Breaking in Gravity. *Phys. Rev.* D91.6 (2015), p. 065034. DOI: 10.1103/PhysRevD.91.065034.

[39] Robert Bluhm. Consequences of Spontaneous Lorentz Violation in Gravity. *Proceedings, 13th Marcel Grossmann Meeting on Recent Developments in Theoretical and Experimental General Relativity, Astrophysics, and Relativistic Field Theories (MG13): Stockholm, Sweden, July 1-7, 2012*. 2015, pp. 1255–1257. DOI: 10.1142/9789814623995_0139.

[40] Robert M. Wald. Quantum gravity and time reversibility. *Phys. Rev. D* 21 (10 May 1980), pp. 2742–2755. DOI: 10.1103/PhysRevD.21.2742. URL: https://link.aps.org/doi/10.1103/PhysRevD.21.2742.

[41] Wendy L. Freedman et al. The Carnegie-Chicago Hubble Program. VIII. An Independent Determination of the Hubble Constant Based on the Tip of the Red Giant Branch (2019). DOI: 10.3847/1538-4357/ab2f73.

[42] W. D'Arcy Kenworthy, Dan Scolnic, and Adam Riess. The Local Perspective on the Hubble Tension: Local Structure Does Not Impact Measurement of the Hubble Constant. *Astrophys. J.* 875.2 (2019), p. 145. DOI: 10.3847/1538-4357/ab0ebf.

[43] Kenneth C. Wong et al. H0LiCOW XIII. A 2.4% measurement of $H_0$ from lensed quasars: 5.3$\sigma$ tension between early and late-Universe probes (2019). arXiv: 1907.04869 [astro-ph.CO].

[44] Adam G. Riess et al. Observational evidence from supernovae for an accelerating universe and a cosmological constant. *Astron. J.* 116 (1998), pp. 1009–1038. DOI: 10.1086/300499.

[45] David H. Weinberg et al. Observational probes of cosmic acceleration. *Physics Reports* 530.2 (Sept. 2013), pp. 87–255. ISSN: 0370-1573. DOI: 10.1016/j.physrep.2013.05.001. URL: http://dx.doi.org/10.1016/j.physrep.2013.05.001.

[46] Jeppe Trøst Nielsen, Alberto Guffanti, and Subir Sarkar. Marginal evidence for cosmic acceleration from Type Ia supernovae. *Sci. Rep.* 6 (2016), p. 35596. DOI: 10.1038/srep35596.

[47] Adam G. Riess. The Expansion of the Universe is Faster than Expected. *Nature Rev. Phys.* 2.1 (2019), pp. 10–12. DOI: 10.1038/s42254-019-0137-0.

[48] Juan Casado. Linear expansion models vs. standard cosmologies: a critical and historical overview. *Astrophys. Space Sci.* 365.1 (2020), p. 16. DOI: 10.1007/s10509-019-3720-z.

[49] Jacques Colin et al. A response to Rubin & Heitlauf: "Is the expansion of the universe accelerating? All signs still point to yes" (2019). arXiv: 1912.04257 [astro-ph.CO].

[50] Mohamed Rameez. Concerns about the reliability of publicly available SNe Ia data (2019). arXiv: 1905.00221 [astro-ph.CO].

[51] Ram Gopal Vishwakarma and Jayant V. Narlikar. Is it no Longer Necessary to Test Cosmologies with Type Ia Supernovae? *Universe* 4.6 (2018), p. 73. DOI: 10.3390/universe4060073.

[52] David Mattingly. Modern tests of Lorentz invariance. *Living Rev. Rel.* 8 (2005), p. 5. DOI: 10.12942/lrr-2005-5.

[53] G. M. Tino et al. Precision Gravity Tests and the Einstein Equivalence Principle (2020). arXiv: 2002.02907 [gr-qc].

[54] Lijing Shao and Quentin G. Bailey. Testing the gravitational weak equivalence principle in the standard model extension with binary pulsars. *Phys. Rev. D* 99 (8 Apr. 2019), p. 084017. DOI: 10.1103/PhysRevD.99.084017. URL: https://link.aps.org/doi/10.1103/PhysRevD.99.084017.

[55] Lijing Shao. Pulsar tests of the gravitational Lorentz violation. *8th Meeting on CPT and Lorentz Symmetry (CPT'19) Bloomington, Indiana, USA, May 12-16, 2019*. 2019. arXiv: 1905.08405 [gr-qc].

[56] Joao Magueijo and Lee Smolin. Gravity's rainbow. *Class. Quant. Grav.* 21 (2004), pp. 1725–1736. DOI: 10.1088/0264-9381/21/7/001.

[57] Ahmed Farag Ali and Mohammed M. Khalil. A Proposal for Testing Gravity's Rainbow. *Europhys. Lett.* 110.2 (2015), p. 20009. DOI: 10.1209/0295-5075/110/20009.

[58] Adel Awad, Ahmed Farag Ali, and Barun Majumder. Nonsingular Rainbow Universes. *JCAP* 1310 (2013), p. 052. DOI: 10.1088/1475-7516/2013/10/052.

[59] Yi Ling. Rainbow universe. *JCAP* 0708 (2007), p. 017. DOI: 10.1088/1475-7516/2007/08/017.

[60] Bogeun Gwak, Wontae Kim, and Bum-Hoon Lee. Note on the speed of GW150914 in gravity's rainbow (2016). arXiv: 1608.04247 [gr-qc].

[61] M. Khodadi, K. Nozari, and H. R. Sepangi. More on the initial singularity problem in gravity's rainbow cosmology. *Gen. Rel. Grav.* 48.12 (2016), p. 166. DOI: 10.1007/s10714-016-2160-0.

[62] Yi Ling, Song He, and Hong-bao Zhang. The Kinematics of particles moving in rainbow spacetime. *Mod. Phys. Lett.* A22 (2007), pp. 2931–2938. DOI: 10.1142/S0217732307022980.

[63] Yi Ling and Qingzhang Wu. The Big Bounce in Rainbow Universe. *Phys. Lett.* B687 (2010), pp. 103–109. DOI: 10.1016/j.physletb.2010.03.028.

[64] M. Khodadi et al. On the Stability of Einstein Static Universe in Doubly General Relativity Scenario. *Eur. Phys. J.* C75.12 (2015), p. 590. DOI: 10.1140/epjc/s10052-015-3821-y.

[65] Chengzhou Liu and Haiwen Liu. Spectroscopy of a charged black hole in gravity's rainbow via an action invariance. *Astrophys. Space Sci.* 357.2 (2015), p. 114. DOI: 10.1007/s10509-015-2342-3.

[66] Remo Garattini and Barun Majumder. Electric Charges and Magnetic Monopoles in Gravity's Rainbow. *Nucl. Phys.* B883 (2014), pp. 598–614. DOI: 10.1016/j.nuclphysb.2014.04.005.

[67] Pablo Galan and Guillermo A. Mena Marugan. Length uncertainty in a gravity's rainbow formalism. *Phys. Rev.* D72 (2005), p. 044019. DOI: 10.1103/PhysRevD.72.044019.

[68] Pablo Galan and Guillermo A. Mena Marugan. Quantum time uncertainty in a gravity's rainbow formalism. *Phys. Rev.* D70 (2004), p. 124003. DOI: 10.1103/PhysRevD.70.124003.

[69] Ahmed Farag Ali, Mir Faizal, and Mohammed M. Khalil. Absence of Black Holes at LHC due to Gravity's Rainbow. *Phys. Lett.* B743 (2015), pp. 295–300. DOI: 10.1016/j.physletb.2015.02.065.

[70] Amani Ashour et al. Branes in Gravity's Rainbow. *Eur. Phys. J.* C76.5 (2016), p. 264. DOI: 10.1140/epjc/s10052-016-4124-7.

[71] Ahmed Farag Ali et al. Gravitational Collapse in Gravity's Rainbow. *Int. J. Geom. Meth. Mod. Phys.* 12.09 (2015), p. 1550085. DOI: 10.1142/S0219887815500851.

[72] Joao Magueijo and Lee Smolin. Lorentz invariance with an invariant energy scale. *Phys. Rev. Lett.* 88 (2002), p. 190403. DOI: 10.1103/PhysRevLett.88.190403.

[73] Joao Magueijo and Lee Smolin. Generalized Lorentz invariance with an invariant energy scale. *Phys. Rev.* D67 (2003), p. 044017. DOI: 10.1103/PhysRevD.67.044017.

[74] G. Amelino-Camelia et al. Distance measurement and wave dispersion in a Liouville string approach to quantum gravity. *Int. J. Mod. Phys.* A12 (1997), pp. 607–624. DOI: 10.1142/S0217751X97000566.

[75] Anzhong Wang. Hořava gravity at a Lifshitz point: A progress report. *Int. J. Mod. Phys.* D26.07 (2017), p. 1730014. DOI: 10.1142/S0218271817300142.

[76] Petr Hořava. Quantum Gravity at a Lifshitz Point. *Phys. Rev.* D79 (2009), p. 084008. DOI: 10.1103/PhysRevD.79.084008.

[77] D. Blas, O. Pujolas, and S. Sibiryakov. Consistent Extension of Hořava Gravity. *Phys. Rev. Lett.* 104 (2010), p. 181302. DOI: 10.1103/PhysRevLett.104.181302.

[78] Ted Jacobson. Einstein-aether gravity: A Status report. *PoS* QG-PH (2007), p. 020. DOI: 10.22323/1.043.0020.

[79] Christopher Eling, Ted Jacobson, and David Mattingly. Einstein-Aether theory. *Deserfest: A celebration of the life and works of Stanley Deser. Proceedings, Meeting, Ann Arbor, USA, April 3-5, 2004*. 2004, pp. 163–179. arXiv: gr-qc/0410001 [gr-qc].

[80] Ted Jacobson and David Mattingly. Gravity with a dynamical preferred frame. *Phys. Rev.* D64 (2001), p. 024028. DOI: 10.1103/PhysRevD.64.024028.

[81] Kent Yagi et al. Strong Binary Pulsar Constraints on Lorentz Violation in Gravity. *Phys. Rev. Lett.* 112.16 (2014), p. 161101. DOI: 10.1103/PhysRevLett.112.161101.

[82] Kent Yagi et al. Constraints on Einstein-Æther theory and Hořava gravity from binary pulsar observations. *Phys. Rev.* D89.8 (2014). [Erratum: Phys. Rev.D90,no.6,069901(2014)], p. 084067. DOI: 10.1103/PhysRevD.90.069902, 10.1103/PhysRevD.90.069901, 10.1103/PhysRevD.89.084067.

[83] Clifford M. Will. The Confrontation between general relativity and experiment. *Living Rev. Rel.* 9 (2006), p. 3. DOI: 10.12942/lrr-2006-3.

[84] Yungui Gong et al. Gravitational waves in Einstein-aether and generalized TeVeS theory after GW170817. *Phys. Rev.* D97.8 (2018), p. 084040. DOI: 10.1103/PhysRevD.97.084040.

[85] Brendan Z. Foster and Ted Jacobson. Post-Newtonian parameters and constraints on Einstein-aether theory. *Phys. Rev.* D73 (2006), p. 064015. DOI: 10.1103/PhysRevD.73.064015.

[86] Brendan Z. Foster. Strong field effects on binary systems in Einstein-aether theory. *Phys. Rev.* D76 (2007), p. 084033. DOI: 10.1103/PhysRevD.76.084033.

[87] Joshua W. Elliott, Guy D. Moore, and Horace Stoica. Constraining the new Aether: Gravitational Cerenkov radiation. *JHEP* 08 (2005), p. 066. DOI: 10.1088/1126-6708/2005/08/066.

[88] Sean M. Carroll and Eugene A. Lim. Lorentz-violating vector fields slow the universe down. *Phys. Rev.* D70 (2004), p. 123525. DOI: 10.1103/PhysRevD.70.123525.

[89] David Mattingly and Ted Jacobson. Relativistic gravity with a dynamical preferred frame. *CPT and Lorentz symmetry. Proceedings: 2nd Meeting, Bloomington, USA, Aug 15-18, 2001*. 2002, pp. 331–335. DOI: 10.1142/9789812778123_0042.

[90] T. Jacobson and D. Mattingly. Einstein-Aether waves. *Phys. Rev.* D70 (2004), p. 024003. DOI: 10.1103/PhysRevD.70.024003.

[91] Christopher Eling and Ted Jacobson. Static postNewtonian equivalence of GR and gravity with a dynamical preferred frame. *Phys. Rev.* D69 (2004), p. 064005. DOI: 10.1103/PhysRevD.69.064005.

[92] Michael D. Seifert. Generalized bumblebee models and Lorentz-violating electrodynamics. *Phys. Rev.* D81 (2010), p. 065010. DOI: 10.1103/PhysRevD.81.065010.

[93] Michael D. Seifert. Vector models of gravitational Lorentz symmetry breaking. *Phys. Rev.* D79 (2009), p. 124012. DOI: 10.1103/PhysRevD.79.124012.

[94] O. Bertolami and J. Paramos. The Flight of the bumblebee: Vacuum solutions of a gravity model with vector-induced spontaneous Lorentz symmetry breaking. *Phys. Rev.* D72 (2005), p. 044001. DOI: 10.1103/PhysRevD.72.044001.

[95] R. Casana et al. Exact Schwarzschild-like solution in a bumblebee gravity model. *Phys. Rev.* D97.10 (2018), p. 104001. DOI: 10.1103/PhysRevD.97.104001.

[96] A. F. Santos et al. Gödel solution in the bumblebee gravity. *Mod. Phys. Lett.* A30.02 (2015), p. 1550011. DOI: 10.1142/S021773231550011X.

[97] Y. Nambu. Quantum electrodynamics in nonlinear gauge. *Prog. Theor. Phys. Suppl.* E68 (1968), pp. 190–195. DOI: 10.1143/PTPS.E68.190.

[98] Clifford M. Will and Kenneth Nordtvedt Jr. Conservation Laws and Preferred Frames in Relativistic Gravity. I. Preferred-Frame Theories and an Extended PPN Formalism. *Astrophys. J.* 177 (1972), p. 757. DOI: 10.1086/151754.

[99] Ronald W. Hellings and Kenneth Nordtvedt. Vector-Metric Theory of Gravity. *Phys. Rev.* D7 (1973), pp. 3593–3602. DOI: 10.1103/PhysRevD.7.3593.

[100] V. Alan Kostelecky and Ralf Lehnert. Stability, causality, and Lorentz and CPT violation. *Phys. Rev.* D63 (2001), p. 065008. DOI: 10.1103/PhysRevD.63.065008.

[101] Alejandro Jenkins. Spontaneous breaking of Lorentz invariance. *Phys. Rev.* D69 (2004), p. 105007. DOI: 10.1103/PhysRevD.69.105007.

[102] Per Kraus and E. T. Tomboulis. Photons and gravitons as Goldstone bosons, and the cosmological constant. *Phys. Rev.* D66 (2002), p. 045015. DOI: 10.1103/PhysRevD.66.045015.

[103] Don Colladay and V. Alan Kostelecky. Lorentz violating extension of the standard model. *Phys. Rev.* D58 (1998), p. 116002. DOI: 10.1103/PhysRevD.58.116002.

[104] Don Colladay and V. Alan Kostelecky. CPT violation and the standard model. *Phys. Rev.* D55 (1997), pp. 6760–6774. DOI: 10.1103/PhysRevD.55.6760.

[105] Cheng-Gang Shao et al. Limits on Lorentz violation in gravity from worldwide superconducting gravimeters. *Phys. Rev. D* 97 (2 Jan. 2018), p. 024019. DOI: 10.1103/PhysRevD.97.024019. URL: https://link.aps.org/doi/10.1103/PhysRevD.97.024019.

[106] Natasha A. Flowers, Casey Goodge, and Jay D. Tasson. Superconducting-Gravimeter Tests of Local Lorentz Invariance. *Phys. Rev. Lett.* 119.20 (2017), p. 201101. DOI: 10.1103/PhysRevLett.119.201101.

[107] Jay D. Tasson. Lorentz violation, gravitomagnetism, and intrinsic spin. *Phys. Rev. D* 86 (12 Dec. 2012), p. 124021. DOI: 10.1103/PhysRevD.86.124021. URL: https://link.aps.org/doi/10.1103/PhysRevD.86.124021.

[108] Benjamin P. Abbott et al. Gravitational Waves and Gamma-rays from a Binary Neutron Star Merger: GW170817 and GRB 170817A. *Astrophys. J.* 848.2 (2017), p. L13. DOI: 10.3847/2041-8213/aa920c.

[109] Alan V. Kostelecky and Jay D. Tasson. Matter-gravity couplings and Lorentz violation. *Phys. Rev.* D83 (2011), p. 016013. DOI: 10.1103/PhysRevD.83.016013.

[110] A. Hees et al. Testing Lorentz symmetry with planetary orbital dynamics. *Phys. Rev. D* 92 (6 Sept. 2015), p. 064049. DOI: 10.1103/PhysRevD.92.064049. URL: https://link.aps.org/doi/10.1103/PhysRevD.92.064049.

[111] Michael A. Hohensee, Holger Müller, and R. B. Wiringa. Equivalence Principle and Bound Kinetic Energy. *Phys. Rev. Lett.* 111 (15 Oct. 2013), p. 151102. DOI: 10.1103/PhysRevLett.111.151102. URL: https://link.aps.org/doi/10.1103/PhysRevLett.111.151102.

[112] Michael A. Hohensee et al. Equivalence Principle and Gravitational Redshift. *Phys. Rev. Lett.* 106 (15 Apr. 2011), p. 151102. DOI: 10.1103/PhysRevLett.106.151102. URL: https://link.aps.org/doi/10.1103/PhysRevLett.106.151102.

[113] Helene Pihan-Le Bars et al. New Test of Lorentz Invariance Using the MICROSCOPE Space Mission. *Phys. Rev. Lett.* 123.23 (2019), p. 231102. DOI: 10.1103/PhysRevLett.123.231102.

[114] Geoffrey Mo et al. The MICROSCOPE Space Mission and Lorentz Violation. *8th Meeting on CPT and Lorentz Symmetry (CPT'19) Bloomington, Indiana, USA, May 12-16, 2019*. 2019. arXiv: 1912.07591 [hep-ph].

[115] Lijing Shao. Lorentz-Violating Matter-Gravity Couplings in Small-Eccentricity Binary Pulsars. *Symmetry* 11.9 (2019), p. 1098. DOI: 10.3390/sym11091098.

[116] C. Le Poncin-Lafitte, A. Hees, and S. Lambert. Lorentz symmetry and Very Long Baseline Interferometry. *Phys. Rev.* D94.12 (2016), p. 125030. DOI: 10.1103/PhysRevD.94.125030.

[117] V. Alan Kostelecky and Neil Russell. Data Tables for Lorentz and CPT Violation. *Rev. Mod. Phys.* 83 (2011), pp. 11–31. DOI: 10.1103/RevModPhys.83.11.

[118] Yuri Bonder and Gabriel Leon. Inflation as an amplifier: the case of Lorentz violation. *Phys. Rev.* D96.4 (2017), p. 044036. DOI: 10.1103/PhysRevD.96.044036.

[119] Yuri Bonder. Lorentz violation in the gravity sector: The t puzzle. *Phys. Rev.* D91.12 (2015), p. 125002. DOI: 10.1103/PhysRevD.91.125002.

[120] Giovanni Amelino-Camelia. Testable scenario for relativity with minimum length. *Phys. Lett.* B510 (2001), pp. 255–263. DOI: 10.1016/S0370-2693(01)00506-8.

[121] Giovanni Amelino-Camelia. Relativity in space-times with short distance structure governed by an observer independent (Planckian) length scale. *Int. J. Mod. Phys.* D11 (2002), pp. 35–60. DOI: 10.1142/S0218271802001330.

[122] G. P. de Brito et al. Effective models of quantum gravity induced by Planck scale modifications in the covariant quantum algebra (2016). arXiv: 1610.01480 [hep-th].

[123] Niloofar Abbasvandi et al. Quantum gravity effects on charged microblack holes thermodynamics. *Int. J. Mod. Phys.* A31.23 (2016), p. 1650129. DOI: 10.1142/S0217751X16501293.

[124] A. Tawfik, H. Magdy, and A. Farag Ali. Lorentz Invariance Violation and Generalized Uncertainty Principle. *Phys. Part. Nucl. Lett.* 13 (2016), pp. 59–68. DOI: 10.1134/S1547477116010179.

[125] Iarley P. Lobo, Niccoló Loret, and Francisco Nettel. Rainbows without unicorns: Metric structures in theories with Modified Dispersion Relations (2016). arXiv: 1610.04277 [gr-qc].

[126] Aurélien Hees et al. Tests of Lorentz symmetry in the gravitational sector. *Universe* 2.4 (2016), p. 30. DOI: 10.3390/universe2040030.

[127] R. J. Protheroe and H. Meyer. An Infrared background TeV gamma-ray crisis? *Phys. Lett.* B493 (2000), pp. 1–6. DOI: 10.1016/S0370-2693(00)01113-8.

[128] John R. Ellis, N. E. Mavromatos, and Dimitri V. Nanopoulos. Space-time foam effects on particle interactions and the GZK cutoff. *Phys. Rev.* D63 (2001), p. 124025. DOI: 10.1103/PhysRevD.63.124025.

[129] F. W. Stecker and Sheldon L. Glashow. New tests of Lorentz invariance following from observations of the highest energy cosmic gamma-rays. *Astropart. Phys.* 16 (2001), pp. 97–99. DOI: 10.1016/S0927-6505(01)00137-2.

[130] Floyd W. Stecker. Constraints on Lorentz invariance violating quantum gravity and large extra dimensions models using high energy gamma-ray observations. *Astropart. Phys.* 20 (2003), pp. 85–90. DOI: 10.1016/j.astropartphys.2003.08.006.

[131] G. Amelino-Camelia et al. Tests of quantum gravity from observations of gamma-ray bursts. *Nature* 393 (1998), pp. 763–765. DOI: 10.1038/31647.

[132] Giovanni Amelino-Camelia. Quantum-Spacetime Phenomenology. *Living Rev. Rel.* 16 (2013), p. 5. DOI: 10.12942/lrr-2013-5.

[133] Giovanni Amelino-Camelia et al. Quantum-gravity-induced dual lensing and IceCube neutrinos (2016). arXiv: 1609.03982 [gr-qc].

[134] Giacomo Rosati et al. Planck-scale-modified dispersion relations in FRW spacetime. *Phys. Rev.* D92.12 (2015), p. 124042. DOI: 10.1103/PhysRevD.92.124042.

[135] Uri Jacob and Tsvi Piran. Lorentz-violation-induced arrival delays of cosmological particles. *JCAP* 0801 (2008), p. 031. DOI: 10.1088/1475-7516/2008/01/031.

[136] Tadashi Kifune. Invariance violation extends the cosmic ray horizon? *Astrophys. J.* 518 (1999), pp. L21–L24. DOI: 10.1086/312057.

[137] Jay D. Tasson. The Standard-Model Extension and Gravitational Tests (2016). arXiv: 1610.05357 [gr-qc].

[138] John Ellis et al. A Search in Gamma-Ray Burst Data for Nonconstancy of the Velocity of Light. *The Astrophysical Journal* 535.1 (2000), p. 139. URL: http://stacks.iop.org/0004-637X/535/i=1/a=139.

[139] Andreas Albrecht and Joao Magueijo. A Time varying speed of light as a solution to cosmological puzzles. *Phys. Rev.* D59 (1999), p. 043516. DOI: 10.1103/PhysRevD.59.043516.

[140] John D. Barrow. Cosmologies with varying light speed. *Phys. Rev. D* 59 (4 Jan. 1999), p. 043515. DOI: 10.1103/PhysRevD.59.043515.

[141] John D. Barrow and Joao Magueijo. Varying alpha theories and solutions to the cosmological problems. *Phys. Lett.* B443 (1998), pp. 104–110. DOI: 10.1016/S0370-2693(98)01294-5.

[142] Katarzyna Leszczyńska, Adam Balcerzak, and Mariusz P. Dabrowski. Varying constants quantum cosmology. *JCAP* 1502.02 (2015), p. 012. DOI: 10.1088/1475-7516/2015/02/012.

[143] Mariusz P. Dabrowski and Konrad Marosek. Regularizing cosmological singularities by varying physical constants. *JCAP* 1302 (2013), p. 012. DOI: 10.1088/1475-7516/2013/02/012.

[144] A. Abramowski et al. Search for Lorentz Invariance breaking with a likelihood fit of the PKS 2155-304 Flare Data Taken on MJD 53944. *Astropart. Phys.* 34 (2011), pp. 738–747. DOI: 10.1016/j.astropartphys.2011.01.007.

[145] Petr Horava. Membranes at Quantum Criticality. *JHEP* 03 (2009), p. 020. DOI: 10.1088/1126-6708/2009/03/020.

[146] S. H. Hendi et al. Modified TOV in gravity's rainbow: properties of neutron stars and dynamical stability conditions. *JCAP* 1609.09 (2016), p. 013. DOI: 10.1088/1475-7516/2016/09/013.

[147] V. B. Bezerra et al. Exact solutions and phenomenological constraints from massive scalars in a Gravity's Rainbow spacetime (2017). arXiv: 1704.01211 [gr-qc].

[148] Ricardo Gallego Torromé, Marco Letizia, and Stefano Liberati. Phenomenology of effective geometries from quantum gravity. *Phys. Rev.* D92.12 (2015), p. 124021. DOI: 10.1103/PhysRevD.92.124021.

[149] Sunandan Gangopadhyay and Abhijit Dutta. Constraints on rainbow gravity functions from black hole thermodynamics. *Europhys. Lett.* 115.5 (2016), p. 50005. DOI: 10.1209/0295-5075/115/50005.

[150] Fernando Quevedo. Is String Phenomenology an Oxymoron? *[arXiv:1612.01569]* (2016). arXiv: 1612.01569 [hep-th].

[151] Florian Girelli, Franz Hinterleitner, and Seth Major. Loop Quantum Gravity Phenomenology: Linking Loops to Observational Physics. *SIGMA* 8 (2012), p. 098. DOI: 10.3842/SIGMA.2012.098.

[152] Benjamin P. Abbott et al. Observation of Gravitational Waves from a Binary Black Hole Merger. *Phys. Rev. Lett.* 116.6 (2016), p. 061102. DOI: 10.1103/PhysRevLett.116.061102.

[153] Benjamin P. Abbott et al. GW170817: Observation of Gravitational Waves from a Binary Neutron Star Inspiral. *Phys. Rev. Lett.* 119.16 (2017), p. 161101. DOI: 10.1103/PhysRevLett.119.161101.

[154] E. Troja et al. The X-ray counterpart to the gravitational wave event GW 170817. *Nature* 551 (2017). [Nature551,71(2017)], pp. 71–74. DOI: 10.1038/nature24290.

[155] C. Brans and R. H. Dicke. Mach's Principle and a Relativistic Theory of Gravitation. *Phys. Rev.* 124 (3 Nov. 1961), pp. 925–935. DOI: 10.1103/PhysRev.124.925.

[156] Diego Blas and Hillary Sanctuary. Gravitational Radiation in Hořava Gravity. *Phys. Rev.* D84 (2011), p. 064004. DOI: 10.1103/PhysRevD.84.064004.

[157] A. Emir Gümrükçüoğlu, Mehdi Saravani, and Thomas P. Sotiriou. Hořava gravity after GW170817. *Phys. Rev.* D97.2 (2018), p. 024032. DOI: 10.1103/PhysRevD.97.024032.

[158] Jacob Oost, Shinji Mukohyama, and Anzhong Wang. Constraints on Einstein-aether theory after GW170817. *Phys. Rev.* D97.12 (2018), p. 124023. DOI: 10.1103/PhysRevD.97.124023.

[159] Benjamin P. Abbott et al. First search for nontensorial gravitational waves from known pulsars. *Phys. Rev. Lett.* 120.3 (2018), p. 031104. DOI: 10.1103/PhysRevLett.120.031104.

[160] Benjamin P. Abbott et al. A Search for Tensor, Vector, and Scalar Polarizations in the Stochastic Gravitational-Wave Background (2018). arXiv: 1802.10194 [gr-qc].

[161] Nima Arkani-Hamed, Savas Dimopoulos, and G. R. Dvali. The Hierarchy problem and new dimensions at a millimeter. *Phys. Lett.* B429 (1998), pp. 263–272. DOI: 10.1016/S0370-2693(98)00466-3.

[162] Gia Dvali. Black Holes and Large N Species Solution to the Hierarchy Problem. *Fortsch. Phys.* 58 (2010), pp. 528–536. DOI: 10.1002/prop.201000009.

[163] Petr Hořava and Charles M. Melby-Thompson. General Covariance in Quantum Gravity at a Lifshitz Point. *Phys. Rev.* D82 (2010), p. 064027. DOI: 10.1103/PhysRevD.82.064027.

[164] Shinji Mukohyama. Hořava-Lifshitz Cosmology: A Review. *Class. Quant. Grav.* 27 (2010), p. 223101. DOI: 10.1088/0264-9381/27/22/223101.

[165] Elias Kiritsis and Georgios Kofinas. Hořava-Lifshitz Cosmology. *Nucl. Phys.* B821 (2009), pp. 467–480. DOI: 10.1016/j.nuclphysb.2009.05.005.

[166] Gianluca Calcagni. Cosmology of the Lifshitz universe. *JHEP* 09 (2009), p. 112. DOI: 10.1088/1126-6708/2009/09/112.

[167] Emmanuel N. Saridakis. Hořava-Lifshitz Dark Energy. *Eur. Phys. J.* C67 (2010), pp. 229–235. DOI: 10.1140/epjc/s10052-010-1294-6.

[168] Robert Brandenberger. Matter Bounce in Hořava-Lifshitz Cosmology. *Phys. Rev.* D80 (2009), p. 043516. DOI: 10.1103/PhysRevD.80.043516.

[169] Ewa Czuchry. Bounce scenarios in the Sotiriou-Visser-Weinfurtner generalization of the projectable Hořava-Lifshitz gravity. *Class. Quant. Grav.* 28 (2011), p. 125013. DOI: 10.1088/0264-9381/28/12/125013.

[170] Ewa Czuchry. The Phase portrait of a matter bounce in Hořava-Lifshitz cosmology. *Class. Quant. Grav.* 28 (2011), p. 085011. DOI: 10.1088/0264-9381/28/8/085011.

[171] Sourish Dutta and Emmanuel N. Saridakis. Observational constraints on Hořava-Lifshitz cosmology. *JCAP* 1001 (2010), p. 013. DOI: 10.1088/1475-7516/2010/01/013.

[172] Mu-in Park. A Test of Hořava Gravity: The Dark Energy. *JCAP* 1001 (2010), p. 001. DOI: 10.1088/1475-7516/2010/01/001.

[173] Noemi Frusciante et al. Hořava Gravity in the Effective Field Theory formalism: From cosmology to observational constraints. *Phys. Dark Univ.* 13 (2016), pp. 7–24. DOI: 10.1016/j.dark.2016.03.002.

[174] B. Audren et al. Cosmological constraints on deviations from Lorentz invariance in gravity and dark matter. *JCAP* 1503.03 (2015), p. 016. DOI: 10.1088/1475-7516/2015/03/016.

[175] B. Audren et al. Cosmological constraints on Lorentz violating dark energy. *JCAP* 1308 (2013), p. 039. DOI: 10.1088/1475-7516/2013/08/039.

[176] Thomas P. Sotiriou, Matt Visser, and Silke Weinfurtner. Quantum gravity without Lorentz invariance. *JHEP* 10 (2009), p. 033. DOI: 10.1088/1126-6708/2009/10/033.

[177] Thomas P. Sotiriou. Hořava-Lifshitz gravity: a status report. *J. Phys. Conf. Ser.* 283 (2011), p. 012034. DOI: 10.1088/1742-6596/283/1/012034.

[178] D. Blas, O. Pujolas, and S. Sibiryakov. On the Extra Mode and Inconsistency of Horava Gravity. *JHEP* 10 (2009), p. 029. DOI: 10.1088/1126-6708/2009/10/029.

[179] Christos Charmousis et al. Strong coupling in Hořava gravity. *JHEP* 08 (2009), p. 070. DOI: 10.1088/1126-6708/2009/08/070.

[180] Daniele Vernieri and Thomas P. Sotiriou. Hořava-Lifshitz Gravity: Detailed Balance Revisited. *Phys. Rev.* D85 (2012), p. 064003. DOI: 10.1103/PhysRevD.85.069901,10.1103/PhysRevD.85.064003.

[181] Corrado Appignani, Roberto Casadio, and S. Shankaranarayanan. The Cosmological Constant and Horava-Lifshitz Gravity. *JCAP* 1004 (2010), p. 006. DOI: 10.1088/1475-7516/2010/04/006.

[182] Daniele Vernieri. On power-counting renormalizability of Hořava gravity with detailed balance. *Phys. Rev.* D91.12 (2015), p. 124029. DOI: 10.1103/PhysRevD.91.124029.

[183] Mattia Colombo, A. Emir Gümrükçüoğlu, and Thomas P. Sotiriou. Hořava gravity with mixed derivative terms: Power counting renormalizability with lower order dispersions. *Phys. Rev.* D92.6 (2015), p. 064037. DOI: 10.1103/PhysRevD.92.064037.

[184] H. Lü, J. Mei, and C. N. Pope. Solutions to Hořava Gravity. *Phys. Rev. Lett.* 103 (2009), p. 091301. DOI: 10.1103/PhysRevLett.103.091301.

[185] Maxim Pospelov and Yanwen Shang. On Lorentz violation in Horava-Lifshitz type theories. *Phys. Rev.* D85 (2012), p. 105001. DOI: 10.1103/PhysRevD.85.105001.

[186] Andrew Coates et al. Uninvited guest in mixed derivative Hořava gravity. *Phys. Rev.* D94.8 (2016), p. 084014. DOI: 10.1103/PhysRevD.94.084014.

[187] Sean M. Carroll. The Cosmological Constant. *Living Reviews in Relativity* 4.1 (Feb. 2001), p. 1. ISSN: 1433-8351. DOI: 10.12942/lrr-2001-1. URL: https://doi.org/10.12942/lrr-2001-1.

[188] D. M. Scolnic et al. The Complete Light-curve Sample of Spectroscopically Confirmed SNe Ia from Pan-STARRS1 and Cosmological Constraints from the Combined Pantheon Sample. *Astrophys. J.* 859.2 (2018), p. 101. DOI: 10.3847/1538-4357/aab9bb.

[189] Jing Liu and Hao Wei. Cosmological models and gamma-ray bursts calibrated by using Padé method. *Gen. Rel. Grav.* 47.11 (2015), p. 141. DOI: 10.1007/s10714-015-1986-1.

[190] P. A. R. Ade et al. Planck 2015 results. XIII. Cosmological parameters. *Astron. Astrophys.* 594 (2016), A13. DOI: 10.1051/0004-6361/201525830.

[191] Michele Moresco. Raising the bar: new constraints on the Hubble parameter with cosmic chronometers at z $\sim$ 2. *Mon. Not. Roy. Astron. Soc.* 450.1 (2015), pp. L16–L20. DOI: 10.1093/mnrasl/slv037.

[192] M. Betoule et al. Improved cosmological constraints from a joint analysis of the SDSS-II and SNLS supernova samples. *Astron. Astrophys.* 568 (2014), A22. DOI: 10.1051/0004-6361/201423413.

[193] Chris Blake et al. The WiggleZ Dark Energy Survey: Joint measurements of the expansion and growth history at z < 1. *Mon. Not. Roy. Astron. Soc.* 425 (2012), pp. 405–414. DOI: 10.1111/j.1365-2966.2012.21473.x.

[194] Shadab Alam et al. The clustering of galaxies in the completed SDSS-III Baryon Oscillation Spectroscopic Survey: cosmological analysis of the DR12 galaxy sample. *Submitted to: Mon. Not. Roy. Astron. Soc.* (2016). arXiv: 1607.03155 [astro-ph.CO].

[195] Andreu Font-Ribera et al. Quasar-Lyman $\alpha$ Forest Cross-Correlation from BOSS DR11: Baryon Acoustic Oscillations. *JCAP* 1405 (2014), p. 027. DOI: 10.1088/1475-7516/2014/05/027.

[196] C. L. Bennett et al. The 1% Concordance Hubble Constant. *Astrophys. J.* 794 (2014), p. 135. DOI: 10.1088/0004-637X/794/2/135.

[197] Charalampos Bogdanos and Emmanuel N Saridakis. Perturbative instabilities in Hořava gravity. *Classical and Quantum Gravity* 27.7 (2010), p. 075005. URL: http://stacks.iop.org/0264-9381/27/i=7/a=075005.

[198] Keith A. Olive, Gary Steigman, and Terry P. Walker. Primordial nucleosynthesis: Theory and observations. *Phys. Rept.* 333 (2000), pp. 389–407. DOI: 10.1016/S0370-1573(00)00031-4.

[199] Kaoru Hagiwara et al. Review of particle physics. Particle Data Group. *Phys. Rev.* D66 (2002), p. 010001. DOI: 10.1103/PhysRevD.66.010001.

[200] Gary Steigman. Primordial nucleosynthesis: successes and challenges. *Int. J. Mod. Phys.* E15 (2006), pp. 1–36. DOI: 10.1142/S0218301306004028.

[201] Richard H. Cyburt et al. Big Bang Nucleosynthesis: 2015. *Rev. Mod. Phys.* 88 (2016), p. 015004. DOI: 10.1103/RevModPhys.88.015004.

[202] Isabel M. Oldengott and Dominik J. Schwarz. Improved constraints on lepton asymmetry from the cosmic microwave background. *EPL* 119.2 (2017), p. 29001. DOI: 10.1209/0295-5075/119/29001.

[203] Andrew R. Zentner and Terry P. Walker. Constraints on the cosmological relativistic energy density. *Phys. Rev.* D65 (2002), p. 063506. DOI: 10.1103/PhysRevD.65.063506.

[204] Rachel Bean, Steen H. Hansen, and Alessandro Melchiorri. Constraining the dark universe. *Nucl. Phys. Proc. Suppl.* 110 (2002), pp. 167–172. DOI: 10.1016/S0920-5632(02)01475-5.

[205] V. Bonvin et al. H0LiCOW - V. New COSMOGRAIL time delays of HE 0435-1223: $H_0$ to 3.8 per cent precision from strong lensing in a flat ΛCDM model. *MNRAS* 465 (Mar. 2017), pp. 4914–4930. DOI: 10.1093/mnras/stw3006.

[206] A. G. Riess et al. A 3% Solution: Determination of the Hubble Constant with the Hubble Space Telescope and Wide Field Camera 3. *ApJ* 730, 119 (Apr. 2011), p. 119. DOI: 10.1088/0004-637X/730/2/119.

[207] Sourish Dutta and Emmanuel N. Saridakis. Overall observational constraints on the running parameter $\lambda$ of Horava-Lifshitz gravity. *JCAP* 1005 (2010), p. 013. DOI: 10.1088/1475-7516/2010/05/013.

[208] Nima Arkani-Hamed, Savas Dimopoulos, and G. R. Dvali. Phenomenology, astrophysics and cosmology of theories with submillimeter dimensions and TeV scale quantum gravity. *Phys. Rev.* D59 (1999), p. 086004. DOI: 10.1103/PhysRevD.59.086004.

[209] Diego Blas, Oriol Pujolas, and Sergey Sibiryakov. Models of non-relativistic quantum gravity: The Good, the bad and the healthy. *JHEP* 04 (2011), p. 018. DOI: 10.1007/JHEP04(2011)018.

[210] Guido Cognola et al. Covariant Hořava-like and mimetic Horndeski gravity: cosmological solutions and perturbations. *Class. Quant. Grav.* 33.22 (2016), p. 225014. DOI: 10.1088/0264-9381/33/22/225014.

[211] Alessandro Casalino et al. Alive and well: mimetic gravity and a higher-order extension in light of GW170817. *Class. Quant. Grav.* 36.1 (2019), p. 017001. DOI: 10.1088/1361-6382/aaf1fd.

[212] S. Birrer et al. H0LiCOW - IX. Cosmographic analysis of the doubly imaged quasar SDSS 1206+4332 and a new measurement of the Hubble constant. *Mon. Not. Roy. Astron. Soc.* 484 (2019), p. 4726. DOI: 10.1093/mnras/stz200.

[213] C. Guidorzi et al. Improved Constraints on $H_0$ from a Combined Analysis of Gravitational-wave and Electromagnetic Emission from GW170817. *Astrophys. J.* 851.2 (2017), p. L36. DOI: 10.3847/2041-8213/aaa009.

[214] Stephen M. Feeney et al. Prospects for resolving the Hubble constant tension with standard sirens. *Phys. Rev. Lett.* 122.6 (2019), p. 061105. DOI: 10.1103/PhysRevLett.122.061105.

[215] Zhe Chang et al. Low-redshift constraints on the Hubble constant from the baryon acoustic oscillation "standard rulers" and the gravitational wave "standard sirens". *Eur. Phys. J.* C79.2 (2019), p. 177. DOI: 10.1140/epjc/s10052-019-6664-0.

[216] Adam G. Riess et al. Milky Way Cepheid Standards for Measuring Cosmic Distances and Application to Gaia DR2: Implications for the Hubble Constant. *Astrophys. J.* 861.2 (2018), p. 126. DOI: 10.3847/1538-4357/aac82e.

[217] Adam G. Riess et al. A Redetermination of the Hubble Constant with the Hubble Space Telescope from a Differential Distance Ladder. *Astrophys. J.* 699 (2009), pp. 539–563. DOI: 10.1088/0004-637X/699/1/539.

[218] Bonnie R. Zhang et al. A blinded determination of $H_0$ from low-redshift Type Ia supernovae, calibrated by Cepheid variables. *Mon. Not. Roy. Astron. Soc.* 471.2 (2017), pp. 2254–2285. DOI: 10.1093/mnras/stx1600.

[219] N. Aghanim et al. Planck 2018 results. VI. Cosmological parameters (2018). arXiv: 1807.06209 [astro-ph.CO].

[220] Ashley J. Ross et al. The clustering of the SDSS DR7 main Galaxy sample – I. A 4 per cent distance measure at $z = 0.15$. *Mon. Not. Roy. Astron. Soc.* 449.1 (2015), pp. 835–847. DOI: 10.1093/mnras/stv154.

[221] Éric Aubourg et al. Cosmological implications of baryon acoustic oscillation measurements. *Phys. Rev.* D92.12 (2015), p. 123516. DOI: 10.1103/PhysRevD.92.123516.

[222] E. Macaulay et al. First Cosmological Results using Type Ia Supernovae from the Dark Energy Survey: Measurement of the Hubble Constant. *Mon. Not. Roy. Astron. Soc.* 486.2 (2019), pp. 2184–2196. DOI: 10.1093/mnras/stz978.

[223] Kevin Aylor et al. Sounds Discordant: Classical Distance Ladder & ΛCDM - based Determinations of the Cosmological Sound Horizon. *Astrophys. J.* 874.1 (2019), p. 4. DOI: 10.3847/1538-4357/ab0898.

[224] Supriya Pan et al. Interacting scenarios with dynamical dark energy: observational constraints and alleviation of the $H_0$ tension. *Phys. Rev.* D100.10 (2019), p. 103520. DOI: 10.1103/PhysRevD.100.103520.

[225] Harry Desmond, Bhuvnesh Jain, and Jeremy Sakstein. Local resolution of the Hubble tension: The impact of screened fifth forces on the cosmic distance ladder. *Phys. Rev.* D100.4 (2019), p. 043537. DOI: 10.1103/PhysRevD.100.043537.

[226] Kyriakos Vattis, Savvas M. Koushiappas, and Abraham Loeb. Dark matter decaying in the late Universe can relieve the H0 tension. *Phys. Rev.* D99.12 (2019), p. 121302. DOI: 10.1103/PhysRevD.99.121302.

[227] Zhe Chang and Qing-Hua Zhu. Reference frame dependence of local measured Hubble constant (2019). arXiv: 1909.13252 [gr-qc].

[228] Adam G. Riess et al. A 2.4% DETERMINATION OF THE LOCAL VALUE OF THE HUBBLE CONSTANT. *The Astrophysical Journal* 826.1 (July 2016), p. 56. DOI: 10.3847/0004-637x/826/1/56. URL: https://doi.org/10.3847%2F0004-637x%2F826%2F1%2F56.

[229] E. Lusso et al. Tension with the flat Lambda CDM model from a high redshift Hubble Diagram of supernovae, quasars and gamma-ray bursts. *Astron. Astrophys.* 628 (2019), p. L4. DOI: 10.1051/0004-6361/201936223.

[230] Guido Risaliti and Elisabeta Lusso. A Hubble Diagram for Quasars. *Astrophys. J.* 815 (2015), p. 33. DOI: 10.1088/0004-637X/815/1/33.

[231] Nils A. Nilsson and Ewa Czuchry. Hořava-Lifshitz cosmology in Light of New Data II: The case of $\lambda$ (2020). In preparation.

[232] Adam G. Riess et al. Large Magellanic Cloud Cepheid Standards Provide a 1% Foundation for the Determination of the Hubble Constant and Stronger Evidence for Physics beyond $\Lambda$CDM. *Astrophys. J.* 876.1 (2019), p. 85. DOI: 10.3847/1538-4357/ab1422.

[233] Alejandro Aviles et al. Precision cosmology with Padé rational approximations: Theoretical predictions versus observational limits. *Phys. Rev.* D90.4 (2014), p. 043531. DOI: 10.1103/PhysRevD.90.043531.

[234] Orlando Luongo, Marco Muccino, and Hernando Quevedo. Kinematic and statistical inconsistencies of Hořava–Lifshitz cosmology. *Phys. Dark Univ.* 25 (2019), p. 100313. DOI: 10.1016/j.dark.2019.100313.

[235] Salvatore Capozziello, Rocco D'Agostino, and Orlando Luongo. Cosmographic analysis with Chebyshev polynomials. *Mon. Not. Roy. Astron. Soc.* 476.3 (2018), pp. 3924–3938. DOI: 10.1093/mnras/sty422.

[236] Micol Benetti and Salvatore Capozziello. Connecting early and late epochs by f(z)CDM cosmography. *JCAP* 1912.12 (2019), p. 008. DOI: 10.1088/1475-7516/2019/12/008.

[237] R. U. Abbasi et al. INDICATIONS OF INTERMEDIATE-SCALE ANISOTROPY OF COSMIC RAYS WITH ENERGY GREATER THAN 57 EeV IN THE NORTHERN SKY MEASURED WITH THE SURFACE DETECTOR OF THE TELESCOPE ARRAY EXPERIMENT. *The Astrophysical Journal* 790.2 (July 2014), p. L21. DOI: 10.1088/2041-8205/790/2/l21. URL: https://doi.org/10.1088%2F2041-8205%2F790%2F2%2Fl21.

[238] Kellie O'Neal-Ault, Nils A. Nilsson, and Quentin G. Bailey. The ADM Formulation of the Minimal Standard-Model Extension Gravitational Sector. To be submitted.

[239] Thomas W. Baumgarte and Stuart L. Shapiro. *Numerical Relativity: Solving Einstein's Equations on the Computer*. Cambridge University Press, 2010. DOI: 10.1017/CBO9781139193344.

[240] Quentin G. Bailey and V. Alan Kostelecky. Signals for Lorentz violation in post-Newtonian gravity. *Phys. Rev.* D74 (2006), p. 045001. DOI: 10.1103/PhysRevD.74.045001.

[241] Vincenzo Salzano and Mariusz P. Dabrowski. Statistical hierarchy of varying speed of light cosmologies. *Astrophys. J.* 851.2 (2017), p. 97. DOI: 10.3847/1538-4357/aa9cea.

[242] Antony Lewis and Sarah Bridle. Cosmological parameters from CMB and other data: A Monte Carlo approach. *Phys. Rev.* D66 (2002), p. 103511. DOI: 10.1103/PhysRevD.66.103511.

[243] B. Audren et al. Conservative constraints on early cosmology with MONTE PYTHON. *JCAP* 2, 001 (Feb. 2013), p. 001. DOI: 10.1088/1475-7516/2013/02/001.

[244] David W. Hogg. Distance measures in cosmology (1999). arXiv: astro-ph/9905116 [astro-ph].

[245] Daniel J. Eisenstein and Wayne Hu. Baryonic features in the matter transfer function. *Astrophys. J.* 496 (1998), p. 605. DOI: 10.1086/305424.

[246] Yun Wang and Mi Dai. Exploring uncertainties in dark energy constraints using current observational data with Planck 2015 distance priors. *Phys. Rev.* D94.8 (2016), p. 083521. DOI: 10.1103/PhysRevD.94.083521.

[247] Wayne Hu and Naoshi Sugiyama. Small scale cosmological perturbations: An Analytic approach. *Astrophys. J.* 471 (1996), pp. 542–570. DOI: 10.1086/177989.